Performance estimation and optimization of the IEEE802.11 MAC layer for long distance point-to-point links

Michael Rademacher

Publisher: Dean Prof. Dr. Wolfgang Heiden

University of Applied Sciences Bonn-Rhein-Sieg,
Department of Computer Science

Sankt Augustin, Germany

March 2015

Technical Report 01-2015

Hochschule
Bonn-Rhein-Sieg
University of Applied Sciences

ISSN 1869-5272

Hochschule
Bonn-Rhein-Sieg
University of Applied Sciences

Fachbereich Informatik
Department of Computer Science

Fraunhofer
FOKUS

Network Research

Performance estimation and optimization of the IEEE802.11 MAC layer for long distance point-to-point links

by

Michael Rademacher

First supervisor:	Prof. Dr. Karl Jonas
Second supervisor:	Prof. Dr. Kerstin Uhde
Handed in:	January 15,2014

Contents

List of Tables

List of Figures

List of abbreviations

AP	Access Point
AIFS	Arbitration Interframe Space
AC	Access Category
ACK	acknowledgement
BER	Bit Error Rate
CW	Contention Window
CSMA/CD	Carrier Sense Multiple Access/Collision Detection
CSMA/CA	Carrier Sense Multiple Access/Collision Avoidance
CSMA	Carrier Sense Multiple Access
CPU	Central Processing Unit
DCF	Distributed Coordination Function
DIFS	DCF Interframe Space
SIFS	Short Interframe Space
DSSS	Direct-Sequence Spread Spectrum
EDCF	Enhanced Distributed Coordination Function
EDCA	Enhanced Distributed Coordination Access
EIFS	Extended Interframe Space
EIRP	Equivalent isotropically radiated power
FCS	Frame Check Sequence
FEC	Forward Error Correction
FIFO	First-In-First-Out
FSPL	Free-space path loss
GPS	Global Positioning System
HCF	Hybrid Coordination Function
HOL	Head-of-line
IBSS	Independent Basic Service Set
ISM	Industrial, Scientific and Medical
IP	Internet Protocol
IFS	Interframe Space
MAC	Media Access Control
ISP	Internet Service Provider
LoS	Line of Sight
MIMO	Multiple Input Multiple Output
MTU	Maximum Transmission Unit
MCS	Modulation and Coding Scheme
MSDU	MAC Service Data Unit
MPLS	Multiprotocol Label Switching

MPDU	MAC Protocol Data Unit
NAV	Network Allocation Vector
NTP	Network Time Protocol Unit
OSI	Open Systems Interconnection
OFDM	Orthogonal Frequency-Division Multiplexing
QoS	Quality of Service
SNR	Signal-to-noise ratio
PER	Packet Error Rate
PPDU	Physical Protocol Data Unit
TCP	Transmission Control Protocol
TDMA	Time Division Multiple Access
TSFT	Time Synchronization Function Timer
TXOP	Transmit opportunity
PCF	Point Coordination Function
PLCP	Physical Layer Convergence Protocol
PTP	Precision Time Protocol
UDP	User Datagram Protocol
UP	User Priorities
VoIP	Voice over Internet Protocol
WiBACK	Wireless Back-Haul
WiLD	WiFi based Long Distance networks
WMN	Wireless Mesh Network

1. Introduction

Rural areas often lack affordable broadband Internet connectivity, mainly due to the CAPEX and especially OPEX of traditional operator equipment [HEKN11]. This digital divide limits the access to knowledge, health care and other services for billions of people. Different approaches to close this gap were discussed in the last decade [SPNB08]. In most rural areas satellite bandwidth is expensive and cellular networks (3G,4G) as well as WiMAX suffer from the usually low population density making it hard to amortize the costs of a base station [SPNB08].

WiFi based Long Distance networks (WiLD) offer an alternative as cost efficient back-haul connectivity. In the last decade, several publications described WiLD deployments, providing connectivity to rural areas [SPNB08, RC07, PSGS12, MFL05, HEKN11] including their technical and economical constraints. All these approaches use IEEE802.11 [iee12] off the shelf hardware. Due to their distribution in the consumer sector these radios are well developed, well priced and offer a stable performance in the license free Industrial, Scientific and Medical (ISM)-Band[1]. The Fraunhofer Institute for Open Communication System (FOKUS) has developed their own approach called Wireless Back-Haul (WiBACK). A self-managed, heterogeneous Wireless Back-Haul architecture which is based on long-distance IEEE802.11 point-to-point links as well as technology independent Multiprotocol Label Switching (MPLS)-based traffic engineering [HEKN11].

To address Quality of Service (QoS)-requirements as well as the increasing demand for triple-play content, high bandwidth in the back-haul is a crucial factor for a modern operator. In general there are two different possibilities to increase the capacity inside a wireless back-haul: maximize the efficiency of the radios[2] used or enlarge the overall number of devices and channels. Under the assumption of minimizing the costs of a network (CAPEX and OPEX) the first opportunity should always be considered before choosing the second one.

As already shown in [RKJ13], the physical layer data rate of an 802.11 radio can be increased to 270 Mbps over a distance of 10 km through exploiting the so called next generation wireless standard 802.11n in combination with cross polarized (MIMO) high gain antennas. To define the maximum throughput for the upper layers as well, an academic traffic pattern[3] and parameters were chosen for the experiments. The combination of large Media Access Control (MAC) layer aggregation factors and uni-directional traffic leads to 200 Mbps real throughput. However, the usage of bi-directional traffic could

[1] Extensive development took mainly place for 2.4 GHz and 5 GHz.
[2] Hardware and software.
[3] Uni-directional, UDP, large payload and high aggregation factors.

lead to a decrease of the throughput by several factors and a large number of aggregated packets introduces additional delay. This reduction in quality is caused by different characteristics of the IEEE802.11 MAC layer [iee12]. After defining in previous work the maximum capacity on the physical layer[4] this thesis provides a complete view on the capabilities of the default 802.11 MAC layer for long-distance links in bi-directional and saturated traffic conditions.

The 802.11 MAC layer exploits a technique called Distributed Coordination Function (DCF) which employs the Carrier Sense Multiple Access/Collision Avoidance (CSMA/CA) protocol with a binary exponential back-off algorithm. As the term collision avoidance indicates, collisions will occur leading to an inevitable retransmission of the frame and reducing the overall throughput. By increasing the possible chances for stations to apply for a new transmission, the probability of a collision can be reduced. However, this increases the idle time on the medium and therefore reduces the overall throughput especially on long-distance links. Providing the optimum trade-off between collisions and idle times is one of the main issues addressed in this work.

The DCF was specifically designed by the IEEE 802.11 task group compromising contiguous stations in a cell and spatial restrictions of a few hundred meters at most. However, the topology of a WiLD network is based on point-to-point links with distances from a few hundred meters up to several kilometers. Instead of numerous stations applying for time on the shared medium, only two participants get into contention with a non-negligible propagation delay. Those two circumstances make the scenario crucially different from the one intentionally specified for the CSMA/CA protocol but also indicates the optimization potential of the MAC layer for long-distance point-to-point links.

To optimize the 802.11 MAC layer for point-to-point links the fixed MAC parameters defined in the standard need to be adopted for a gain in throughput and QoS. While the number of adjustable parameters are relatively low, the assumption is a strong dependency on individual link[5] and traffic[6] related facts leading to a rather dynamic task. Instead of a one time simulation, a model describing the MAC characteristics of long-distance IEEE802.11 links can be used to calculate individual parameters for each link depending on the propagation environment[7] and traffic conditions. This model and a suitable process of optimization will be described in this thesis.

The successful development of this model leads beside the optimization potential of the MAC layer parameters to the possibility of estimating the capacity and delay of WiLD

[4] Using a traffic pattern highly aiming at throughput maximization.
[5] E.g. Modulation and Coding Scheme (MCS), propagation delay.
[6] E.g. Payload-size, UDP/TCP.
[7] This includes the possible Modulation and Coding Scheme (MCS) well as the propagation delay.

links. This estimation provides an operator of WiLD networks with the possibility of capacity planing before setting up the infrastructure. Depending on the knowledge about the characteristics of the topology, a dimensioning of the network can be carried out beforehand.

An important factor is the accuracy of the model, which needs to be determined through real experiments instead of simulations usually conducted in this field of study. For this purpose a measurement environment was implemented, capable of precisely measuring the throughput and delay of the 802.11 MAC layer utilizing UDP traffic. With the gained data from these experiments an additional adaption of the modeling approach (to account for real-world deployments) might be possible.

Overall, this leads to two main tasks of this thesis. First, the estimation of throughput and delay of the 802.11 MAC layer for long-distance point-to-point links in saturated and bi-directional traffic conditions. If this estimation can be carried out with a sufficient accuracy, the second goal of this thesis can be proceeded: The optimization of the MAC parameters to increase the throughput and decrease the delay on this type of links.

The remainder of this work is structured as follows. In section 2 the reader is briefly introduced to the main concepts of the 802.11 MAC layer and WiLD links. Afterwards, in the state of the art section, current modeling techniques for the 802.11 MAC are reviewed. This review includes a detailed description about the already conducted research about MAC layers for WiLDs. Section 4 will deal with the methodology of this work. In this part, the selection of an modeling approach will be justified as the base for this work. This approach will be evaluated in detail to prepare the reader with an appropriate understanding of the mathematical background before the developed model extensions will be proposed. These additions provide the possibility to account for long-distance point-to-point links and current 802.11 standards. In section 5 the implementation of the model, the measurement system as well the exploited WiFi links will be evaluated. A detailed validation of the model with the need for additional adoptions to precisely account for real-world deployments is described in section 6. The successfully developed model will then be used in 7 to first, estimate different characteristic of long-distance links and afterwards, optimize the 802.11 MAC parameters. This thesis will close in section 8 with a detailed discussion of the results. In the future work section the influence of different transport layer protocols like TCP, as well first ideas about different MAC layer techniques for long-distance point-to-point links will be briefly illustrated.

2. Background

The purpose of this section is to provide the reader with a short introduction to the main concepts of IEEE802.11 with a special focus on the MAC layer mechanism. Several publications, books [LÖ07, Rec12] and the different versions of the standard itself [iee07, iee09, iee12] already deal with this topic, therefore the main ideas will be briefly summarized and the focus will be laid on the important aspects related to upcoming sections.

The 802.11 standard defines the first two layers of the Open Systems Interconnection (OSI) reference model leaving the upper ones unspecified for ambiguous technologies and distinguishes between two different modes of operation: the infrastructure mode and the ad-hoc mode. The main difference is the need for at least one Access Point (AP) in the infrastructure mode operating as a central distributor in the wireless cell. In the ad-hoc mode the different clients communicate directly with each other. Wireless Mesh Networks (WMNs) exploit WiFi-radios by setting up a multi-hop wireless infrastructure. This technology has the potential to provide communication services where traditional equipment like fixed-line is not profitable for an operator. In the case of WMN (including WiBACK) the operation mode is ad-hoc. In most cases, one radio per client (that is associated to a certain ad-hoc cell) is used. WiBACK exploits a multi-radio technology operating on different frequencies. In contrast to traditional WMN, this can be characterized as a chain connection of point-to-point WiFi links.

The physical layer specifications strongly depend on the version of the standard used. Over the years, several extensions have been published increasing the maximum throughput from 11 Mbps (802.11b [iee07]) to 150 Mbps (802.11n [iee12]). With the usage of Multiple Input Multiple Output (MIMO) a further increase of the physical data rate is possible by transmitting data simultaneously on spatial streams.

As a sublayer of the data link layer, the MAC provides rules and protocols regulating the communication channel shared among different network nodes. These rules are needed to handle simultaneous access of different terminals. Otherwise, frequent packet collisions would occur. For stations in a wired network it is possible to detect collisions on the medium and stop the transmission immediately. This is defined in the so called Carrier Sense Multiple Access/Collision Detection (CSMA/CD) protocol for example used by IEEE802.3 (Ethernet). Wireless radios are not capable of detecting a collision in the shared medium. This applies due to the lack of possibility to trace their own transmission and to determine if the packet is received correctly [Bia98], because just one antenna is used for sending and receiving packets and the transmission power is significantly higher than the receiving sensitivity. All WiFi radios sense the medium for an

idle state beforehand (listen before talking [LÖ7]) to avoid collisions as defined in the so called Carrier Sense Multiple Access/Collision Avoidance (CSMA/CA) protocol.

The rest of this section is structured as follows. First, the 802.11 Media Access Control (MAC) layer mechanisms are elaborated since knowledge is prerequisite to the understanding of this work. Afterwards, the challenges for 802.11 in the context of long-distance links are summarized, which closes the background section.

2.1. IEEE802.11 Medium Access Control

The 802.11 standard defines two basic functions on the MAC layer: the Distributed Coordination Function (DCF) and the Point Coordination Function (PCF). As PCF is not available with a current implementation in a commercial product nor the Linux network stack it is not used by any known WiLD deployement and will not be considered any further in this thesis. The next subsections describe DCF and its QoS enhancement: the Enhanced Distributed Coordination Function (EDCF) in more detail.

2.1.1. Distributed Coordination Function (DCF)

In general there are two different techniques specified under the name DCF. The basic access technique is a two-way handshake characterized by the transmission of a packet immediately followed by an acknowledgement sent by the receiver. In addition to the basic access method a four way hand-shake (often referred as request-to-send/clear-to-send (RTS/CTS)) is specified in the standard [iee12]. Before transmitting data on the medium a node sends a short RTS frame to all other stations, reserving the medium for the needed amount of time. The receiver sends a CTS-frame, to signal the willingness to receive the data which is followed by the basic access method. In the following the basic method is presented in more detail.

When a frame arrives at the head of the First-In-First-Out (FIFO)-transmission-queue, a station monitors the channel for an idle time of a DCF Interframe Space (DIFS). To detect an idle channel, 802.11 uses a carrier sense function on the physical layer and a virtual carrier sense function on the MAC layer. The physical carrier sense function monitors the channel for any ongoing transmission. The virtual carrier sense function is based on a timer called Network Allocation Vector (NAV). Every station manages its own NAV which represents the time the medium is estimated busy. The NAV is propagated in a header-field of every 802.11 frame called the Duration/ID field. All stations can receive this information and update their NAV accordingly. Only when the NAV reaches zero and the physical carrier sense function detects no transmission for the time of a DIFS, the medium is sensed idle.

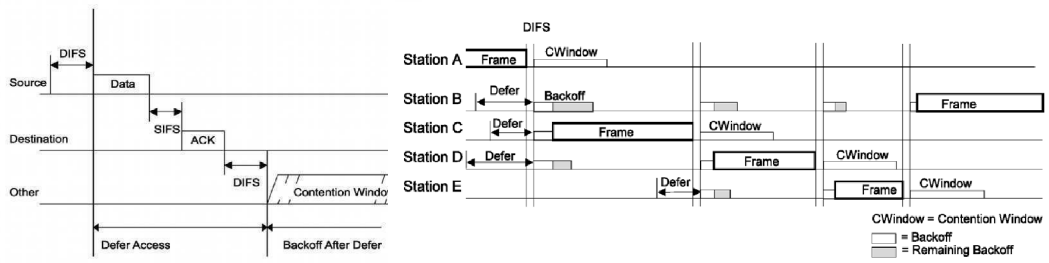

(a) Basic access [iee12, p. 838] (b) Back-off procedure [iee12, p. 839]

Figure 1: Distributed Coordination Function (DCF)

To prevent all stations transmitting at the same time when the medium is sensed idle, the so called back-off process starts (cf. figure 1a and 1b). In the beginning of this collision avoidance action a random number, uniformly distributed between zero and the current Contention Window (CW) size, is generated.

$$CW = rand[0 : CW_i - 1] \quad , CW_{min} \leq CW_i \leq CW_{max} \tag{1}$$

This number is used to generate a random back-off interval (time) which every station has to wait before their transmission. After defining the first equation of this work, the reader is invited to use the list of variables in the appendix section A.

The back-off procedure employs a slotted and discrete time scale. A station is allowed to transmit in the beginning of each slot. The slot time duration depends on the underlying physical layer and should be equal to the time needed for every station to detect a transmission on the medium. The randomly generated number represents the back-off time counter which is decremented by the time of a slot as long the carrier sense functions reports an idle medium. If a transmission starts and the channel becomes busy during a back-off decrease, the value is frozen and the process pauses. When the channel becomes idle again for the time of a DIFS, the process is resumed with the frozen value [Bin08]. When the counter reaches zero, the station is allowed to start the transmission in the current slot. There is one possibility to overcome the back-off procedure: when a frame arrives at an empty queue and the medium has been idle longer than a DIFS, the transmission starts immediately.

The receiving station waits the time of a Short Interframe Space (SIFS) to sent an acknowledgement back to the transmitter to confirm the successful transmission. This time is needed to ensure the medium is idle again. Since the time of a SIFS is shorter than the time of a DIFS, the transmission of the acknowledgement is protected from other stations' contention (see figures 1a and 2). If the acknowledgement is not received within the so called ACK timeout, the frame is considered as lost and needs to be retransmit-

ted after another random back-off. One possibility[8] for an aborted transmission is that another station randomly picked the same transmission slot. Initially assigned to CW_{min} ,the back-off scheme doubles the value of CW in this case until it reaches CW_{max}.

$$CW_{i+1} = 2(CW_i + 1) - 1 \tag{2}$$

This decreases the probability of two stations picking the same back-off slot, but increases the back-off time. After a successful transmission the station sets CW back to CW_{min} to re-improve the channel utilization and performs a DIFS deference as well as a random back-off - even if there is no packet in the queue [Bin08]. This so called post back-off ensures that there is at least one back-off interval between two transmissions (see figure 1b). Another important IFS besides SIFS and DIFS is called Extended Inter-

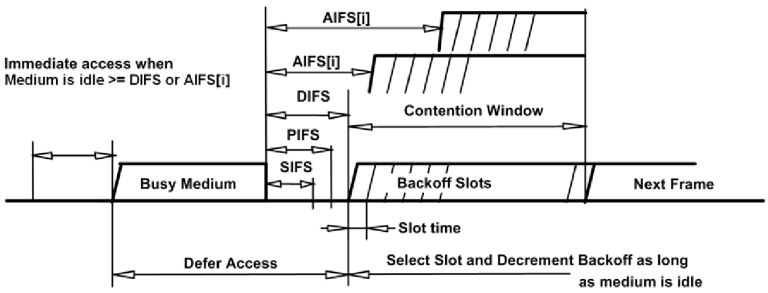

Figure 2: IFS relationships [iee12, p. 826]

frame Space (EIFS). This IFS shall be used when a received frame contains a detected error. There are two different cases this error can be reported [Bin08]:

1. The PHY detects and reports an error, e.g. carrier lost.
2. The MAC detects and reports an incorrect Frame Check Sequence (FCS).

For stations receiving an erroneous packet it is in most cases possible to detect this error, however it is not possible to determine the identity of the receiver. To provide a station (the proper receiver) with the chance to send an acknowledge, these nodes wait the time of an EIFS.All the presented MAC parameters depend on the underlying PHY. Figure 2 shows their general relationship, table 1 sums up the parameters for common 802.11 PHYs. However, all IFS depend on the slot time leading to the possibility of generic calculations which are given below.

$$DIFS = SIFS + 2 * SlotTime \tag{3}$$

$$EIFS = SIFS + DIFS + ACKTxTime \tag{4}$$

[8] This could also occur due to interference or any other error on the channel.

Table 1: MAC parameters for 802.11 PHY [Rec12, iee07, iee09, iee12]

Parameter Standard	Slot (μs)	SIFS (μs)	DIFS (μs)	CW_{min}	CW_{max}
802.11-1997 (FHSS)	50	28	128	15	1023
802.11-1997 (DSSS)	20	10	50	31	1023
802.11b	20	10	50	31	1023
802.11a	9	16	34	15	1023
802.11g	9/20	10	28/50	31	1023
802.11n (2.4 GHz)	9/20	10	28/50	15	1023
802.11n (5 GHz)	9	16	34	15	1023
802.11ac	9	16	34	15	1023

2.1.2. Enhanced Distributed Channel Access (EDCA)

In the year 2005 the IEEE published the 802.11e standard - a MAC extension for QoS provisioning. The standard defines a new coordination function called Hybrid Coordination Function (HCF) which combines DCF and PCF with the contemplated QoS extensions. For the case of Independent Basic Service Set (IBSS) networks[9], HCF employs the contention-based channel access referred to Enhanced Distributed Coordination Access (EDCA), which is described below in more detail.

The EDCA distinguishes between 8 different User Prioritiess (UPs) from 0 to 7 to provide differentiated access on a per frame basis. For every MAC Service Data Unit (MSDU) arriving at the MAC layer, higher layers need to provide a UP to take advantage of this differentiation. Frames transmitted by stations exploiting the IEEE802.11e standard are called QoS-data frames. The UP can be found in the header of each packet. Before transmitting QoS-data frames, each station maps the UP to one of the four so-called Access Category (AC). Each AC distinguishes itself by individual MAC timings, still utilizing the basic DCF scheme to guarantee interoperability. For every AC, values for AIFS[AC], $CW_{min}[AC]$ and $CW_{max}[AC]$ are assigned which correspond to DIFS, CW_{min} and CW_{max} in the case of DCF (cf. figure 2) [Bin08]). In general Arbitration Interframe Space (AIFS) are calculated as

$$AIFS(AC) = SIFS + AIFSN(AC) * SlotTime \tag{5}$$

where AIFSN(AC) is represented as an integer greater one. Table 2 sums up all important values for the EDCA.

[9] Synonym for ad-hoc networks.

Table 2: MAC parameters for EDCA [Bin08]

AC	Designation	AIFSN	$CW_{min}(AC)$	$CW_{max}(AC)$	TXOPLimit[AC]
AC_BK	Background	7	CW_{min}	CW_{max}	0
AC_BE	Best Effort	3	CW_{min}	CW_{max}	0
AC_VI	Video	2	$\frac{CW_{min}+1}{2}-1$	CW_{min}	3.008 ms
AC_VO	Voice	2	$\frac{CW_{min}+1}{4}-1$	$\frac{CW_{min}+1}{2}-1$	1.504 ms

In the infrastructure mode, an AP distributes the contemplated EDCA parameters to the stations. In ad-hoc mode, predefined values shown in table 2 are used since a distribution is not possible.

As pictured in figure 3, every traffic class employs a complete DCF entity so all ACs apply for the medium in parallel. After the back-off counter of an AC reaches zero it applies for a transmission on the medium, usually also competing against other stations. All other ACs freeze their back-off counters until the medium becomes idle again. A so called virtual transmission handler is required for the case when multiple ACs reach zero at the same time. In this case, the station with the higher priority wins and all other stations increase their Contention Window (CW) size.

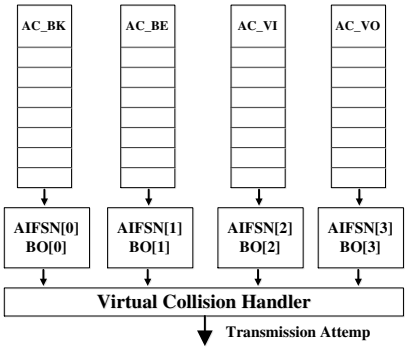

Figure 3: Access Class differentiation [Bin08]

An important difference between EDCA and DCF is the way the back-off counter is decremented. For the EDCA case the first countdown occurs at the end of the AIFS[AC] interval, while in the DCF case the first decrement occurs at the end of the first slot after the DIFS interval. Moreover, for EDCA either a decrement or a transmission occurs in one slot, whereas the DCF transmits a frame when the counter reaches zero in the same slot.

2.1.3. Additional MAC functions

There are several other MAC layer aspects and functions which are not directly related to any kind of coordination function. Those are briefly described in this subsection.

The 802.11e standard introduces an additional function to increase the efficiency of the channel by omitting the back-off and therefore reduce the gap between physical and MAC-layer throughputs [Rec12]. This so-called concept of Transmit opportunity (TXOP) is defined as "a time interval one particular station has the right to initiated a transmission" [Bin08]. This right can be obtained by any station or particular AC winning the back-off and having several packets queued for transmission. During a TXOP a station is allowed to send multiple QoS-data frames with SIFSs in between the frame, the acknowledgement (ACK) and the subsequent frame. The duration of a TXOP is limited by the TXOPLimit[AC] which can be defined individually for each traffic class. The proposed values are presented in table 2.

Besides several changes on the physical layer, IEEE802.11n (approved in 2007) introduces additional and mandatory[10] concepts on the MAC layer. These concepts define a logical extension of the Transmit opportunity (TXOP) to close the gap between the physical- and MAC-layer by surrendering IFS between data frames. This technique called "frame aggregation" represents the main 802.11n MAC enhancement. The 802.11n standard distinguishes between two different types of aggregation:

- The aggregate MAC Service Data Unit (MSDU)
- The aggregate MAC Protocol Data Unit (MPDU).

The difference between both methods is the type of aggregated payload. While the A-MSDU logically resides above, the A-MPDU technique operates below the MAC layer [SNC+08]. The A-MPDU method aggregates completely formated MAC frames including a MAC header for every sub-frame thus the A-MSDU method is more efficient. Both mechanisms share the same restriction that each sub-frame in one block has to share the same address and traffic class. To acknowledge or demand a retransmission of an aggregated frame structure, the receiver utilizes the Block ACK protocol (BACK) which efficiently confirms multiple sub-frames through a bitmap in a single packet. A description and a comparison between both techniques is provided in [PS10], a complete summary of the 802.11 MAC layer is provided by [Rec12].

[10] [PS10] shows that using the 802.11n PHY in combination with the 802.11a MAC layer leads to a decrease from 150 Mbps to a maximum of 65 Mbps throughput.

2.2. IEEE802.11 long distance links

After summarizing the 802.11 MAC layer features and functions in section 2.1, the purpose of this section is to describe long distance 802.11 links and their challenges and constraints. Some publications use a special notation for this type of networks: WiFi based Long Distance networks (WiLD) [PNS+07, SSN08]. In the last decade several authors wrote about aspects of WiLDs [PNS+07, SSN08]. Real-world deployments came up bringing connectivity to rural areas [SPNB08, RC07, PSGS12, MFL05, HEKN11].

In the following section the main physical- and MAC-layer constraints are briefly summarized, while a particular view on these aspects is presented in [Rad11,SMFRLSP10].

2.2.1. Physical Layer constraints

The mayor constraint limiting the range of WiLDs is the Signal-to-noise ratio (SNR) needed for higher modulations, leading to an increased throughput. The SNR is mainly[11] reduced by two major physical conditions [Rec12]:

- Free-space path loss (FSPL)
- Fresnel zone.

Both circumstances add attenuation to the radio signal and are affected by the selected frequency and the distance between receiver and transmitter. Through the usage of high gain antennas (up to 34 dBi) and high-power wireless cards up to (600 mW) it is possible to overcome these constraints and provide high throughput over long distance [RKJ13]. However, common WiFi-cards operate in the ISM-band which is under regulatory restriction by different organizations and governments. Table 3 summarizes the biggest regulators in charge.

Table 3: Spectrum regulators

Regulator	Region
Federal Communications Commission (FCC)	USA
Industry Canada	Canada
Association of Radio Industries and Businesses (ARIB)	Japan
European Telecommunications Standards Institute (ETSI)	Europe

Despite the fact of regulatory efforts by the organizations, the maximum allowed Equivalent isotropically radiated power (EIRP) still varies significantly - depending on country,

[11] Cf. [LÖ7, Rec12] for additional aspects.

frequency, use case and whether a registration is present[12]. In the case of WiLD, 4 Watt or 36 dBm can be seen as a first reference value for the EIRP (E.g. Germany [Bun07]), but these values usually apply not for the full ISM-Band and a registration is needed. Under the assumption of a perfect Line of Sight (LoS) connection (omitting a detailed calculation[13]), this signal strength is sufficient to use high modulations up to a distance of approximately 15 km [Rad11, RKJ13].

In [SSN08] multiple-link interference are mentioned as another significant source of errors, especially for WiLD. These interferences occur between adjacent 802.11 links operating on the same or a nearby channel. Even high gain directional antenna employ side lobes in their radiation pattern ranging from 4 to 8 dBi [MFL05]. Especially when mounted on the same mast, these side lobes (together with high power cards) can overwhelm the reception on other local radios. To avoid this problem radio frequency planing is needed to keep enough bandwidth between the adjacent 802.11 links, as for example by WiBACK.

2.2.2. Medium Access Layer constraints

Where the constraints of WiLDs on the physical-layer are evident, the situation on the MAC-layer is more complex. The main problem is the use case of long-distance links resulting in problematic MAC-layer timings. Basically the increased range needs to be taken into account by increasing the timings respectively for two parameters:

- Slot time
- ACK timeout.

The slot time needs to be increased to give all stations the chance to detect any ongoing transmission on the medium during the back-off interval. The ACK timeout represents the time the transmitter waits for an ACK from the receiver before marking the frame as lost. In the latest revisions of the standard [iee12] both parameters are defined, including a value for the air propagation time of the data (*AirPropTime*) with a default set to $1\mu s$.

$$ACKTimeout = AirPropTime + SIFS + ACKTxTime + AirPropTime \quad (6)$$

$$SlotTime = \text{MAC and PHY delays} + AirPropTime \quad (7)$$

[12] Best known summary: http://wireless.kernel.org/en/developers/Regulatory/Database .
[13] For a complete view, see [LÖ7, Rec12].

Using the default value of $1\mu s$ and the speed of light, this results in a maximum link distance of

$$s = c * t = 3 * 10^8 \frac{m}{s} * 1\mu s \approx 300\ m. \tag{8}$$

A default increase of the air propagation time would result in a decrease of throughput on short links because of the additional overhead during the back-off process. For every further 300 m of distance, 1 μs needs to be added to the slot time and 2 μs to the ACK timeout. For this purpose the standard defines the so called coverage class such that an increase of one equals 3 μs of additional air propagation time with a maximum value of $cc = 255 \mathrel{\widehat{=}} 765\ \mu s \mathrel{\widehat{=}} 229.3\ km$.

3. State of the art

The purpose of this section is to introduce the reader to the concepts and the current state of the art of mathematically modeling the IEEE802.11 MAC layer, which will be utilized as a tool for estimation and optimization. The remainder of this section is structured as follows. First a very simple, yet comprehensive introduction summarized from [Bin08] and based on [BT05] is presented. This introduction describes the main ideas of the modeling well, and provides the reader with the ability to understand further modeling aspects and the extensions conducted in upcoming sections.

In section 3.2 a review of the state of the art of different models is presented. This summary will distinguish between modeling of the DCF and the EDCA as a first differentiation, and describes different problems due to assumptions done by the authors.

Section 3.3 will elaborate the publications dealing with optimization of WiLDs (as the specified field of this thesis) to define the need and starting points for additional work in later sections.

3.1. Basics in Modeling the 802.11 MAC layer - DCF

This subsection introduces the reader to the basics of modeling the 802.11 MAC layer, drawing conceptually from a very comprehensive report in [Bin08] and updating it to the more current[14] IEEE802.11a standard. What follows are considerations about the Distributed Coordination Function (DCF) which is (as described in section 2.1.2) in their main concepts considered equally to EDCA[15].

The first part of this section describes simple calculations to determine the Media Access Control (MAC) protocol overhead, which occurs independently of the number of stations. The second part introduces the main ideas of MAC layer modeling in a situation where several stations compete for time on the medium. This situation is more complex and requires the described modeling approaches even when only two stations (for the case of point-to-point links) are considered.

3.1.1. MAC overhead

First considerations about the DCF overhead can easily be calculated by comparing the ratio of time to transmit the payload with the overall allocation time on the medium. We consider a *single station* transmitting data on the medium without contending to other

[14] [Bin08] used IEEE802.11b which is not contemporary.
[15] In fact DCF can be described as a subset of EDCA.

participants. The payload of the frame aggregates all headers (IP, TCP/UDP, etc.) and we neglect for simplification all interactions with upper layers (e.g. such as TCP congestion control). On a perfect wireless link without any errors due to interference or high noise levels the maximum throughput (S) can be expressed as follows [Bin08]:

$$S_{Station} = \frac{E[Payload]}{E[T_{Frame}] + DIFS + SlotTime * \frac{CW_{min}}{2}}. \tag{9}$$

The payload is described as an expected[16] value of a discrete and finite random variable since a bit can not be further divided and the payload can not be increased to infinity [17]. The ratio is calculated on to the overall busy time of the medium for a single transmission including the payload, a DIFS and the average time spent in the back-off process. This fraction directly leads to the common unit of throughput - data per time. The average time to transmit the frame (T_{Frame}) needs further specification. In this definition it includes the transmission time of the MPDU, the mandatory SIFS as well as the acknowledgement transmitted by the receiving station:

$$T_{Frame} = T_{MPDU} + SIFS + T_{ACK}. \tag{10}$$

T_{MPDU} and T_{ACK} are the times needed for the transmission of an MPDU and ACK respectively. Both times still include physical layer overheads and strongly depend on the transmission rate.

$$T_{MPDU} = T_{PREAM} + T_{PLCP} + N_{SYM}((\text{MAC-HDR} + Payload), MCS_{Data}) * T_{SYM} \tag{11}$$

$$T_{ACK} = T_{PREAM} + T_{PLCP} + N_{SYM}(ACK, MCS_{ACK}) * T_{SYM} \tag{12}$$

The time needed to transmit the preamble as well as the Physical Layer Convergence Protocol (PLCP) are fixed values dependent on the iteration of the standard used (cf. table 16 in the appendix). The PLCP signals the WiFi-card that subsequent bits are plain-data by transmitting a predefined combination of symbols. However, the transmission time depends on the usage of the long or short preamble option. This work only considers the short preamble option which is the de facto standard as Direct-Sequence Spread Spectrum (DSSS) is outdated[18]. For the transmission of the MAC header and the payload, different rates, also called modulations and MCS, are specified. While the word "modulation" usually refers to 802.11a and previous standards, the term MCS is used for 802.11n. In this work the terms modulations and MCS are considered equal for both standards. The acknowledgement transmission has a fixed size including a shortened MAC header. The standard [iee07] prescribed a transmission at the lowest MCS accessible by all involved stations. A Modulation and Coding Scheme (MCS) defines

[16] Indicated with a capital E in equation (9).
[17] It is limited by the Maximum Transmission Unit (MTU).
[18] Note that most publications still use the long preamble in their modeling approaches.

the number of Orthogonal Frequency-Division Multiplexing (OFDM) symbols needed (N_{SYM}) for transmitting a certain amount of data. A higher MCS leads directly to less OFDM symbols while the time needed to transmit one symbol is specified and fixed by the value T_{SYM}. Function (13) calculates the number of symbols dependent on the used MCS and the amount of data bits.

$$N_{SYM}(L[bit], MCS) = \left\lceil \frac{L+22}{N_{DBPS}(MCS)} \right\rceil \tag{13}$$

$N_{DBPS}(MCS)$ matches the MCS to the number of data bits per OFDM symbol (DBPS) (cf. table 12 in the appendix). The constant 22 in equation (13) represents the service and tail bits which are mandatory additions to the data bits as pictured in figure 4.

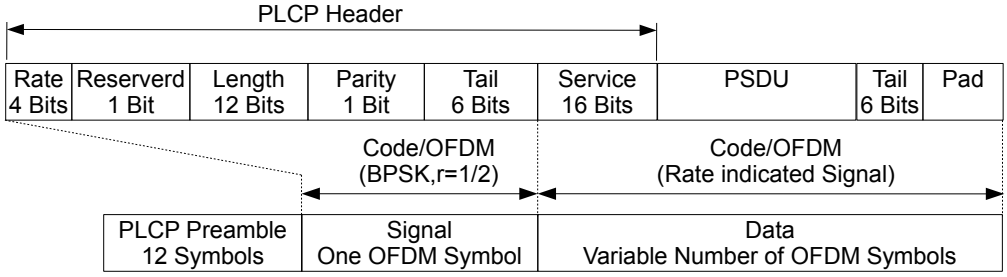

Figure 4: Structure of an 802.11a frame [Rec12]

With the presented equations 9-13 the overhead of the Distributed Coordination Function (DCF) can be calculated for a single transmitting station build up on the utilized MCS, the expected size of the payload and the standard used. To compare the efficiency and overhead of different MCS, the so called normalized throughput is a suitable unit. It compares the maximum possible MAC layer throughput with the utilized MCS defined in the following way.

$$S_{Normal} = \frac{S_{Station}\ [Mbps]}{MCS\ [Mbps]} \tag{14}$$

Figure 5 shows the normalized throughput of different MCS using the default values of the IEEE802.11a standard (cf. table 1) for different payload sizes by utilizing equation (14). It can be noted that the 802.11 MAC layer overhead decreases non-linear with an increasing packet-size. This behavior is clearly linked to the ratio of the fixed overhead time of the back-off process (as well as the IFS) and the variable transmission time of the payload. The same effect also applies to different MCS. A higher MCS directly leads to a shortened transmission time which therefore decreases the value of S_{Normal}, leading to a decreased efficiency of the allocated time on the medium.

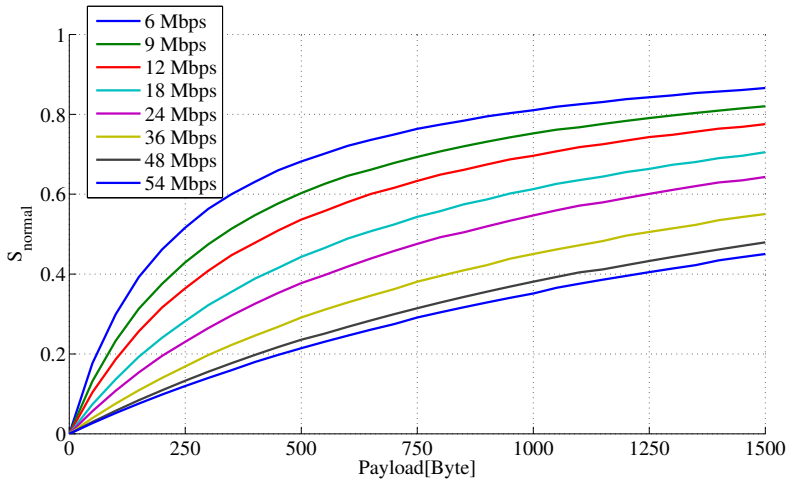

Figure 5: Normalized throughput for 802.11a [iee12]

3.1.2. Maximum saturation throughput with contention

The last section described a situation where only one station is transmitting packets without any contention (with other stations or an Access Point (AP)). In the case of contention with other participants on the network, the situation is much more complex. Each station holds their own back-off state independently from the other stations but dependent on the previous events on the medium as described in section 2.1. This state consists of different variables like the existence of a Head-of-line (HOL) packet, the current back-off value and the number of retries leading to a large state space inside an ad-hoc cell. In [Bia98, TBS04] it has been proven that elementary analytical techniques are sufficient for describing the work of the Distributed Coordination Function (DCF) inside these cells. The main ideas of these techniques will be described in this section and the necessary, more complex models will be summarized in section 3.2.

The *saturation throughput* represents the maximum load that the system can carry under stable and practical conditions. For a single transmitting station this equals $S_{Station}$ (cf. equation (9)). In case of several stations competing for the medium the situation is different [Bin08]. At saturation throughput, every station always has a packet waiting to transmit. In [Bin08, p. 69] an additional definition of the saturation case is provided as the author describes "the practical impossibility to maintain a sustained operation of DCF or EDCA at any load greater than the saturation throughput", which therefore defines the maximum achievable capacity per link. An 802.11 long-distance point-to-point link is in high-load conditions bounded to this maximum capacity as well. The maximization of this capacity will be one of the main issues of this work.

The following defines an analytical approach to determine the maximum saturation throughput for an 802.11 ad-hoc network with N stations competing for the channel access [Bin08, TBS04]. For this analytical approach some basic observations are obligatory. These observations rely on three different assumptions which are presented first:[19]

- One or more stations are in a saturation condition so that at least one packet is always available for transmission.
- A frame is never corrupted due to bad channel conditions.
- The transmission only fails when at least two stations pick the same slot for transmission.

Under these circumstances the possibility to model the DCF with elementary techniques mainly relies on two basic observations.

The first important observation is the possibility to introduce a discrete-time scale which is key for all following analysis. As already described in section 2.1.1 a station is only allowed to transmit a frame in a slot during the back-off procedure and after the idle time of a DIFS has elapsed. This results in a limited number of possibilities to start for every station. Moreover, the size of these slots is fixed by the slot time hereafter indicated as σ.

The second important observation is that there are only three different events occurring on the channel under the above defined assumptions. All three events can be linked to a probability for the event to occur and with an according busy time on the medium.

1. When exactly one station schedules a transmission in a back-off slot the communication will be successful. The other stations will freeze the back-off counter and wait for the transmission to take place including the upcoming IFS and the ACK: $P_{success}$ and T_s for the probability and the time respectively.
2. When two or more stations start a transmission in the same slot, a collision will occur. The medium will be unavailable for the transmission time of the longest frame as well as an EIFS: $P_{collsion}$ and T_c.
3. If no station transmits during the current slot, the slot time will elapse without any action: P_{idle} and σ.

Summarizing both observation leads to the possibility of three different and random events occurring in a slotted and discrete time scale. The size of this model slot is different from the slot size (σ) and varies for each event occurring (T_s, T_c, σ). This will be quantified later in this section.

[19] Some of these assumptions will be reversed later.

To determine the maximum throughput inside an 802.11 ad-hoc cell composed of N different stations, we begin by specifying the probabilities $P_{success}$, $P_{collsion}$ and P_{idle}.

[Bia98] first showed that each station picks a slot with a **constant probability** τ for a transmission, randomly and independently of the other stations. This valid assumption corresponds to one of the four known Carrier Sense Multiple Access (CSMA) access modes: p-persistent[20]. With this single probability it is possible to specify all probabilities corresponding to the contemplated events. The probability that none of N different stations uses a slot to transmit is equal to

$$P_{idle} = (1-\tau)^N. \tag{15}$$

Similar, the probability that just one stations picks a slot for transmission is equal to[21]

$$P_{success} = N\tau(1-\tau)^{(N-1)}. \tag{16}$$

As there are only three possible events in this model, the converse probability defines the last variable

$$P_{collsion} = 1 - P_{idle} - P_{success}. \tag{17}$$

After defining the probabilities for each event the according times need to be specified. For the idle case the duration is equal to the physical layer slot time (σ). For the case of a successful transmission (T_s), this duration is the period where no other station has the chance to access the channel. This duration includes the transmission of the MPDU as well as the mandatory IFSs and the ACK ,where T_{MPDU} and T_{ACK} are already defined through equation (11) in the previous section.

$$T_s = T_{MPDU} + SIFS + T_{ACK} + DIFS \tag{18}$$

$$T_s = T_{Frame} + DIFS \tag{19}$$

For the case of a collision an additional assumption is needed. When frames collide because several stations are randomly picking the same slot, the medium will be unavailable for the transmission time of the largest frame. In this model all frames are assumed to have the same size which is statistically possible by using the average frame size. The duration of T_c can be defined as

$$T_c = T_{MPDU} + EIFS. \tag{20}$$

Using the three specified probabilities in combination with the durations for every event it is possible to calculate an average slot duration. Note that this is the mean model slot

[20] 1-persistent, p-persistent, Non-persistent and O-persistent.
[21] Note that we correct an obvious mistake made in [Bin08].

and not the physical layer specific slot (σ) occurring during the back-off interval.

$$E[slot] = P_{idle}\sigma + P_{success}T_s + (1 - P_{idle} - P_{success})T_c \tag{21}$$

The maximum saturation throughput can now be defined as the average amount of information transmitted in a slot using $E[P]$ as the average MPDU size.

$$S = \frac{P_{success}E[P]}{E[Slot]} = \frac{P_{success}E[P]}{P_{idle}\sigma + P_{success}T_s + (1 - P_{idle} - P_{success})T_c} \tag{22}$$

The outcome of this equation strongly depends on the constant transmission probability τ which donates that a specified station transmits in a slot. For a complete view of the ad-hoc cell, this parameter defines the probabilities $P_{idle}, P_{success}$. In addition to that, τ strongly depends on the number of stations inside the cell, the values for the Contention Window (CW) and the maximum retry limit of a frame.

If DCF did not double the Contention Window after a collision ($CW = CW_{min} = CW_{max}$) the calculation of the parameter would be obvious. The value for τ would then be fixed to

$$\tau = \frac{1}{1 + \frac{CW}{2}}. \tag{23}$$

hence a transmission occurs statistically every $1 + \frac{CW}{2}$ slots. For small values of CW and many stations this would lead to a high number of retransmissions decreasing the throughput inside the cell. Since this is not the case, because DCF exploits an exponential back-off scheme and doubles the value of CW after each unsuccessful transmission, complex modeling is needed to determine the key parameter τ.

3.2. Analytical MAC Layer models

Having described the main idea of throughput calculation inside 802.11 ad-hoc cell with numerous stations contenting for the medium, the identification of the parameter τ still needs to be addressed. This identification of the parameter was studied by numerous researchers over the past years, known as MAC layer modeling of IEEE802.11. This section tries to provide the reader with an appropriate state of the art about this field of research. It is out of the scope of this thesis to explain every modeling technique in detail but the reader is invited to use this summary, especially the provided tables, as an overview for further research.

Besides describing different modeling approaches in general, a focus will be on their assumptions, trade-offs and how these influence further considerations for the use case of point-to-point links. The last part of this section will focus on publications specifically dealing with the topic of optimizing long-distance links. Accumulating both fields of research defines the border for further considerations and concludes the state of the art section.

3.2.1. Origin of the models

After the first IEEE802.11 standard was published in 1997, several researchers focused on developing models for the 802.11 MAC layer. Two different models, both using a different mathematical background, prevail against others due to their accuracy. Bianchi [Bia98, TBS04, BT05] published the first iteration of his model based on Markov chains in 1998. In parallel, Cali et al. developed a model which is based on geometric distributions [CCG98, CCG00].

Bianchi exploits a two dimensional Markov chain model to obtain the parameter τ. The first dimension describes the stochastic process representing the back-off time in a finite and discrete way by setting the time scale in a slotted way. The second dimension describes the current back-off-stage of the station, namely how many retries the HOL-packet has already done. The model assumes a saturated state and ideal channel conditions and there is no provision for limiting the number of retransmission. Calis' approach is based on geometric distributions [CCG98] and a computation of the average contention window size depending on the number of stations in a cell. With this average CW size the collision probability (p)[22] is calculated and the throughput is approximated by a ratio of MPDU transmission time (m) and overall time on the medium for a frame (t_v).

3.2.2. DCF

Several papers were published to further improve the accuracy or to provide the possibilities to remove some of the initial assumptions. In the following a very short summation of the most important publications reviewed is presented.

In 2004, Bianchi published a further enhancement of the Markov chain model and titled it as a revision of his previous publication [TBS04]. He showed that the DCF can be modeled utilizing conditional probabilities (instead of Markov chains) and also included the possibility to limit the maximum retransmission count [TBS04]. The model is defined independent of the underlying back-off sequence, which provides the possibility to account for other schemes than the standard exponential one. With simple changes in the probability and throughput calculation presented in the last section, this model is also capable of accounting for non-ideal channel conditions, which is an important factor for long-distance point-to-links because the chance of erroneous packets is generally higher. Several authors have stated this revision of the original paper as the current best approach for modeling DCF [Bin08].

[22] Which is directly linked to the contemplated parameter τ [HD05].

By adding a post-back-off state modeled as an M/G/1[23] queue, [CNB+00] extends Bianchis original model to account for finite load and compare it against real measurements instead of simulations. A model also taking finite load into account but still assuming ideal channels conditions is presented in [ASS03]. [YWA05] introduced another way to take account of non-ideal channel conditions and focuses on finding an optimal relationship between packet error rate, CW and packet-size. [DV05] reached some similar results in parallel by extending Bianchi's original model for lossy channel conditions. To account for a finite transmission buffer, [LSC10] extended the 2D Markov chain with an additional dimension to model the buffer. However, this model still assumed ideal channel conditions and the calculations are expensive.

Table 4 provides a summarization and the current state of the art regarding publications for modeling the Distributed Coordination Function (DCF).

Table 4: State of the art of analytical models for the DCF

Publication	Assumptions		Metric		Validation		Origin	
	Saturated	Ideal channel	Throughput	Delay	Simul.	Experim.	Cali	Bianchi
[Bia98]	✓	✓	✓		✓			X
[CCG00]	✓	✓	✓		✓		X	
[TBS04]	✓		✓	✓	✓			✓
[CNB+00]		✓	✓	✓		✓		✓
[ASS03]		✓	✓		✓			✓
[YWA05]	✓		✓	✓	✓		✓	
[DV05]	✓		✓		✓			✓
[LSC10]		✓	✓	✓	✓			✓

3.2.3. EDCA

As already theoretically described in section 2.1.2, the Enhanced Distributed Coordination Access (EDCA) first introduced by the IEEE802.11e standard extends DCF for QoS provisioning. Several publications have extended Bianchis approach for the DCF, still using the basic Markov chain. In [RR04] an average collision probability p is calculated weighting the different AC and considerations about post-collision contentions to improve the accuracy. A similar approach can be found in [MHW03]. A three dimensional Markov model, that is capable of predicting the delay, is used in [KTBG04]. The extension of Bianchis model in [EO05] eliminates all assumptions and uses a virtual z-transformation to calculate the delay. However, the calculations are very expensive. [BV05] is the only known extension of Calis' model for EDCA which is only

[23] A queuing model where arrivals are Markovian, service times follow a general distribution and there is a single server.

capable of calculating the delay with both assumptions enabled. An interesting approach is found in [HD05], presenting a unified model combining the two original approaches [Bia98, CCG98] and explaining the similarities between them as well. As already performed for the DCF case, table 5 provides a summary of the most important modeling approaches for EDCA.

Table 5: State of the art of analytical models for the EDCA

Publication	Assumptions		Metric		Validation		Origin	
	Saturated	Ideal channel	Throughput	Delay	Simul.	Experim.	Cali	Bianchi
[RR04]	✓	✓	✓		✓			✓
[MHW03]	✓	✓	✓		✓			✓
[KTBG04]	✓	✓	✓	✓	✓			✓
[EO05]			✓	✓	✓			✓
[BV05]	✓	✓			✓		✓	

3.3. Long distance 802.11 MAC layer

The purpose of this section is to describe the state of the art of optimizing MAC layer parameters for long-distance point-to-point links. All publications about the different analytical models presented in section 3.2 focus heavily on the modeling aspect instead of optimization. The applicability refers to infrastructure scenarios rather than point-to-point links. None of them accounts for the propagation delay of long-distance links, which is an important factor as described in section 2.2.2. A few publications start with considerations about how to optimize the 802.11 MAC layer in the context of WiLDs. These publications will be summarized in the following to describe the current state of the art in this special field of study and to provide the starting points for further research.

The first publication dealing with the impact of distances on the DCF was written by Leung et al. [LMCW02] in 2002. Their research focuses on the feasibility of 802.11b DSSS as an alternative to 3G cellular networks in urban areas instead of the optimization for long-distance point-to-point links. In fact, the propagation delay is considered as an addition to all timings (e.g. the transmission time and the busy channel time). This model is capable of describing the influence of distance and different packet sizes to the normalized saturation throughput. The modeling of the back-off procedure is carried out via an aggregated Poisson process with a fixed packet rate defined in packets per μs. This rate summarizes the contribution of all contending stations. However, it refuses access to different MAC parameters and therefore to a detailed optimization. Nevertheless, the conclusion of this paper is that the MAC throughput is still satisfactory despite the increased propagation delay. This statement is confirmed by our experiments as presented in [Rad11, RKJ13].

Salmerón et al. compare in [SSN08] two different MAC protocols for 802.11 based long-distance links - an optimized version of the CSMA/CA protocol and a Time Division Multiple Access (TDMA) based MAC approach. They conclude that the throughput is nearly identical with both approaches, but the TDMA based solution suffers from high and constant delay mainly due to imprecise time synchronization leading to large time slots. Besides the known adaption of CSMA/CA[24] described in section 2.2.2 experiments with different values of CW_{min} have been done. By exploiting a PropSim C8 wireless channel emulator the influence of CW_{min} on different link distances is evaluated. The authors show that there is an optimal value of $CW_{min} = CW_{opt}$ depending on the link distance. In fact, with an adapted slot time according to the propagation delay, the value for CW_{opt} decreases with an increasing link distance. The throughput gain due to the optimized values increases with link distances in their experiments. For distance larger than 15 km the gain in throughput and QoS is nearly 50 %. However, a fixed modulation of 11 Mbps and a fixed packet size of 1500 Bytes is used which limits the results. Because of the utilization of a simulation rather than the development of a general model, it is not possible to reproduce these results for different link parameters. Traffic differentiation through variant values of AIFS is also not considered.

Simó-Reigadas et al. [SMFRLSP10] propose a model for the IEEE802.11 DCF for long distances as well as some optimizations of the parameters CW_{min} and the slot time. The main considerations are made about large WMN with numerous nodes operating on the same frequency and large, variable distances in-between. Their model is based on Markov chains and takes the propagation delay as an additional factor for the transmission timings and during the back-off into account. Both known assumptions about ideal channels and saturated traffic conditions apply for their model. The assumption of ideal channel conditions is especially questionable in case of long-distance point-to-point links. One fact that justifies their approach is that for long links the round trip time is equal or even larger than the slot time. This leads to collisions when stations pick the same as well as adjacent slots for transmission. Especially with different distances in between nodes the situation is complex. However, their modeling approach is not suitable for the point-to-point links case because of two main reasons.

1. The model is justified for N stations with full visibility among them and large distances in between and a good accuracy of the modeling approach is only given at a large number of stations. This assumption hold not for real world deployments especially not for the WiBACK case. To overcome large distances using 802.11, high gain directional antennas are needed leading to a visible subset of stations only in common topologies[25]. In the WiBACK case this subset is reduced to two stations because of the usage of different frequencies for adjacent links.

[24] As the increased slot time and ACK timeout.

[25] An exception is represented by networks with a star topology on the same frequency.

2. One assumption is the correct adjustments of the ACK timeout (cf. equation (6)) according to the distance while the slot time is still variable. In the current implementation of common hardware and Open Source Linux-drivers[26], an adaption of the ACK timeout always applies an adjustment of the slot time as well.

Simó-Reigadas et al. also consider the point-to-point case, which simplifies their approach dramatically . The propagation delay is now equal between the two stations and the model is now close to the one presented originally by Bianchi [Bia98]. For this case the authors perform an optimization successively with two parameters: slot time and CW_{min}, keeping one respectively to the IEEE802.11b standard value. An optimization using the slot time needs to be evaluated critically. As described in section 2.2.2 the slot time defines the basic timing for all other IFS and for the case of long-distance links it needs to be adapted to provide the carrier sense function with a possibility to detected an ongoing transmission in the current slot. This was found by the authors as well they conclude that an optimization through the CW_{min} parameter should be considered first "because it adapts more integrally to the CSMA/CA protocol" [SMFRLSP10]. A differentiation between packet sizes and different modulations is not considered in their work and they only consider the outdated IEEE802.11b standard.

The last important publication in the field of study prior to this thesis was written by Salmerón et al. [RMSS07] and provides first guidelines for the usage of EDCA for rural 802.11 long-distance links. This paper seems to be unpublished so the results need to be scrutinized. It contains some interesting ideas which are worth considering. The authors of this paper apply a constant value for CW_{min} leading to a constant value for the transmission probability $\tau = \frac{2}{CW+1}$. This constant value for τ along with some other approximations provides the mathematical opportunity to define a simple function for the throughput dependent on CW and the link distance. Through derivation, this function can be maximized, determining the optimal value of CW. Especially for small values of CW_{min} the approximation of a constant CW value, which completely leaves out the back-off process, does not hold since it does not account for any collisions. The other values the authors tried to exploit are TXOP (TX-opportunity) and AIFS. They conclude that the optimal value for CW should be used for all traffic classes and that the usage of different values for AIFS provides a good possibility for traffic class differentiation as defined by the standard. The $TXOP$ value provides an opportunity for frame aggregation leading to a higher throughput as well as the possibility for asynchronous capacities on the link for a specified traffic class.

[26] Referring to the Atheros drivers for Linux wireless ath9k and ath5k.

4. Methodology

After describing the current state of the art of modeling the 802.11 DCF as well as different approaches for long-distance links, this section will start by defining and justifying the need for another advance in this field of study. Afterwards, the reasons for the model selection and the model itself are presented in detail. The realized adaptations of the model to account for long-distance point-to-point links are described in the next part. Details about the used WiFi links as well as the implementation provides the reader with the important facts and the background needed for understanding and reproducing the experiments and results.

4.1. Approach and methodology justification

To enlarge upon the different approaches of modeling and optimizing of WiLDs presented in section 3, this paragraph aims at pointing out the need for an additional research in this field of study.

None of the evaluated publications compare their modeling approach systematically against a real-world deployment. The comparison between a mathematical model and a simulation tool (like the NS-2) is questionable for using the results for optimization since their correlation is not proven. In fact, several publications focused on the discrepancies between simulations and real-world testbeds and found partly huge gaps in the results of throughput and delay [TWCM10, KNG+04]. Since the result should be used to increase the user experiences and the Quality of Service (QoS) of real deployments, a model evaluation on identical hardware in comparable conditions should be carried out.

While several authors focused on the mathematical intricacies of their modeling approaches, just a few of them used their results for optimization. A remarkable fact is that in all publications the value of CW_{min} is increased compared to the value of the standard which is sensible in the case of several stations in an ad-hoc cell. For the optimization of point-to-point link a decrease of this parameter should be considered as well, since there are just two contenting stations and the decrease of the idle time generally leads to a higher possible throughput.

None of the publications about modeling and MAC optimization of long-distance WiFi links [LMCW02,SSN08,RMSS07,SMFRLSP10] systematically justified their modeling approach for different use cases. While diverse distances are usually taken into account, the influence of different modulations and payload sizes is not evaluated yet, which bounds the results to a certain subset of traffic and link parameters. The contemplated

publications used the 802.11b standard which leads at some point to easier calculations. However, this standard is outdated by now and replaced by 802.11g, 802.11a and - for the usage of high-throughput - the next generation wireless standard 802.11n.

4.2. Model selection and description

This section consists of two parts. At first, the selection process for an appropriate modeling using the evaluated publications will be described. Afterwards, this chosen model is delineated.

4.2.1. Model selection

Having evaluated several modeling approaches in section 3.2, one of these needs to be selected to estimate and optimize WiLD links. After carefully evaluating the publications, the revised approach based on conditional probability by Bianchi [BT05] (as an extension to his original approach) was selected because of the following reasons:

- Several authors described this approach as one of the most accurate [Bin08].
- The model based on conditional probability is comparably easy to understand and follows a clear structure. Other approaches suffer from poorly defined equations and assumptions.
- The complexity of the chosen approach is predominantly determined by the solution of a single non-linear equation. This leads to a potential implementation and recalculation of parameters on less powerful hardware, like a router. This is especially useful if a huge variation of the optimum parameters will be found. Other modeling approaches require a complex solution to more dimensional Markov chains for example, requiring powerful processing capabilities [LSC10].
- Compared to other publications [SMFRLSP10], the chosen approach clearly defines all variables and makes them accessible for changes. This accessibility provides the possibility to adopt the approach to long-distance point-to-point links, different iterations of the standard or possible deviants due to the specifics of the Linux implementation - mac80211 [Ber09].

Choosing this model clearly comes with a compromise. It was original designed to be used with the Distributed Coordination Function (DCF) instead of EDCA. However, some authors [Bin08] provide suggestions on how to adopt this approach to account for different traffic classes, which will be pursued and extended in later sections.

4.2.2. Model description

After describing the modeling-basics in section 3.1.2, the parameter τ still needs to be specified. To quantify this parameter the following provides a summary of the chosen modeling technique based on conditional probability. For further details, the reader is referred to the original paper [BT05].

As explained in section 2.1.1, a station doubles its CW value for the upcoming retransmission after a collision occurs until CW_{max} or the retry limit (R) is reached, in which case the frame is dropped. The probability for a station to accesses the medium mainly depends on the current number of retransmission for the HOL packet and the CW_{min} value. Every other station in contention for the medium will retain their own back-off state depending on the status of the current HOL packet. Instead of analyzing each station in a particular moment, which would lead to a large state space (difficult to handle[27]) the contribution of all stations is aggregated. This aggregation is suitable for a stationary condition (saturation throughput) and leads to a constant permission probability τ. A more formal way to phrase this aggregation leads to the following assumptions as presented in [Bin08]:

1. Each frame transmission suffers from a constant and from the history of the HOL packet independent collision probability (p).
2. The collision probability (p) is calculated as the contribution of N-1 remaining stations, each accessing a channel slot with a constant permission probability τ.

The parameter τ accounts with a single value for all presented rules of the Distributed Coordination Function (DCF).

The term back-off-tage is used to describe the number of retransmission the HOL packet has already suffered. A new MPDU arriving at the head of the queue will always be transmitted in back-off-stage zero. In this stage (i=0) the back-off value is drawn from a random distribution B_0. If the packet collides, the next value will be drawn from the distribution B_1 and in general, after i retries from the distribution B_i.

The term "TX" donates that the station is transmitting a frame and $s = i$ correspond to the case that the station is found in back-off-stage i.

The following equation (24) exploits Bayes' Theorem and defines the probability for $\tau = P\{TX\}$ taking the back-off-stage into account

$$P\{s = i|TX\} = \frac{P\{TX|s = i\}P\{s = i\}}{P\{TX\}}, \quad \forall i \in \{0,..,R\} \tag{24}$$

[27] Even for two stations.

which is equal to

$$P\{TX\}\frac{P\{TX|s=i\}}{P\{s=i|TX\}} = P\{s=i\}, \quad \forall i \in \{0,..,R\} \tag{25}$$

and since this is defined for all $i \in 0,...,R$ a summation can be applied on both sides.

$$\sum_{i=0}^{R} P\{TX\}\frac{P\{TX|s=i\}}{P\{s=i|TX\}} = \sum_{i=0}^{R} P\{s=i\} \tag{26}$$

This summation is useful since the right term of the equation is a probability distribution that a station is found in back-off-stage i. The summation over all values of R (all back-off-stages) sums up to 1 since a station is always found in a back-off-stage. After rewriting the equation the following term for τ can be observed:

$$\tau = P\{TX\} = \frac{1}{\sum_{i=0}^{R} \frac{P\{s=i|TX\}}{P\{TX|s=i\}}}. \tag{27}$$

This equation provides the first definition of the desired parameter τ, the constant transmission probability of a station in a slot. However, it is still linked to the successful expression of $P\{s=i|TX\}$ and $P\{TX|s=i\}$ which will be described in the following.

The conditional probability that a transmitting station is found in back-off-stage i can be described by two different approaches, both leading to the same results [28].

A first way to define this probability is provided by the concept of geometric distributions. In general there are two different types of geometric distributions [Pit95]: One accounts for the number of Bernoulli trails needed to get one success. The second (used here) describes the number of failures (k) before the first success occurs with a constant *success probability* q and is given in the following equation:

$$Pr(Y=k) = (1-q)^k q, \quad \forall k \in \{0,1,...\}. \tag{28}$$

In this case of DCF the probability that a collision occurs in the back-off-stage i is defined as the constant[29] probability p. This leads (for the general geometric distribution) to $q = 1-p$ and to

$$P\{s=i \cap TX\} = (1-p)p^i \tag{29}$$

for the DCF case. In other words, the probability for i collisions before a successful transmission takes place or the *joint* probability that a station transmits in back-off-stage i.

[28] These two possibilities are linked to the two original publications by Bianchi and Cali.
[29] Note that this is one of the assumptions defined earlier.

Since the goal is to describe the conditional probability $P\{s = i|TX\}$ that a transmitting station is found in back-off-stage i, $P\{TX\}$ still needs to be expressed. For the case of finite values of R this is possible by following equation

$$P\{TX\} = 1 - p^{R+1} \tag{30}$$

since p^{R+1} is the probability that packet is ultimately dropped after the finite number of retries and is therefore not transmitted. Using the theorem of conditional probability[30] this leads to the desired equation

$$P\{s = i|TX\} = \frac{(1-p)p^i}{1-p^{(R+1)}}. \tag{31}$$

The second way of defining $P\{s = i|TX\}$ is through the usage of Markov chains. The complete mathematical details can be looked up in [BT05] and are skipped in this work. The equation (31) is a steady state probability distribution of a one-dimensional Markov chain describing the back-off-stages [Bin08]. This chain is schematically pictured in figure 6. A Markov time step in this chain represents a transition either to a higher back-off-stage (with the collision probability p) or back to the first back-off-stage, with the converse probability 1-p or 1 for the last stage.

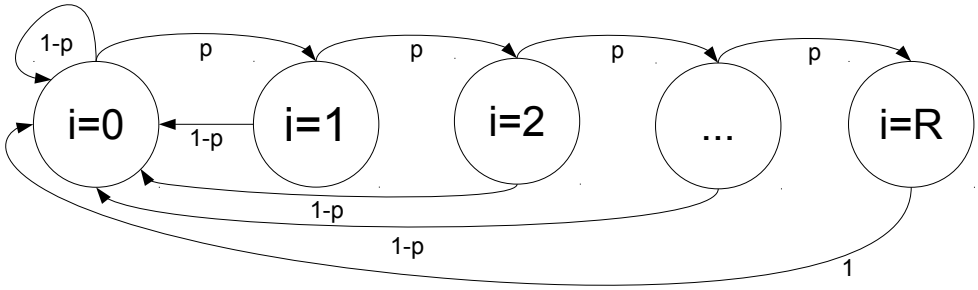

Figure 6: Markov chain for the back-off-stage transition

The second probability needed for the expression of τ is $P\{TX|s = i\}$ which describes the transmission probability of a station inside back-off-stage i. The expression of this probability is straight forward by putting the transmission slots (which equals in this case 1) into perspective with the overall number of back-off slots of the current stage (B_i) [BT05].

$$P\{TX|s = i\} = \frac{1}{1+E[B_i]} = \frac{1}{1+\beta_i}, \quad \forall i \in \{0,..,R\}. \tag{32}$$

[30] $P(A \mid B) = \frac{P(A \cap B)}{P(B)}$.

In the case of DCF, $E[B_i] = \beta_i$ represents a uniform selection of the parameter from zero to CW_{min} of the current back-off-stage. To model the doubling of the CW_{min} parameter after an unsuccessful transmission, β_i is mathematically described as

$$\beta_i = \frac{2^i * W - 1}{2}, \quad W = CW_{min} + 1. \tag{33}$$

Finally an equation for τ can be obtained by substituting the equations (31) and 32 into equation (27) leading to [BT05]

$$\tau = \frac{1}{1 + \frac{(1-p)}{1-p^{(R+1)}} + \sum_{i=0}^{R} p^i \beta_i}. \tag{34}$$

This important equation (34) defines the probability that a station randomly and independently picks a slot for transmission, depending on the collision probability p. The probability p on the other hand just depends on the probability τ and is defined in the following equation (35).

$$p = 1 - (1 - \tau)^{N-1}. \tag{35}$$

This equation accounts for the case when (besides one transmitting station) at least one of the remaining N-1 stations transmits a frame in this slot as well, which is carried out with the same constant permission probability τ [31].

The equations (34) and (35) describe a system of two non-linear functions with two unknowns which can be solved using numerical techniques[32] [Bin08].

4.2.2.1. Throughput estimation

So once the value for τ is calculated it is possible to use equations (15) (P_{idle}), (16) ($P_{success}$) to calculate the saturation throughput inside an 802.11 ad-hoc cell. The required equation (22) was described in a previous section for the saturation throughput.

$$S = \frac{P_{success} E[P]}{E[Slot]} = \frac{P_{success} E[P]}{P_{idle}\sigma + P_{success} T_s + (1 - P_{idle} - P_{success}) T_c} \tag{22}$$

The values for T_s and T_c have been defined through equations (18) and (20) respectively. To calculate and picture different dependencies the model introduced by Bianchi was implemented utilizing MATLAB [MAT13]. More details about the implementation are given in section 5.

In the following, some basic plots showing the throughput performance of the 802.11a-DCF under different conditions are presented. The purpose of these plots is to provide

[31] Note that this probability is different from T_c described above due to different time scales.
[32] We utilize the root of non-linear functions.

the reader with a general idea about the capabilities of the modeling approach as well as illustrating some general connections between different parameters before proceeding with the adaption of the modeling approach to WiLD links.

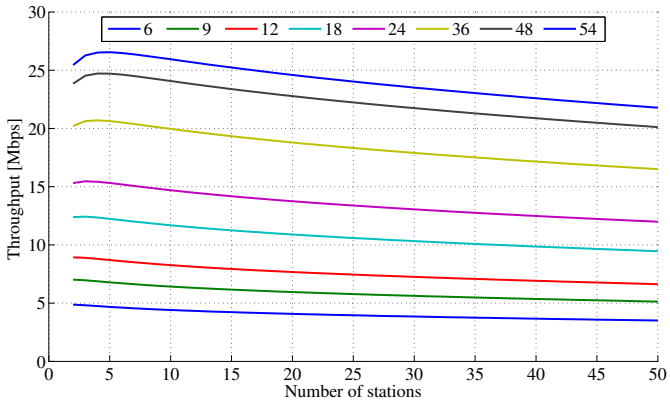

Figure 7: Saturation throughput 802.11a (Modulations in Mbps)

Figure 7 shows the *overall saturation throughput* inside an 802.11a ad-hoc cell for different modulations and an increasing number of stations, while assuming a payload size of 1450 Bytes. Overall, the saturation throughput decreases with an increasing number of stations for all modulations. Initially and for a few stations (< 5), the overall throughput for the ad-hoc cell increases, especially for the higher modulations. This effect is attributed to a decreasing idle time on the medium (mainly during the back-off) because more stations apply for a transmission. For a low number of stations, this decreasing idle time has a bigger effect on the throughput than the increasing probability for a collision. For a small payload this effect is even stronger since T_{Frame} is smaller.

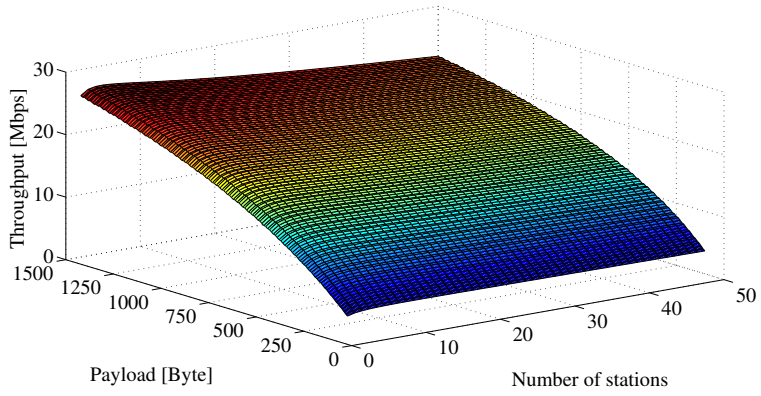

Figure 8: Saturation throughput for different payloads 802.11a

Figure 8 pictures the general relationship between the number of stations, the size of the payload and the maximum saturation throughput. It is observable that the size of the payload has a bigger influence on the maximum throughput than the number of stations. The influence of the maximum throughput decrease for an increasing number of stations is higher with an increased size of the payload, mainly due to the longer duration of a collision T_c.

4.2.2.2. Non-ideal channel conditions One disadvantage of the described model by Bianchi [BT05] is the assumption of ideal channel conditions. This assumption can easily be withdrawn as shown in [Bin08].

The parameters ζ is now defined as the probability that a transmitted frame is corrupted because of noisy channel conditions instead of collisions with other contending stations. This parameter equals the Packet Error Rate (PER) on a wireless channel. A station will not receive an acknowledgement either if a collision due to the back-off procedure occurs, or the frame was corrupted by channel noise. The conclusion is to include ζ into the calculation of the conditional collision probability p leading to a refined version of equation (35):

$$p = 1 - (1-\zeta)(1-\tau)^{N-1}. \tag{36}$$

The probability p describes now the cases in which a frame collides *or* is corrupted. The calculation for τ is not directly affected so equation (34) is still valid. However, the parameter ζ needs to be included in the calculation of the saturation throughput. This adjustment leads to the following definition of S:

$$S = \frac{(1-\zeta) * P_{success} E[P]}{P_{idle}\sigma + (1-\zeta)P_{success}T_s + \zeta * P_{success} * T_e + (1 - P_{idle} - P_{success})T_c}. \tag{37}$$

A new value T_e takes account for the case that a corrupted frame is currently transmitted on the channel and no other station can access the medium. It is calculated as:

$$T_e = T_{MPDU} + EIFS. \tag{38}$$

A station which detects the corrupted frame will wait for the interval of an Extended Interframe Space (EIFS). Again, there are several possible causalities to analyze with this extension.

Figure 9 provides one example picturing the influence of noise on the saturation throughput for a fixed modulation of 54 Mbps along with a large payload. The influence of corrupted frames due to non-ideal channel condition is almost linear for all payload sizes at least for the higher modulations. This linearity can be used for fast approximation purposes on non-ideal channel conditions.

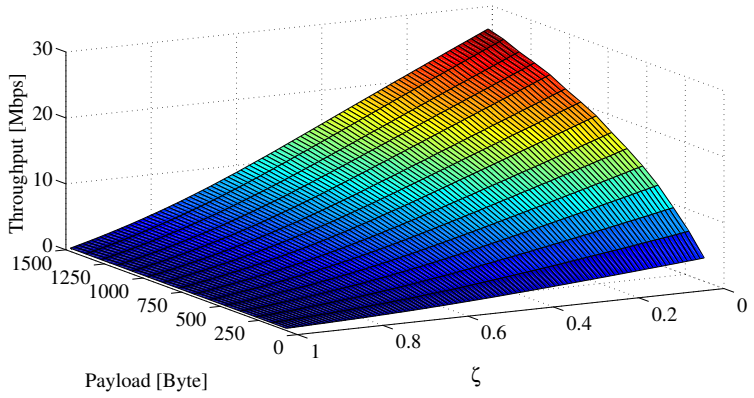

Figure 9: Saturation throughput and non-ideal channel conditions

4.2.2.3. Delay estimation Besides the throughput another important Quality of Service (QoS) factor is the delay of a packet. Therefore an estimation of this parameter is mandatory as well. The visualized modeling approach offers an easy and intuitive way to estimate the average *access delay* of a packet. In [Bin08] this delay is defined as the elapsed time between the frame becoming head of line of the transmission queue and its successful delivery. To determine this average access delay it is possible to use "Little's law" [Ser99]. With its origin in the queuing theory, this law is commonly used in operations research as indicated by its definition. A common definition is provided in [HS11] where the law is stated as

$$TH = \frac{WIP}{CT}. \tag{39}$$

The author defines throughput (TH) as "the average output of production process per unit time," work in process (WIP) is "the inventory between the start and end points of a product routing" and cycle time (CT) as "the average time from release of a job at the beginning of the routing until it reaches an inventory point at the end [...]"[33]. The application of this law to prognosticate the average access delay leads to the following equation, as described in [Bin08]:

$$D = \frac{N}{S/E[P]}. \tag{40}$$

The relationship to the original definition of the law is given by the following translation: The access delay (D) corresponds to the cycle time, the number of nodes inside the cell corresponds to the work in process and the fraction at the denominator represents the throughput (TH) measured in frames per second. This method of calculation is only precise for an infinite retry case [Bin08]. For the finite retry case of frames, the delay

[33] Note that this is not the original definition of the law but the transformation is widely known. The original law stated out that the average number of customers in a system L equals the long-term average arrival rate λ multiplied by the mean time a customer spends on the system W [Ser99].

calculation should only account for successfully transmitted frames and exclude the ones discarded after reaching a maximum retry limit. To account for the finite retry case, [CBV05] found a possibility (while still utilizing Little's law) by exploiting the following equation:

$$D = \frac{N}{S/E[P]} - E[slot] * \frac{p^{(R+1)}}{1-p^{(R+1)}} * \sum_{i=0}^{R}(1+\beta_i). \tag{41}$$

This equation can be interpreted as follows [Bin08]. The first term still accounts for Littles' law and describes the time between two successfully delivered frames. This calculation accounts for frames waiting for a transmission but ultimately being dropped after reaching a certain retry limit are not considered. This time needs to be subtracted from equation (40) in the following way: The fraction in equation (41) defines the average number of dropped frames between two successfully deliveries. Each of this dropped frames passes all back-off-stages which is represented by the sum in equation (41). The sum multiplied by the fraction is weighted with the average modulation slot size as one of the three contemplated events which may occur between a successful transmission[34].

The elegant part of this modeling approach for the delay estimation is, compared to other publications, its simplicity. All needed values are already introduced by the throughput estimation, which makes the usage of another complex modeling approach for the delay expendable.

4.3. Model adaption for 802.11 long-distance links

The described modeling approach for 802.11 ad-hoc cells in the last sections is widely known and well validated against simulations. The goal of this thesis to estimate and optimize long-distance WiFi point-to-point links requires an adaption of this modeling approach. The adaption to the point-to-point case is simple by setting the number of contending stations to two. To utilize the selected model for long-distance WiFi links several changes are proposed in this section. These adoptions focus on applying the modeling approach to long-distance links by combining Bianchis version with the Medium Access Layer constraints of WiLDs (introduced in section 2.2.2). The main idea of this adaption is to increase all MAC layer timings by adding the propagation delay where needed. For this purpose additional functions need to be added to enrich the model. These functions calculate the propagation delay from a given[35] distance and add this additional timings

[34] It is important to not mistake this for the back-off slot size σ.

[35] The distance between two nodes in WiFi based Long Distance networks (WiLD) can be discovered by two different techniques:

1. Before setting up the network by utilizing Global Positioning System (GPS) coordinates.
2. In previous research we have already introduced a link calibration algorithm which is capable of determining the distance [KHB+12].

.

to the model approach where needed. The general calculation of the propagation delay (using the speed of light) and d for the distance in meter between both stations can be described as:

$$AirPropTime[\mu s] = \frac{d\ [m]}{300\frac{m}{\mu s}} \tag{42}$$

The standard [iee07] defines an adaption of the slot time according to the propagation delay in a non-continuous way by utilizing the so called coverage class.

$$CoverageClass = \left\lceil \frac{2 * d\ [m]}{300\frac{m}{\mu s}} * \frac{1}{3} \right\rceil \tag{43}$$

One additional step of the coverage class (cc) correlates to an extra distance of 450 m[36].

Since the assumption is that DCF operates for the back-off scheme similar to normal (non-long-distance) links the presented calculations for the back-off modeling (mainly to find the parameter τ in section 4.2.2) should apply for WiLD as well.

The throughput calculations presented in section 3.1.1 and 3.1.2 need to be adapted. The following presents an adaption of the MAC timings with the propagation time and the coverage class respectively. To account for long-distance links in the chosen approach, two main tasks need to be addressed. First, the adaption of the slot time for long-distance point-to-point links need to be included. The slot time is no longer considered as a fixed value defined by the standard or other modeling approaches, instead it changes dynamically according to the distance of link.

$$\sigma(d) = \sigma + 3 * cc \tag{44}$$

This redefinition of the physical slot time implies a change of all other used IFS for the model calculations as well.

$$DIFS = SIFS + 2 * \sigma(d)$$
$$EIFS = SIFS + DIFS + ACKTxTime(\sigma(d))$$

The second adaptation of the model for long-distance links is to include the propagation time as an addition to the existing transmission timings. It is important to differentiate in this case between the coverage class, used for enlarging the slot time, and the propagation time which is defined in a non-slotted way. This addition implies a redefinition of the three basic event timings of the model T_s, T_c and T_e.

[36] $\frac{3*cc*300[\mu s]}{2} = 450 * cc = \lceil d \rceil$

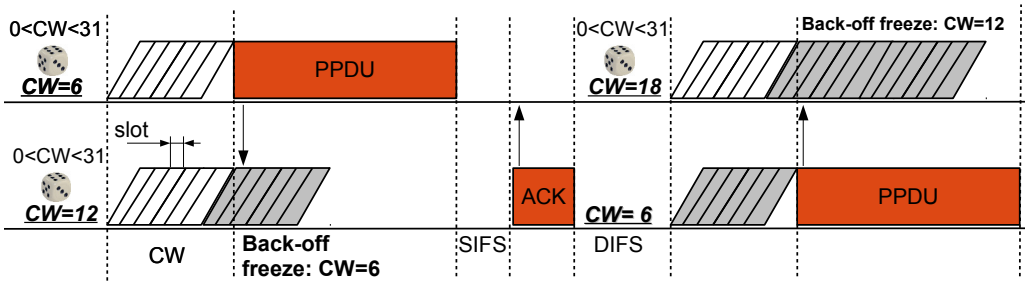

(a) Normal links

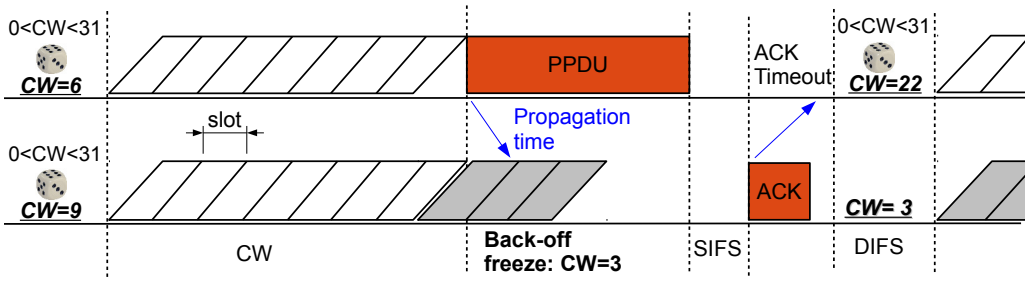

(b) Long-distance links

Figure 10: Distributed Coordination Function (DCF) operation

The propagation time needs to be added to each of the three basic timings *twice*. For T_s the propagation delay will occur for the transmission of the MPDU as well for the acknowledgement. The same applies indirectly for the timings T_c and T_e as well. A frame may not be decoded correctly due to a collision or interferences, however, the receiving station has to wait until the ACKTxTime has elapsed (EIFS) since it assumes a correct transmission may directed to another station. Figure 10 presents a schematic view on the general operation of DCF and the needed model adoptions for WiLD.

4.4. Model adaption for 802.11n

The 802.11n standard offers a radical increase in throughput by several changes to the physical and MAC layer as briefly described in section 2.1.3 and explicitly in a previous publication [RKJ13]. In the reminder of this section Bianchis modeling approach will be adapted to account for this standard in combination with long-distance point-to-point links. Instead of introducing a complete new modeling approach for 802.11n the goal of the following extensions is to reuse many parts from the 802.11a model. This proceeding introduces the possibility to have a unified modeling approach for 802.11a and 802.11n long-distance point-to-point links.

4.4.1. Physical layer extensions

The integration of the physical layer extensions into the chosen approach are possible by taking the different MCS into account. The generally higher MCS for 802.11n define more databits per OFDM symbol. These higher MCS result mainly from a better channel utilization of the allocated 20 MHz channel width by using an increased number of OFDM sub-carriers (cf. table 13 in the appendix). Another important throughput increasing feature is the bandwidth doubling to 40 MHz by bounding two adjacent channels. The possibility to include this is provided by multiplying each 802.11n MCS-rate with a constant factor of $\frac{108}{52}$. This fraction defines the relation for the increase of OFDM sub-carrier due to channel bounding.

As an extraordinary physical layer extension Multiple Input Multiple Output (MIMO) has been extensively described and successfully tested for the case of long-distance links in [RKJ13]. The inclusion of this technique into the approach is again possible by enlarging the MCS-rates. 802.11n MIMO in combination with spatial multiplexing introduces new MCS labeled from 8 to 15 for the two times two antenna case at sender and receiver.

The extension to MIMO implies a redefinition of the duration of the physical preamble. For MIMO, the 802.11n physical layer preamble is enlarged by several fields in different operation modes. A complete description of these Physical Protocol Data Unit (PPDU) formats is provided in the standard [iee12, p.1682] as well as in [Rec12, p.272]. For the case of point-to-point links the HT-Greenfield-Frame-Format is assumed. This PPDU format implies that only 802.11n stations are active in an ad-hoc cell in contrasts to the so called HT-Mixed-Frame-Format. In the greenfield mode an additional training field for every spatial stream is added to the preamble which provides predefined symbols to train the receiver for spatial multiplexing (cf. table 16 in the appendix). This additional field in the preamble enlarges the preamble time by 4 μs for every spatial stream.

4.4.2. MAC layer extensions - frame aggregation

Frame aggregation is the main 802.11n MAC layer extension. To include this into the modeling approach, several changes are needed. As delineated in [RKJ13] the current Linux implementation of the ath9k driver [Lin12] and the mac80211 [Ber09] only implements one of the standardized MAC layer aggregation techniques: A-MPDU. This technique aggregates completely formated MAC frames. The block ACK protocol is used to efficiently acknowledge sub frames through a bitmap. Several authors [TC05, Che12] propose ideas about modeling extensions for the Block ACK case. However, instead of evaluating the 802.11n MAC layer aggregation techniques the focus is on the 802.11e

transmission opportunity scheme which differs in many ways (cf. [Rec12]). A noticeable work of A-MPDU extensions is presented in [LW06] and defines the base for the following considerations.

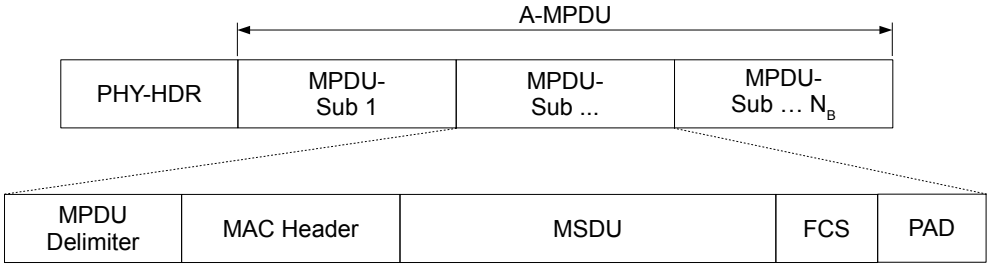

Figure 11: A-MPDU packet structure

The aggregation factor, described in the standard [iee12] as well is in the Linux driver implementation [Lin12], is controllable by defining the maximum number of aggregated Bytes represented through the following equation:

$$AMPDU_{max} = 2^{13+i} \quad \text{Bytes}, \quad \forall i \in \{-3,..,0,..3\}. \tag{45}$$

This leads to a maximum aggregation size between 1024 and 65536 Bytes, stepwise increased by the power of two. There is an important detail to consider which is not described yet in any publication found. Due to fairness considerations among stations the maximum transmission time on the medium for an PPDU shall not exceed a certain amount of time. For the current implementation of the ath9k driver this is limit is set to 4 ms. In contrast, the standard defines a maximum limit of 10 ms [iee07, p. 1762]. This limitation has a direct influence on the maximum possible A-MPDU factor especially for lower MCS. To calculate the number of aggregated packets in a block (N_B) the following equations hold

$$N_{\text{B-calc}} = \left\lfloor \frac{2^{13+i}}{PAYLOAD + L_{\text{MAC-HDR}}} \right\rfloor, \quad \forall i \in \{-3,..,0,..3\} \tag{46}$$

$$N_{\text{B-4ms}} = \left\lfloor \frac{4\ [\text{ms}] * \text{MCS}\ [\text{Bps}]}{PAYLOAD + L_{\text{MAC-HDR}}} \right\rfloor \tag{47}$$

$$N_B = \min(N_{\text{B-4ms}}, N_{\text{B-calc}}). \tag{48}$$

For convince of the reader table 14 and 15 in the appendix provide the maximum aggregation length due to the 4 ms limitation of the driver for the different MCS. The influence of this limitation is immense. The maximum aggregation factor is not available for any non MIMO MCS for 20 MHz and 40 MHz bandwidth alike. For the case of

a transmission of 1450 Bytes the following tables provide the values for N_{B-calc} (table 6) and N_{B-4ms} (table 7) to illustrate the huge influence of the 4 ms transmission limit. In both tables the columns define the MCS and the rows the A-MPDU factors alike. Note that for every cell the minimum value is taken as the number of aggregated frames (N_B). To add the A-MPDU aggregation technique to the modeling approach the transmission

Table 6: $N_{\text{B-calc}}$

	0	1	2	3	4	5	6	7
-3	**1**	**1**	**1**	**1**	**1**	**1**	**1**	**1**
-2	**1**	**1**	**1**	**1**	**1**	**1**	**1**	**1**
-1	**2**	**2**	**2**	**2**	**2**	**2**	**2**	**2**
0	5	5	**5**	**5**	**5**	**5**	**5**	**5**
1	10	10	10	10	**10**	**10**	**10**	**10**
2	21	21	21	21	21	21	21	**21**
3	43	43	43	43	43	43	43	43

Table 7: $N_{\text{B-4ms}}$

	0	1	2	3	4	5	6	7
-3	2	4	6	8	12	17	19	21
-2	2	4	6	8	12	17	19	21
-1	2	4	6	8	12	17	19	21
0	**2**	**4**	6	8	12	17	19	21
1	**2**	**4**	**6**	**8**	12	17	19	21
2	**2**	**4**	**6**	**8**	**12**	**17**	**19**	21
3	**2**	**4**	**6**	**8**	**12**	**17**	**19**	**21**

time needs to be enlarged to account for the longer overall frame length. This implies an adaption of equation (11) which is for convenience of the reader again given below

$$T_{MPDU} = T_{PREAM} + T_{PLPC} + N_{SYM}(L_{\text{MAC-HDR}} + Payload, MCS) * T_{SYM}.$$

A successful transmission now includes N_B frames which are in the contemplated case of A-MPDU completely formatted MAC frames with a delimiter in between (cf. figure 11). Equation (11) is redefined in the following way to take this into account

$$T_{MPDU} = T_{PREAM} + T_{PLCP} + N_{SYM}(N_B * (L_{\text{MAC-HDR}} + Payload + 4), MCS) * T_{SYM}. \quad (49)$$

The additional 4 Bytes represent the delimiter in this case.

To utilize the Block ACK protocol with the contemplated selective acknowledgement through a bitmap the length of the ACK increases for 802.11n. However, the increase of the length is less than proclaimed by the standard [iee12] or different publications [LW06]. The Linux mac layer implementation [Ber09] use a compressed version of this bitmap the which leads to an increase to 34 Bytes while other publications used a length of 58 Bytes [LW06].

The collisions due to identical back-off slots still lead to collisions of a complete block and therefore for a retransmission of all aggregated frames. The erroneous case is not valid anymore. For the case of 802.11a the parameter ζ accounted for the packet loss as a percentage. With the introduction of the selective retransmission using the Block ACK bitmap this parameter needs to be exchanged. As described in [LW06] the error case occurs when all the A-MPDU subframes become corrupted. To express this case, the Bit Error Rate (BER) after the Forward Error Correction (FEC) is used and described

through the probability BER. A single bit shift after the FEC leads to a wrong checksum and therefore to a detected error for a sub-frame. The probability that an error in all sub-frames occurred can be expressed as [LW06]:

$$\zeta = \begin{cases} (1-(1-BER)^{L})^{N_B}, & \text{for } N_1 = N_i \quad \forall i \in \{1,..,N_B\} \\ \prod_{i=1}^{N_B}(1-(1-BER)^{L_i}), & \text{else} \end{cases} \tag{50}$$

where L represents the overall length of an A-MPDU sub-frame in Bit. For typical values of $BER \approx 10^{-6}$ on a wireless link this probability is nearly negligible. However the strength of the block ACK is the selective retransmission which needs to be addressed in the model. To account for selective retransmission it is possible to redefine the average number of transmitted payload bits ($E[Payload]$) needed for the throughput estimation in equation (22). This redefinition relies on the knowledge about an average BER.

$$E[Payload] = \begin{cases} N_B * (L-32) * (1-BER)^{L}, & \text{for } N_1 = N_i \quad \forall i \in \{1,..,N_B\} \\ \sum_{i=1}^{N_B}(L_i-32) * (1-BER)^{L_i}, & \text{else} \end{cases} \tag{51}$$

Both presented equations simplify through the assumption that a mean value for the packet size is present. The knowledge about an average BER may be not available at the physical layer. A common connection between BER and the packet error rate is given in the following equation:

$$\text{PER} = 1-(1-BER)^{L}. \tag{52}$$

For delay calculation an additional effect needs to be considered. The so called block ACK reordering in 802.11n takes place at the receiver if one or more packets of an aggregated transmission are damaged due to channel errors. In this case, the receiver buffers the complete block of received frames for a defined time and waits for the damaged packets to arrive. If the frames arrive during this time the packets get reordered to their original arrangement and afterwards handed to higher layers. This reordering time leads to additional delay especially on error-prone wireless channels. The following equation accounts for this effect:

$$D = D + (N_B * P_{BER} * (T_{\text{Reorder}})). \tag{53}$$

A defined value for T_{Reorder} in the standard is not available so this is open to the implementation. In this thesis this value is assumed to be 10 ms which is used by the measuring tools described in the following section. To still use the ideas behind Little's Law the calculation of the delay needs to adapted with the calculated maximum number frames inside a block. The adaption is needed since the interest[37] is still the delay per frame and not per aggregated block.

[37] The used measurement system account for the per packet delay as well.

$$D = \frac{N}{\left(S/E[P]\right) * N_B} - E[slot] * \frac{p^{(R+1)}}{1-p^{(R+1)}} * \sum_{i=0}^{R}(1+\beta_i) \tag{54}$$

The difference between this delay calculation for 802.11n and the calculation for 802.11a (equation (41)) is the numerator in the first fraction.

This closes the current section about the theoretical aspects of the modeling approach for long-distance 802.11 links. A further refinement of the described calculations is going to be held in section 6 to precisely account for additional issues arising from a comparison to real hardware.

5. Implementation and Setup

The purpose of this section is to briefly describe the implementation of the model and the measurement system, to provide the reader with the ability to understand the experiments conducted in the next section. For the implementation, a strict separation of modeling and measurement code was performed to provide the possibility to use each part separately or exchange the model if desired. All implementations and the gained data are available on the CD-ROM attached to this work. This section will maintain this separation by describing each part in separate subections. Afterwards this section will end with a description of the WiFi links and hardware used.

5.1. Model

The implementation of the presented model is realized in Mathworks MATLAB [MAT13] because of its abilities in numerical calculations and big data handling. This implementation follows the calculation of the presented equations in section 4. In this implementation the solution for the system of the contemplated non-linear equations needs to be addressed. For this purpose MATLAB provides the function ”fzero“ which numerically searches for the root of non-linear functions. To exploit this function, equation (35) was substituted in (34) and solved to zero. By utilizing the well-known bisection method[38] the process is robust and sufficient in terms of speed and complexity.

5.2. Measurement Software

The main implementation work was done for the measurement system which is implemented in the MATLAB front-end to provide the possibility for easy comparison of measured and modeled values. Two main tools provide the core functionalities of the system:

1. The ”80211Analyzer“ developed at the Fraunhofer Institute Fokus and based on the SENF C++ framework [sen10]. This Analyzer uses a so called monitor device which works parallel to the standard interface but offers the ability to access all packet data (including information about the physical layer provided by the radiotap API [Joh07]). The Analyzer is capable of calculating the average delay and throughput on a predefined time base. For the upcoming measurements this timebase was chosen to one second as a trade-off between log-file size and resolution.

[38] Also known as binary search method.

2. The MGEN traffic generator [Lab04] for creating data packets at the transmitter. This traffic generator was chosen because of its ability to access all relevant traffic parameters. In addition to that, it is well known tool used in several publications to evaluate traffic in computer networks.

Almost all upcoming measurements will deal with *bi-directional traffic* between two stations in contention. Both stations host their own instances of the 80211Analyzer and the MGEN traffic generator. They are controlled by a third system running MATLAB. Figure 12 provides an overview of the measurement system with the most important components involved. To distinguish between upstream and downstream the traffic is separated via different User Datagram Protocol (UDP) ports.

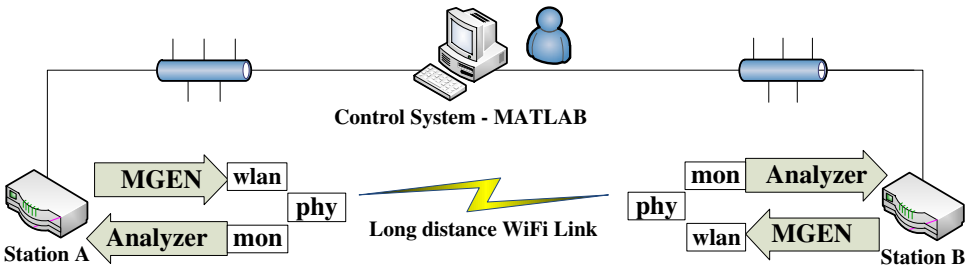

Figure 12: Schematic representation of the measurement system

5.2.1. Delay Measurements and IEEE 1588-2008

Measuring the delay across distributed systems is a difficult task because of the non-synchronous hardware clocks. For uni-directional delay measurements a synchronisation of these clocks is however needed with the current approach. This section will provide the reader with a briefly description of several possibilities to synchronize clocks in Internet Protocol (IP) networks. Afterwards an approach to measure the delay by utilizing the assumption of a linear clock drift will be described. However, this approach is only needed if both stations use different MAC or traffic parameters. For the case of identical, hardware and traffic condition it will be justified why a precise synchronization is not needed for the evaluation of the average access delay. This justification will be confirmed by the conducted measurements in the next section.

To synchronize clocks across IP-networks, the Network Time Protocol Unit (NTP) is widely used. Some simple experiments showed that the accuracy of this protocol is not sufficient for delay measurements in the range of a few milliseconds. In fact the best

accuracy reached with the current Linux Debian implementation of NTP[39] over a single long-distance links in a direct server client communication was around 10 ms in self conducted measurements.

In the last decade, several researchers focused on using the Global Positioning System (GPS) for time synchronization because of its outstanding accuracy (in the range of nano seconds). A good overview of this technique as well as a comparison to NTP is provided in [BF+06]. However, this technique has some disadvantages in the current use case. Every station needs to be equipped with an outdoor capable GPS receiver leading to additional effort and costs. The timestamps of the generated IP packets need to utilize the GPS clock instead of the hardware one. This is a non-trivial task and could affect the results of the measurements.

The Precision Time Protocol (PTP) defined in its newer version through the IEEE standard 1588 defines itself as an "IEEE Standard for Precision Clock Synchronization Protocol for Networked Measurement [...]" [iee08].

In [Eid06] the purpose of this standard is described as follows: The "IEEE 1588 is designed to fill a niche not well served by either of the two dominant protocols, NTP and GPS. IEEE 1588 is designed for local systems requiring accuracies beyond those attainable using NTP. It is also designed for applications that cannot bear the cost of a GPS receiver at each node, or for which GPS signals are inaccessible". Following this description the PTP seems to be a good choice to solve the synchronization problem for delay measurements. In fact, by utilizing an open-source implementation [Har13] of the protocol an improvement compared to NTP was reached. The synchronization utilizing PTP results in accuracy of about 1 ms which is tolerable for bi-directional delay approximation on WiLDs.

The PTP can only be used for an initial synchronization of the clocks and not during the measurements because of two reasons. First, the constant re-synchronization would lead to a sawtooth wave result. Second, for the adjustment, an exchange of packets is needed which would affect the results of the measurement.

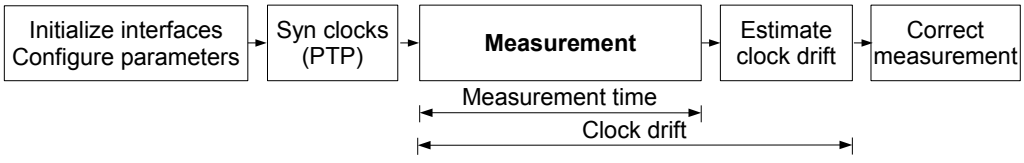

Figure 13: Schematic representation of delay measurement principles

[39] Version: 1:4.2.6.

An idea to deal with this problem is to correct the drift of the clocks afterwards. Self-conducted experiments and different researchers [WD06] have shown that (assuming a constant temperature) the clock drift of commercial available quartzes is nearly linear. This fact can be used to correct the clock drift after the measurement. Figure 13 provides an overview of the delay measurement process. An additional challenge for the time correction is the difference between measurement time and clock drift time as indicated in figure 13. This requires a precise knowledge about the duration of the different sub-processes.

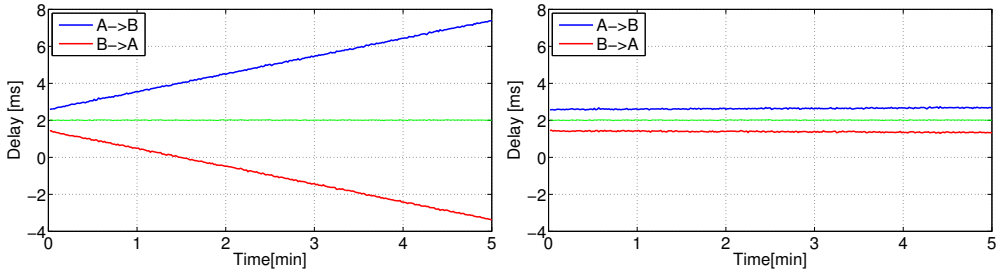

(a) Before correction (b) After correction

Figure 14: Delay measurement with linear clock drift correction

Figure 14 shows an example of a 5 minute long measurement before and after the the correction of the clock drift factor.

The precise time synchronization of the PTP is only needed for the evaluation of different MAC layer parameters across stations which is not the main use case in this work. For the case of identical MAC layer parameters and traffic conditions on both stations the mean value of the measured packet delay provides a precise view on the overall delay for the ad-hoc cell. The accuracies of the delay measurement is for the identical case independent from the synchronization quality of the results because of the following reasons: Both station suffer the same access delay of a packet. The overall error between the different clocks is identical for both stations. This error decreases the measured delay for one direction and increases the delay for the other direction compared to the real access delay alike. When taking the mean value of the measured and aggregated delays from station A to B and from station B to A, this error is subtracted out. This is indicated in figure 14 with the green line. This technique will be used for evaluating the described delay modeling for an 802.11 point-to-point link under saturated conditions.

The feature to evaluate the delay for different MAC layer parameters is an important attribute for further considerations in this thesis. For this case and when using the PTP the synchronization quality needs to be considered with an additional error calculation which bounds the results to a certain level of quality.

5.3. Utilized WiFi-Links and hardware

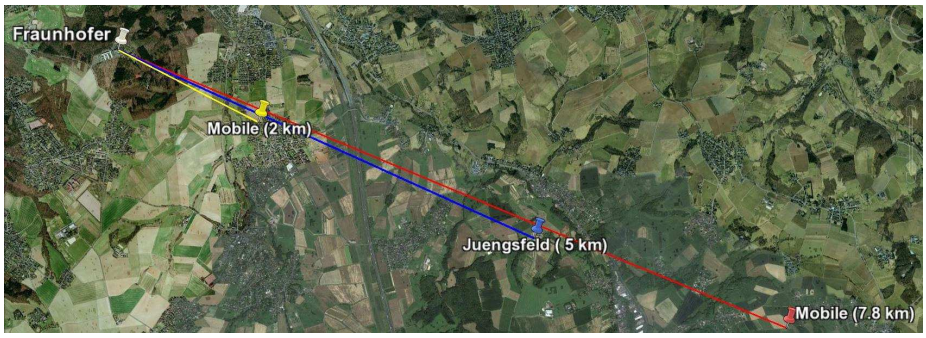

(a) Geographical visualization of the two long-distance links

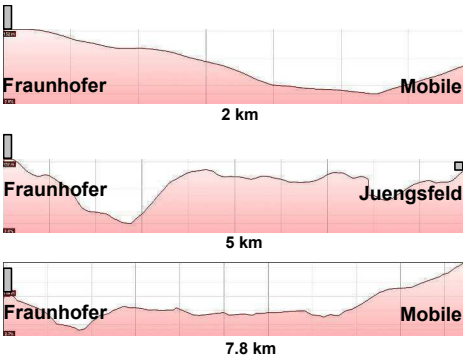

(b) Elevation profiles in descending order of distance

(c) Example of the mobile build-up

Figure 15: Long-distance links

The purpose of this section is to describe the installed test scenarios used for all forthcoming experiments in the next subsections. To compare the modeling approach with long-distance WiFi links, different test links have been set up or used:

- Laboratory environment utilizing high-frequency cables for a nearly non-interfering measurement without distance.
- Static long-distance link from Fraunhofer Campus to a tree nursery at Juengsfeld (distance 5 km).
- Mobile long-distance links from Fraunhofer Campus to different locations in the vicinity (distances 2 km and 7.89 km).

Taken from Google-Earth, a visualization of the long-distance links as well as their elevation profile is shown in figure 15. This profile indicates that the links are in straight line of sight and no corrections due to the Fresnel zone are needed since the antennas at the Frauhofer campus are mounted additionally on top on a 20 m height building. To calculate the overall link budget, the free space loss should be the only attenuation due

to the propagation environment that takes into account. Since the focus of this work is the evaluation of the MAC layer a detailed link budget calculation and presentation of the antennas is skipped. This work was conducted by the author in [Rad11] as well as [RKJ13] and the reader is invited to use this for further reading for calculations on the physical layer. To evaluate all available modulations the dimension of the antennas and the output power was chosen to provide a sufficient SNR for higher modulations[40].

The mobile measurement system was set up to provide additional distances to test. This system includes the same hardware but is powered with a battery and a mobile antenna pole. An example of a measurement build up is provided in figure 15c. The chosen locations for the mobile measurements were precisely selected based on their link properties. On the one hand different link distances need to be evaluated to estimate the accuracy of the long-distance model, on the other hand a perfect line of sight condition is needed to have the possibility to test all available modulations with comparable properties. Two location were chosen at a distance of 2 km and 7.8 km (cf. figure 15a). Together with the laboratory environment which corresponds to a link distance of zero and the static 5 km link to Juengsfeld these places provide enough variance on the distance to evaluate the modeling approach.

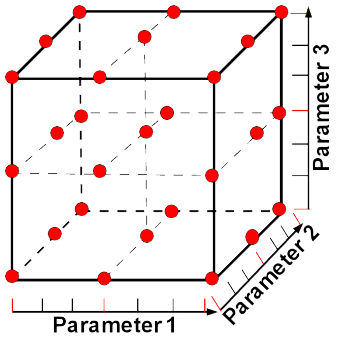

Figure 16: Design of Experiments for the mobile measurements

It will be elaborated in the next section that a complete test run of all possible parameters for 802.11a sums[41] up to 448 different measurements which last at least eight hours to complete for the chosen measurement time. For 802.11n the situation even more parameter combination are possible. For the mobile measurement a subset of the parameters needs to be determined. The choice of these parameters follows the ideas behind the topic - Design of experiments. This scientific topic deals with the issue of conducing a minimal number of experiments and still providing a valid analysis of a system in general. Since this is a complex topic, the reader is referred to [Ant03] for further reading.

[40] The antennas features a gain between 24 and 30 dbi with a 3 dB beam-width between 5 and 15 degress.
[41] Seven values of retry, eight values of CW_{min} and eight different modulations.

The main idea of this topic is utilized in this thesis by conducting a subset of experiments as visualized in figure 16. Instead of testing all values, the border for every combination is tested (corners of the cube) as well as a slice in the middle of every dimension. For the case of a 802.11a this reduces the needed test to 27 for a determined payload.

All three scenarios use the same hardware for unsophisticated comparison of the results. On both sides, as transmitting and receiving devices, a tailor-made embedded computer from the company "Airberry" [Air12] is used. The devices are equipped with a dual core Intel Atom CPU N2800 (1.86GHz) and three Ubiquity SR71 wireless cards using the Atheros AR9280 chipset. The operating system is Debian Squeeze 6.0 with a modified kernel. This kernel is based on the source revision 3.7.11, including some modifications to the wireless driver.

These modifications allow a reliable transmission over longer distance due to adaptations in the MAC layer timings, especially the acknowledgement timeout as describe in [Rad11].

5.4. Atheros driver adaption

The used WiFi driver implementation is one of the most important parts of this thesis since a comparison between the modeling approach and the implementation of this driver will take place. So the following analysis and experiments in this thesis have a strong dependency on the used driver and its capabilities. The ath9k[42] is an Open Source wireless driver for all Atheros IEEE 802.11an PCI/PCI-Express WiFi based chip-sets [Lin12]. Mainly community developed, the ath9k is (besides the MadWiFi project) the most advanced WiFi driver available for Linux today.

Table 8: Variable MAC parameter of the ath9k driver

Parameter	**Adjustable range**
CW_{min}	$2^i - 1, \quad \forall i \in \{1,2,..10\}$
CW_{max}	$2^i - 1, \quad \forall i \in \{1,2,..10\}, >= CW_{min}$
AIFS	0,1,...,
A-MPDU factor	$2^{13+i}, \quad \forall i \in \{-3,2,..,3\}$
Retry	1,2,..,7

An important factor of this thesis is to adopt the different MAC layer parameters successfully to predefined values. This possibility will be briefly validated in the following

[42]The name is used because it supports all devices from the Atheros 9000 series.

through the utilization of the so called Time Synchronization Function Timer (TSFT) field provided in the radio header. This field is described as a "Value in microseconds of the MAC's 64-bit 802.11 Time Synchronization Function timer when the first bit of the MPDU arrived at the MAC" [Joh07] and applies to received frames only. By calculating the TSFT time difference between two directly subsequent frames and plotting them in a histogram like manner, the back-off scheme of the DCF can be visualized. Figures 17a and 17b show the TSFT histogram for the default values of the IEEE802.11a and an adjustment respectively. For better comparison a logarithmic scale was applied on the frequency axis.

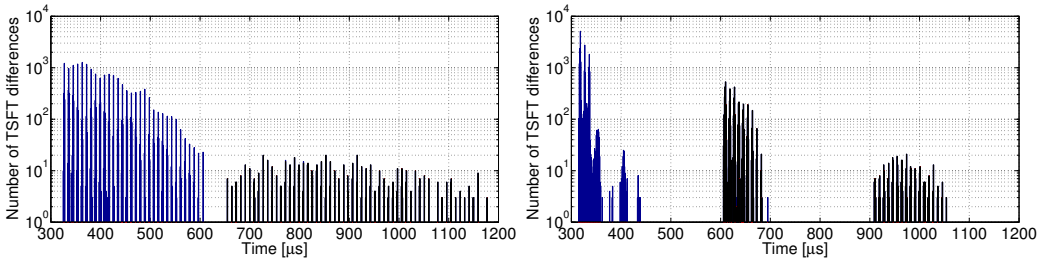

(a) 802.11a default values (cf. table 1).

(b) $CW_{min} = 4$ and AIFS=0

Figure 17: MAC layer parameter adaption

The histograms show that the adjustment is carried out successfully in general. The first observable difference is the reduction of CW_{min} from 31 to 3 between the two plots. The exponential back-off theme is successfully applied for both values of CW_{min} which lead in figure 17b to a back-off scheme of $[3,7,15,...]$ slots. Regarding the figures, two possible problems are observable. In figure 17a the slot times seem not to be uniformly distributed between zero and CW_{min} as claimed by the standard. The second problem is that the slot distribution in figure 17b becomes unstable for small values of CW_{min}. A possible effect of this problem will be picked up in later sections if needed. Another small but visible adjustment and difference between the two figures is the adaptation from AIFS=2 to AIFS=0 leading to a small but overall lower transmission time. This is observable by the lower position for the first bar. Generally the Atheros driver seems to carry out the changes to the MAC protocol successfully and (despite of the described problems) as predicted.

5.5. Measurement parameter and description

The conducted test in the next section evaluates all available modulations for the different standards against all possible values for CW_{min} against all combinations for the number of retries. Since a limitation of the retries also involves a bounding of CW_{max}, this parameter is included as well. These variables have the biggest influence on the

modeling approach as described in section 4.2.2, first on the parameter τ and therefore on the probability of a successful transmission or collision. The payload size can be seen as an additional variable having a strong impact on the throughput. However, its influence on the evaluation of the model is relatively low because of the following reasons:

- The payload can be utilized as an expected value of a distribution.
- According to the statistics of the Amsterdam Internet Exchange[43] peering point, the frame size distribution of the Internet is mainly determined by two different payload sizes: small packets between 50-100 Bytes and large ones around 1500 Bytes [Ams13].
- The time needed to transmit a frame is defined as a static value, mainly characterized through the modulation utilized in the modeling approach. The assumption is that a correct representation of one payload size correlates directly to the results of other frame sizes since the modeling of the back-off behavior is not influenced.
- The measurement of all different payload sizes in the range of 50-1500 Bytes would dramatically increase the needed number of validations.

All upcoming tests will utilize IP as layer three protocol and UDP as layer four protocol. Peculiarities with the Transmission Control Protocol (TCP), especially with its slow start and sliding window mechanisms, are commonly known [LÖ07]. The study of its influence on the modeling approaches will be considered as future work of this thesis. Nevertheless, at suitable points of the next section a possible influence of TCP will be discussed.

To evaluate the modeling approach, UDP seems overall the better choice because of its simplicity and predictability of its behavior. The following experiments will deal with saturated and aggregated throughput inside an ad-hoc cell which means the summation of the throughput from station A to station B, and from station B to station A. Both participants are contenting for time on the medium. Since the choice of the MAC parameters is equal on both stations the overall link capacity is divided by two for up- and downlink between the two concerned stations.

This equality between the two stations is watched during the experiments through the usage of the so called "Jain's fairness index" defined through the following equation:

$$F_i(x_1, x_2, ..., x_n) = \frac{(\sum_{i=1}^{n} x_i)^2}{n \sum_{i=1}^{n} x_i^2} \tag{55}$$

[43] Founded 1994, the Amsterdam Internet Exchange is one of the biggest Internet peering points worldwide.

The origin of this index is found in [JCH84] and an explanation of this commonly known number is provided in [JDB99]. The range of this index is found between zero and one where a value close to one signifies an equal throughput spreading among the stations. If a station occupies significantly more throughput than the other this is reported in the measurement protocol and will be mentioned in the next section.

For the IEEE802.11a DCF case table 9 provides other important parameters influencing the measured throughput and therefore the accuracy of model. Note that these values are carefully verified utilizing wireshark. Since the 80211Analyzer calculates the throughput on the base of an UDP packet size, the IP-header (as well as all lower[44] layers) are summarized under the term L_{HDR}. This definition is highly customizable, by including additional headers for MPLS, for example. For the case of 802.11n nearly the same variables apply. However, a required change will be mentioned in the next section.

Table 9: Variables influencing the throughput of 802.11a

Parameter	**Value**	**Comment**
T_{SYM}	4 μs	Time for one OFDM-Symbol
T_{PLCP}	4 μs	PLCP-Header length
$T_{Preamble}$	16 μs	PLCP-Header length
$L_{HDR} =$	58 Bytes	MAC+LLC+IP Header
$+L_{\text{MAC-HDR}}$	30 Bytes	802.11 QoS-Data MAC Header
$+L_{\text{LLC-HDR}}$	8 Bytes	Logical-Link Control
$+L_{\text{IP-HDR}}$	20 Bytes	IPv4
AC	2	Best effort TC equals DIFS
R_{ACK}	6 Mbps	Defined in the standard [iee12]
$Payload$	8 Bytes+Payload	UDP_{HDR}+Payload

[44] Lower in the context of the standard OSI-model.

6. Model validation and additional adaption

To follow the contemplated ideas about optimizing the 802.11 MAC layer, the model needs to predict the reality with a sufficient quality. The validation of the model using the presented links will be described in this section starting with a general evaluation of Binachis modeling approach against a current Linux implementation of the Linux SoftMAC - mac80211 [Ber09]. This evaluation will picture the need for changes to the standard modeling approach to account precisely for real hardware instead of simulations[45]. Afterwards the developed model extensions for 802.11a long-distance links are evaluated. The section will close with the validation of the model extensions to account for the 802.11n standard using experiments conducted on the laboratory environment as well as on the long-distance links.

A sufficient accuracy of the model would lead to the first goal of this thesis: the possibility to estimate the capacity of WiLD links under given circumstances and for bi-directional traffic. To evaluate the accuracy, the relative deviation between model and measurements needs be quantified. The accuracy measurement in this thesis is defined in the following way:

$$T_{Diff} = \frac{T_{measure}(MCS, CW_{min}, Retry) - T_{model}(MCS, CW_{min}, Retry)}{T_{measure}(MCS, CW_{min}, Retry)}. \tag{56}$$

Since the measurement defines the bias of this definition the result is a positive value for T_{diff}, if the throughput of the measurement is higher than the model and vice versa for negative values. This results in a percentage like definition of the accuracy with a value of zero representing a perfect match between the calculated model and the conducted measurement. This accuracy value is calculated for every measurement using all possible combinations of MCS, CW_{min}, retry and different payload sizes. This provides a detailed possibility for an evaluation of the model but results in a huge amount of data as well. Since all value can not be included entirely[46] in this thesis, a single value is used to aggregate the accuracy of the modeling.

$$T_{\text{Diff}} = \text{mean}(|T_{Diff}(MCS, CW_{min}, Retry)|) \tag{57}$$

This value is a summation of all *absolute* values of the throughput difference divided by the overall number of conducted experiments for every parameter combination. Therefore, it defines the overall accuracy of the model as a percentage like deviation. If not otherwise described, the value T_{Diff} describes now the aggregation of a set of conducted experiments using the contemplated mean value.

[45] A description of these changes to the model will be carried out in this section since their existence was found during the conducted experiments.

[46] Overview purposes.

6.1. Linux implementation

The general accuracy test of the model will take place on the contemplated laboratory link introduced in section 5.3. Through the usage of cables, it is assumed that the transmission errors of this link are very low. A lost packet in this link will exclusively arise from collisions, making it a suitable environment for a general model validation. First the accuracy of the throughput model will be evaluated followed by the same procedure for the delay.

For this first conducted experiments the average difference between the implemented model and the measurements is $T_{\text{Diff}} = 0.035$. This is a higher magnitude of the difference as described in other publications which mainly compared the 802.11b standard to simulations (cf. table 4).

What follows is a closer analysis of this deviation with the goal of further improving this value. By carefully evaluating the conducted experiments a clear tendency is visible. The deviation is not constant for all different values of CW_{min} and number of retries. Moreover, for all different modulations the deviation is comparably high for low values of CW_{min} and a lower number of retries. This trend is visualized in figure 18.

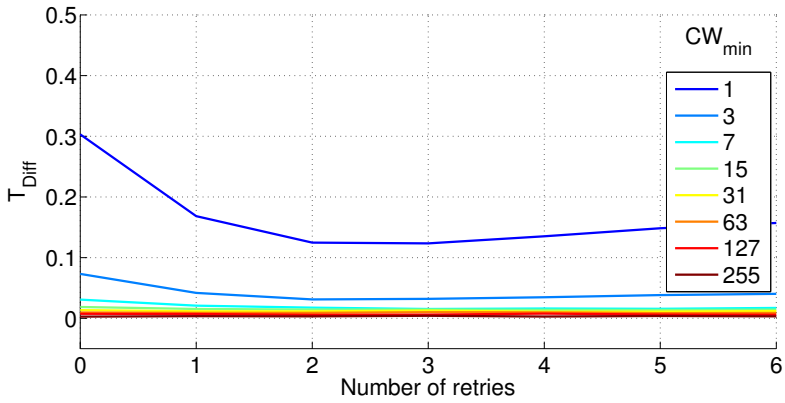

Figure 18: Throughput deviation dependencies

The plot shows for all different values of CW_{min} (indicated by different lines) and all possible retry values on the x-axis (with aggregated stats for the every modulation) the deviation between modeling approach and measurement. The result is a clear tendency towards a significant deviation for small values of CW_{min}. For values of CW_{min} larger than 7 the approximation of the model holds well.

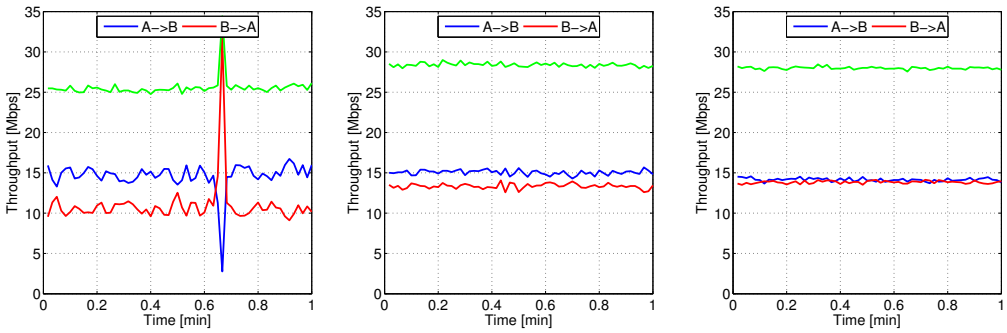

(a) CW_{min}=1 (b) CW_{min}=3 (c) CW_{min}=31

Figure 19: Per station throughput for different CW_{min} values

During the experiments with small values of CW_{min} the fairness index between the two station decreases. Figure 19 visualizes this unfairness among both stations for different values of CW_{min} at every subplot and no possibility for retransmission which defines the worst-case in the case of deviation.

Especially in figure 19a (for $CW_{min} = 1$) it is clearly observable that one station is provided with an advantage when contending for time on the medium despite of identical parameters and hardware on both stations. This unfairness is in weakened version reproducible also with a value for $CW_{min} = 3$ shown in plot 19b. For comparison purpose 19c shows a symmetric traffic behavior with a value of $CW_{min} = 31$.

A reason for this behavior can be a failure in the implementation of the Linux softmac [Ber09] or Bianchis modeling approach does not account for a detail in the standard. In fact there are two additional details which need to be considered for an accurate modeling of the DCF. These details are especially important when taking real hardware into account which justifies their description in this section. The first detail is called Back-off-freezing and was first discovered by [ZAZA02]. The second needed adaption is called anomalous slots [FT05] or slot differentiation [TBX10]. Both adaption will be described in the following to improve the model accuracy.

The reason for the adaption due to Back-off-freezing is described in the latest standard [iee12], namely in the way the back-off counter is decremented. The standard [iee12] specifies that the decrement of the back-off timer should be suspended immediately if a transmission occurs in the current slot. In other words, a decrease of the back-off counter always takes place at the end of the current slot. This leads to the fact that the subsequent slot after a successful transmission cannot be used for transmissions by any other station, except the transmitting one and only if this station starts immediately a transmission through a back-off value of 0. All other stations have at least one value on the back-off counter to decrement, otherwise they would have already tried to access the medium before the transmission occurred. In [Bin08] a way to adopt Bianchis modeling approach

to account for this behavior is provided. This adaption is carried out by redefining the time for a successful transmission T_s. With a probability of $\frac{1}{CW_{min}+1}$, the station starts with a back-off counter 0 and transmits again in the next possible slot. This increases the time it takes to successfully transmit a frame.

$$\bar{T}_s = T_s + \sum_{k=1}^{\infty} (\frac{1}{CW_{min}+1})^k T_s + \sigma = T_s \frac{CW_{min}+1}{CW_{min}} + \sigma \tag{58}$$

The number of successful transmitted bits needs to be changed as well since with the contemplated probability the transmission of an additional frame takes place.

$$\bar{E}[P] = E[P] \frac{CW_{min}+1}{CW_{min}} \tag{59}$$

Since a successful transmission includes an extra idle slot time, this slot is not available for getting picked by a station. Therefore, the back-off counter is now uniformly in the range $[0, CW_{min}-1]$ [47].

These changes are applied to the model and the newly introduced values are used to recalculate the throughput. Instead of an increase in the accuracy the overall quality of the model deteriorates from $T_{\text{Diff}} = 0.035$ to $T_{\text{Diff}} = 0.054$. The implications of this adaption and the decrease in quality is not directly evident for the modeling approach but is again observable with a closer evaluation of the results.

For higher values of CW_{min} the deviation between model and measurement decreases. However, the accuracy was already sufficient before applying the last changes. The main reason for the decease in accuracy is a deviation value of one for $CW_{min} = 1$ and no possibility to retry the frame. This value of one has its origin inside Bianchis modeling approach which estimates now a throughput of *zero* because of the following reason. With setting $W = CW_{min} = 1$, the model assumes that just one slot is available for transmitting and that every station is going to apply for this slot. For a retry value of zero (no retransmission), this would result in a constant collision. In reality just one station has transmitted in the previous model slot. Therefore not all stations are bounded to the first slot. Nevertheless, this differentiation among stations is not accounted for in the modeling approach of Bianchi. One fundamental assumption of (as described in section 3.1.2) is that every station sees the ad-hoc cell in the same condition.

The described inaccuracy is called an anomalous slot [FT05] or slot differentiation [TBX10] and was found nearly parallel by the two different publications. Both publications introduce a multi-dimensional Markov chain which dramatically increases the complexity of the modeling approach. Its influence is negligible for default values of

[47] For the calculation of equation (34) it is important to set ($W = CW_{min}$) for the uniformly distribution of CW_{min}.

CW_{min} and retry. Despite these publications none of the evaluated paper (especially the one for the long-distance case) took this case into account since usually an evaluation of the model takes place with many stations instead of point-to-point links. A mathematically accurate correction of the model based on conditional probability seems not possible without dramatically increasing the complexity since one of the fundamental assumptions is violated in this case. In this thesis an approximation to overcome this inaccuracy is used for the case of point-to-point links[48]. By utilizing the idea of split slots the accuracy can be overall increased for the point-to-point case. Keeping the back-off-freezing adaption through equations (58) and (59), but setting the decreased value of $W = CW_{min}$ to $W = CW_{min} + 0.75$, accounts best for the unfairness among both contenting stations. This was carefully verified for every new set of measurements conducted and applies for 802.11a and 802.11n alike. This move increases the overall of the model accuracy to $T_{\text{Diff}} = 0.0231$ due to a huge improvement for the low values of CW_{min} and the number of retries.

An additional improvement, which is especially important for long-distance point-to-point links, is the usage of the ACK timeout after a collision occurred. This is different from [Bin08] but is accurate according to the newer revisions of the standard [iee12]. This adaption redefines T_c through the following equation.

$$\bar{T_c} = T_{E[MPDU]} + ACKtimeout \tag{60}$$

The value for an ACK timeout was already calculated in equation (6) and is now used in the modeling approach. This improves the overall accuracy of the model to a value of $T_{\text{Diff}} = 0.020$ even in the laboratory environment. The influence of this adaption is assumed to be even higher on long-distance links.

The last improvement to precisely account for real deployments is the transmission rate of the ACK. Different from the standard or the reviewed publications, the Linux implementation of mac80211 [Ber09] does not utilize the lowest possible bit rate for the transmission of the ACK. It increases the acknowledgement bit rate according to the payload bit rate as shown in table 10.

The Acknowledgement bit rates in table 10 are defined in the standard [iee12] as the mandatory bit rates that every station utilizing 802.11 has to support. Especially for higher modulations where the relation between transmission of the payload and the acknowledgement is fairly low this has a significant influence on the modeling approach. By utilizing this new values the overall accuracy of the model changes to $T_{\text{Diff}} = 0.0132$.

[48] Without giving a complete mathematical proof.

Table 10: ACK rates

Payload rate [Mbps]	ACK rate [Mbps]
6	6
12	12
18	12
24	24
36	24
48	24
54	24

To close this section of evaluating Bianchis model and adapting it to the more accurate 802.11a standard, figure 20 provides the final results for the comparison between the introduced model and the linux MAC layer implementation. Besides the overall accuracy, the standard deviation in comparison to figure 18 (representing the beginning of the section) has improved as well.

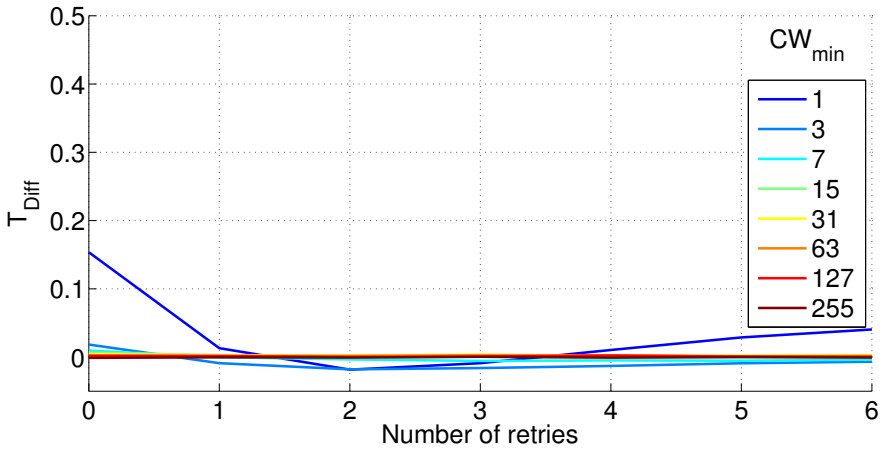

Figure 20: Throughut deviation dependencies after adaption

With one notable exception for a value for $CW_{min} = 1$ and no possibility to retry the frame[49] *all* deviation values are well below 2%. For values equal or higher than $CW_{min} = 7$ the accuracy of the model is larger than 99.5%. This can also be shown by substituting the mean value with the median in equation (57) to calculate the average difference. It is commonly known that the median is (compared to the mean value) solid for the case of extreme values which in these experiments still occurred for lower values of CW_{min}

[49]This value will be excluded in the process of the optimization in later sections. The still large amount of deviation as well as the unsymmetrical traffic distribution among both stations makes this combination an undesirable choice for real-world deployments. Nevertheless, it will still be included in the calculation of the overall accuracy to provide a complete view on the quality of the modeling approach.

especially for the contemplated exception. The overall results for the model deviant utilizing the median is in this case $T_{\text{Diff-median}} = 0.005$. In the following the mean as well as the median value will be used to indicate the model accuracies.

Table 11 provides the development of the model deviation with the different presented adaption.

Table 11: Separate effects of the model adaptation

Model adaption	Accuracy T_{diff}
Original apprach	0.035
Backoff-freezing and splitted Slots	0.023
ACK-Timeout	0.020
Accurate ACK bit rate	0.013

During this chapter one parameter was fixed to a certain value - the payload size. To calculate with both extrema the same tests were done with a Payload size of 50 Bytes. The overall model accuracy with this small packet size is with a value of $T_{\text{Diff}} = 0.0144$ a little worse, but still sufficient. The difference in accuracy between the Payload sizes can have multiple reasons. For smaller packet sizes the overall duration is less so that a timing difference of just a few μs leads to a higher deviation between model and measurement.

After successfully modeling the throughput in the laboratory environment, the following will evaluate the possibility to predict the delay using the techniques introduced in section 4.2.2.3 based on "Little's law", extended with the possibility to account for ultimately dropped frames. When comparing the measured results with the model an additional tasks comes up. The model accounts for the average access delay, but the measured delay includes additional times which need to be evaluated as well to provide a fair comparison. These further timings arise mainly from the two following interactions:

- Buffer-Delay: In saturated conditions a buffer is needed to fulfill the assumption that a packet for transmission is always available[50]. The access delay was defined in section 4.2.2.3 as the time between the packet becoming head of line of the queue and the successful delivery at the receiver. The Linux socket buffer has a minimum size so that there is at least space for one packet [Sie13]. However, this size can be increased to different levels, which will be evaluated later.

[50] In Linux this buffer is called driver queue in and is implemented as a ring buffer. A comprehensive article about network buffers in Linux is provided in [Sie13].

- Processing time: It is assumed that there is a processing time for the path of the packet through the different stages in the Linux kernel. This time includes for example the generation and addition of needed headers. The amount of this delay is assumed to be very low in comparison to the access and the buffer delay. An exact analysis of this value seems to be out of scope of this thesis since during its way through the Kernel a packet crosses several functions and procedures, as indicated by the networking flow diagram provided in [Han13]. In addition to that another assumption is a strong dependency of this value on the frequency and load of the Central Processing Unit (CPU).

Besides the benefit of its simplicity, the contemplated approach of utilizing "Littles law" has the disadvantage that the accuracy of modeling the delay strongly depends on the modeling of the throughput, hence the predicted packets per seconds are used. This implies that the delay prediction can not be more accurate than the forecasting of the throughput. Since the presented results for throughput comparison were satisfactory a usage of this methodology still seems to be a valid approach.

To evaluate the delay prediction the same conducted experiments as in the previous section are utilized. In addition to that and for unified comparison of the results, equation (56) is redefined to account for the percentage deviation of the delay between model and measurement.

$$D_{Diff} = \frac{D_{measure}(MCS, CW_{min}, Retry) - D_{model}(MCS, CW_{min}, Retry)}{D_{measure}(MCS, CW_{min}, Retry)} \tag{61}$$

Again the mean and the median can be used to summarize D_{Diff} for all measured values. For the conducted experiments with a payload size of 1450 Bytes the average deviation is $D_{\text{Diff}} = 0.0817$ for the usage of the mean and $D_{\text{Diff}} = 0.0641$ for the median case. As a first visualization of this accuracy, figure 21 provides a comparison of the measured delay in 21a as well as the modeled in 21b.

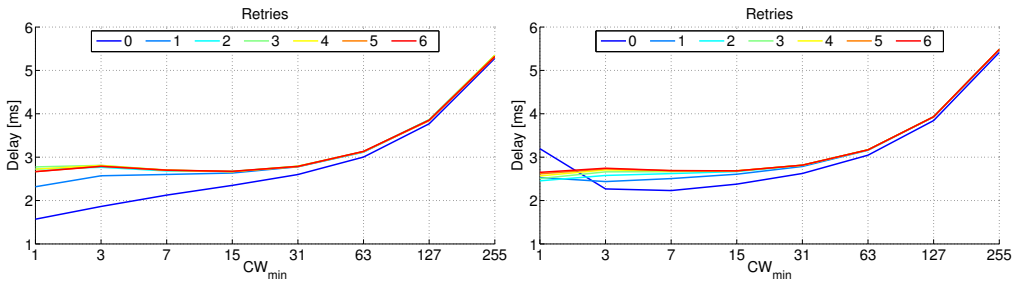

(a) Measurement (b) Model

Figure 21: Delay comparision experiments and model

Different findings can be observed in this figure. The overall form of the plots seems identical. Again for low values of CW_{min} and the number of retries the deviation levels off. This is a continuation for the same difference modeled with the throughput but now with a stronger impact. Another important observation can be made by closely comparing the absolute values of the delay. The model approach has a small, lower delay value for all different parameter combinations. This effect is clearly related to the contemplated processing time since it is a constant value. Analyzing the difference for all conducted experiments the processing time is estimated with 0.2 ms. Including this factor in the modeling approach through a simple addition improves the accuracy. The now calculated values for the average deviation are $D_{\text{Diff}} = 0.04$ for the usage of the mean and $D_{\text{Diff}} = 0.0131$ for the median case which mainly excludes the extreme value. These values are as expected worse than the prediction of the throughput but still sufficient when taking the simplicity of the calculation into account. For example with a delay of 1 ms the average deviation for all measurements is just 40 μs.

The influence of the buffer size still needs to be evaluated. On the transmitting side the influence on the delay is significant since a transmitting queue needs to wait before the previous packet is successfully delivered or discarded after reaching a certain limit of retries. For delay aware applications this buffer should be as low as possible. However, without any queuing mechanism the throughput decreases, since the MAC layer could miss a chance on the medium to transmit a data packet. This trade-off between starvation and delay is described in [Sie13] and the reader is invited to use this for further information.

In this work the influence of the buffer to the delay shall be quantified by adding this to the model if needed. For this purpose, a single test utilizing the laboratory environment was conducted. This test should evaluate the buffer for different sizes of the payload since the assumption is that the buffer is determined by the number of packets inside. To include this in the model the following extension to the current modeling approach of the delay is proposed. The buffer is included as an additional and separated system from the MAC layer and the access delay. Since the departure rate of the buffer is strongly connected to the delay of the MAC layer, the following relation is proposed for the case of point-to-point links:

$$D_{System} = D_{Access} + \frac{D_{Access}}{2} * (N_{Buffer}). \tag{62}$$

Utilizing this equation the following plot provides the relationship between buffer size and delay and confirms the validity of equation (62) by using two different payload sizes as well.

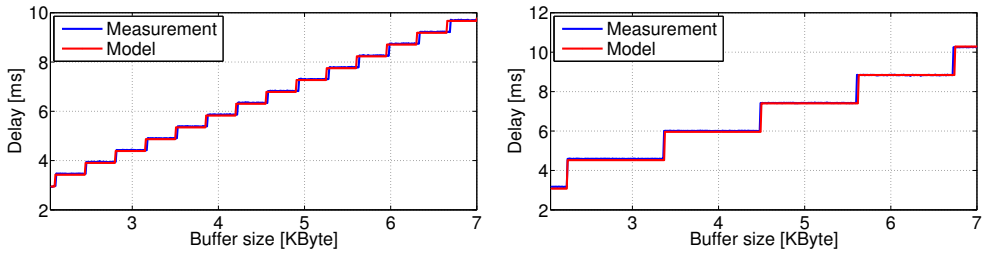

(a) Payload: 100 Bytes (b) Payload: 1450 Bytes

Figure 22: Validation of the buffer modeling approach

6.2. Long-distance links

After comparing and adapting the model carefully to a laboratory environment this section deals with the validation of the long-distance case. All gained results from the previous section will still be used. The purpose of this subsection is the applicability of the introduced adaption for long-distance point-to-point links described in section 4.3. For the static long-distance 5 km link the exact tests as in the laboratory environment were performed. For the mobile measurements, the described idea behind the Desing of Experiments is applied.

Figure 23 shows the results for the conducted test on the long-distance links. It can be observed that the adaption of Bianchis approach was successful since the distance has no effect on the deviation between model and measurement.

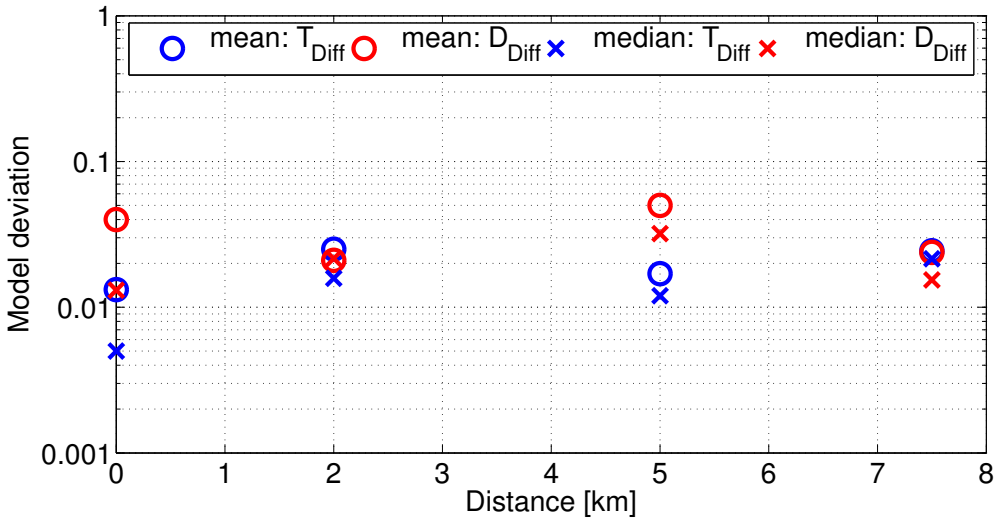

Figure 23: Model accuracy for long-distance links

The highest measured deviation is about 0.04 and the majority is well below 0.02 for delay as well as throughput comparison.

Interim summary The conclusion of this section is that the well known Bianchi approach was adapted in two different ways. At first it was successfully modified to account for current Linux implementations including a partial fix for the deviation for low values of CW_{min} due to anomalous slots. Second, the proposed changes to the model account successfully for long-distance 802.11a links. It is now possible to estimate the maximum capacity[51] for long-distance WiFi links. This leads to the possibility of optimization as well as to evaluate the behavior of these links under different conditions without the need for expensive testing on different distances.

6.3. 802.11n

After evaluating the 802.11a standard in the laboratory environment and on long-distance links the proposed model extensions for 802.11n needs to be classified as well. This section will first evaluate the PHY enhancement of 802.11n (cf. section 4.4.1) and afterwards the A-MPDU frame aggregation including the block ACK protocol (cf. section 4.4.2).

For the following experiments the laboratory environment and the long-distance links have been used. For the mobile long-distance links the contemplated concept for design of experiments are used. The results are presented in figure 24. To provide an aggregate view on the results, all model accuracy values for all long-distance links have been aggregated to provide a suitable representation of the physical layer extensions.

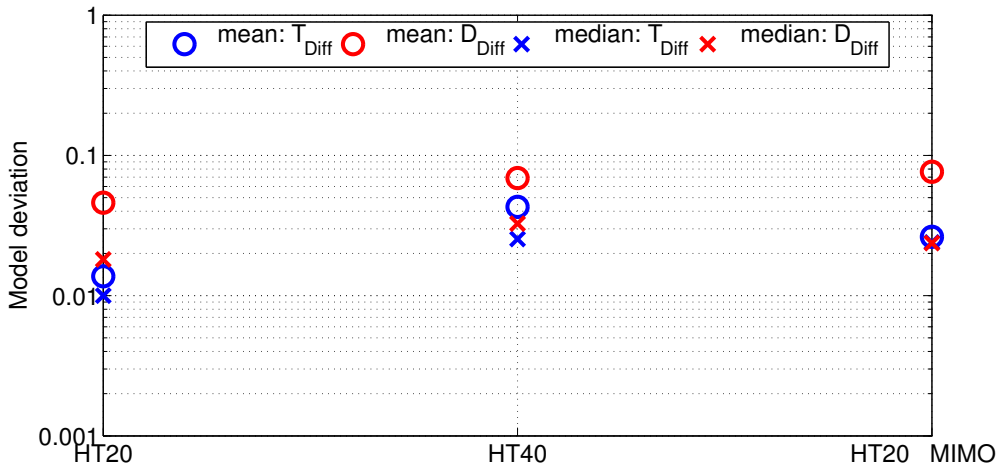

Figure 24: Deviation 802.11n physical layer extensions

[51] Saturated conditions.

During the evaluation of the results an additional modeling feature needed to be tested at this point. For the long-distance links the higher MCS are effected by physical layer loss even in non-saturated conditions as additional test have shown. This can be accounted in the approach by setting the parameter ζ to a determined value for higher modulations.To account for the packet loss on the 5 km static link the following map for ζ is used for the MCS 0-7 and 8-15 alike. Especially for higher 802.11n modulations the static link to Juengsfeld suffers from a non-negligible packet loss.

$$\zeta[MCS] = [0\ 0\ 0\ 0\ 0.01\ 0.02\ 0.02\ 0.05]$$

The plots show that the model accuracy is slightly worse compared to 802.11a laboratory and 802.11a long-distance links. However, it is still well below three percent for the throughout and well below 4 percent for the delay and the median case.

The following will evaluate the model extension to account for 802.11n frame aggregation technique, which will be again carefully verified against all available WiFi links. The results are presented in an aggregated way for representation purpose. To classify the experiments the A-MPDU factor is still used although it is not the main defining factor for the number of aggregated frames due the 4 ms limitation in the Linux driver implementation as described in section 4.4.2. Because of two reasons the assumption of a complete error-free "wireless" channel in the laboratory environment does not hold for 802.11n and the aggregation technique. The generally higher modulations and the less redundant FEC for 802.11n (cf. table 13 in the appendix). The following values for the BER are used for the calculation of the modeling results. Note that these values are well below typical error rates for wireless links [LÖ07].

$$BER[MCS] = [0\ 0\ 0\ 0.3*10^{-6}\ 0.4*10^{-6}\ 0.5*10^{-6}\ .5*10^{-6}\ 0.9*10^{-6}]$$

Using this BER map, the results for the laboratory environment are presented in figure 25.

It can be observed that the extension of Bianchis modeling approach to account for aggregated frames and the selective Block ACK feature was successful for the throughput case. Expect for an aggregation factor of zero the deviation for the mean and the median is well below 3%. For higher aggregation factors ($i > 1$) the delay accuracy found around 10%.

This larger deviation can be explained in the following way: For the usage of large aggregation factors the application needs to buffer a huge amount of packets to provide them to the MAC layer if needed. To provide an accurate modeling of the throughput this buffer size was chosen to have at least three times the amount of packets queued to account for the case that a stations wins several times in a row the back-off. On the other

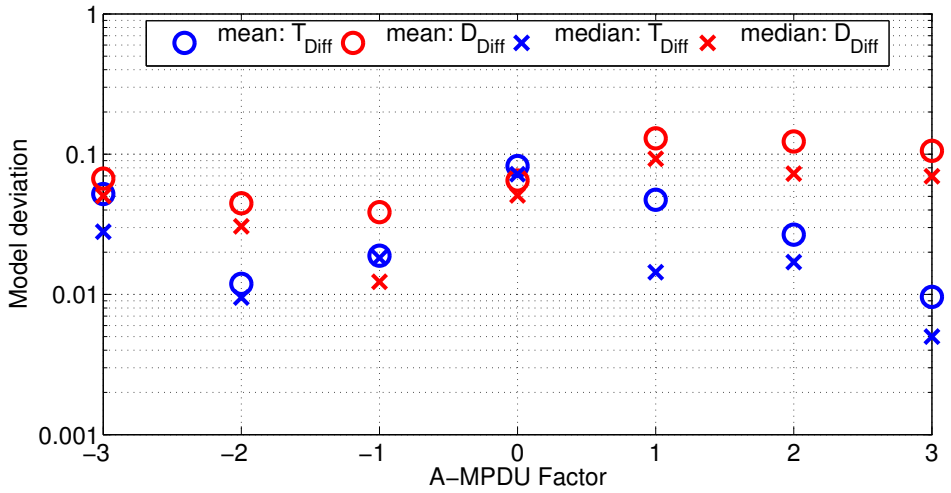

Figure 25: Deviation MAC layer extensions (lab)

side this buffer leads to a large amount of additional delay. To provide an idea about the influence of this buffer, additional experiments were conducted similar to the one already presented for 802.11a in figure 21.

Figure 26 represents the results for different MCS using the highest possible A-MPDU factor (which defines the worst case for the accuracy) to visualize the higher deviations for the delay.

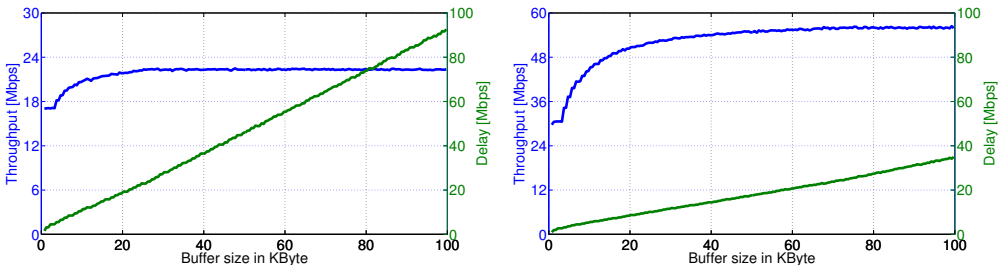

(a) MCS 3 (b) MCS 7

Figure 26: Influence of the buffer to A-MPDU aggregation

To ensure that the buffer has no influence on the throughput measurement it was initially chosen for the A-MDPU factor three to a value of 80 KByte. When conducting the measurements the 4 ms limitation was unknown which leading to a greatly decreased needed buffer size. It can still be observed that for the higher MCS the buffer size is needed as the throughput increases with an increased buffer (blue lines figures 26a and 26b). The current modeling approach predicts the average access delay underlying the assumption that enough packets are available at any time, but does not account for any

delay due to buffering. It can be observed that the assumption of using the average access delay in combination with high throughput does not hold.

As already described for 802.11a it is possible to account for the buffering delay by multiplying the access delay with the number of queued packets in the case of point-to-point links (cf. equation (62)). As the delay nearly increases linear with the size of the buffer for 802.11n as well the same calculation can be applied. For a large buffer size the multiplication factor is accordingly high. The model error of the access delay therefore multiplies with this buffer factor. This effect leads to the higher model deviations for the delay in combinations with the larger aggregation factors. Since the delay accuracies depends on the throughput accuracy as well, this leads to the gap between T_{Diff} and D_{Diff} in figure 25 for the A-MPDU factor three.

Despite the correct estimation of the delay the size of buffer has a strong influence on the throughput (which can be observed especially at figure 26) the current state of the modeling approach takes the delay increase into account but neglects the negative influence on the throughput. To best of the authors knowledge, [LSC10] is the only publication which takes a finite buffer and the related throughput decrease into account. This publication is limited to non 802.11n standards and uses a multi-dimensional Markov model. The additional implementation and solving is out of scope of this thesis. An additional problem with the modeling approach in [LSC10] is that it does not account for Back-off freezing and anomalous slots. This thesis will introduce an approximation for calculating the finite buffer influence on the 802.11n aggregation throughput.

The maximum saturation throughput for 802.11 A-MPDU aggregation and the buffer size share several dependencies. If the buffer size (in packets) is lower than the maximum amount of to be aggregated packets (N_B) only the buffer-size is available for transmission and therefore equals N_B. If the buffer size is equal or greater than N_B, N_B packets can be send in an aggregated way defined by the maximum aggregation factor. If the station wins the back-off several times in a row and assuming a realistic and non infinity arrival rate of packets[52], the buffer size needs to be greater than the maximum aggregation size. Utilizing the conducted experiments presented in figure 26 the modeling approach will be extended to account for 802.11n A-MPDU aggregation with finite buffers in the following way.

[52]For the conducted experiments the mgen rate was set approximately to the physical data rate.

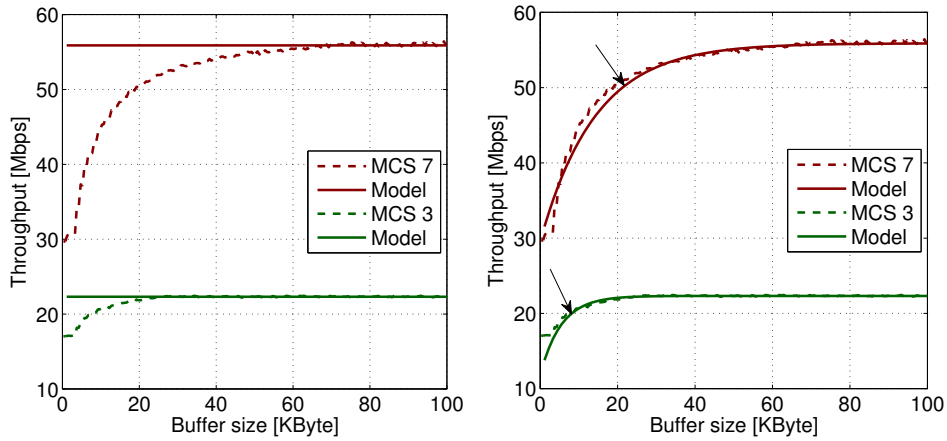

(a) Without buffer modeling (b) With buffer modeling

Figure 27: Validation of the buffer modeling approach for 802.11n

A redefinition of the transmitted payload is needed. This definition will lower the overall transmitted payload to account for the case when there are not enough packets available.

$$E[Payload] = E[Payload] - E[Payload] * (\sum_{k=0}^{\infty} P_{Success}^{k} - \sum_{k=0}^{(1+\frac{N_{Buffer}}{N_B})} P_{Success}^{k}) \qquad (63)$$

Several aspects of this calculation need further description. The first sum defines the probability that a single station wins (after wining the initial back-off) again every following back-off. After a certain number of times wining the contention again, there are no packets queued in the buffer to send. This certain number of times wining the contention is expressed by the second sum which takes the current buffer as well as N_B into account. The difference of the sums approximates the probability when a station won the back-off but none or not enough packets are available for transmission. Using this probability the average transmitted payload size decreases accordingly. For ease of calculation the sums can be expressed using geometric series.

The effect of this approximation is pictured in figure 27 for two experiments. The first figure 27a shows the experiment without the adaption while the second 27b takes equation (63) into account. It can be observed that the approximation using equation (63) holds as an approximation well.

The ability to model finite buffer values for 802.11n A-MPDU aggregation pictures the clear trade-off between delay and throughput for this technique. In fact when observing the measurement result in figure 26 and the modeling in 27 the non-linear relationship between throughput and delay increase is visible. On the other hand the influence of this

factor is only given with a combination of high A-MPDU factors and modulations. For huge buffer sizes the throughput increase is fairly small compared to the delay growth. The goal of the thesis is to optimize the 802.11 MAC layer for both QoS-parameter: throughput and delay for the saturation condition. From this point on the buffer will be seen as an additional factor (F_{Buff}) strongly influencing the delay and the throughput. However, to keep the complexity of the developed modeling approach tractable a reasonable choice for this factor needs to be done. If not mentioned, this choice is used for all upcoming considerations. The buffer size will be held equal to the maximum number of blocks for an A-MPDU. This choice was taken because it is equal to the inflection point of the throughput curve in figure 27b. After the inflection point the ratio between throughput increase and delay growth is getting lower. Since the delay increase is linear, the inflection point defines a reasonable trade-off from a mathematical point of view. The choice of this factor has a positive influence on the accuracy of the delay prediction for higher A-MPDU factors since the multiplication factor is significantly lower compared to the conducted experiments.

This choice of the buffer factor (F_{Buff}) strongly depends on the current traffic situation on the link and the desired optimization goal. Different types of applications or use case for WiLD lead to a stronger focus on throughput or delay optimization. The choice of this factor also depends on the distribution of the used transport layer protocols. TCP for example (also considering different algorithms for this protocol) has a strong dependency on congestion situations which could lead to a throughput decrease if a large buffer size is chosen. Another idea of setting this buffer is to define a maximum tolerable delay for a single 802.11 link in the case of congestion. This tolerable delay could be used to optimize the throughput under this given boarder. An orientation to set the maximum tolerable delay is provided by the ITU-T in its recommendation G.114 [It03].

After describing the model validation for the laboratory environment, the long-distance case still needs to be addressed for 802.11n A-MPDU transmissions. Figure 28 aggregates the complete results for the static 5 km long-distance links as well as the results from the mobile measurements for 2.5 and 7.8 km.

The overall deviations are slightly higher as in the laboratory environment while the tendency are identical. Providing still moderate deviation values the modeling approach is valid for long-distance links as well. The assumption for the higher deviations is that the BER values (which are constantly higher for the long-distance case) are more difficult to handle. A slightly wrong definition of this error can lead to a different prediction of the throughput.

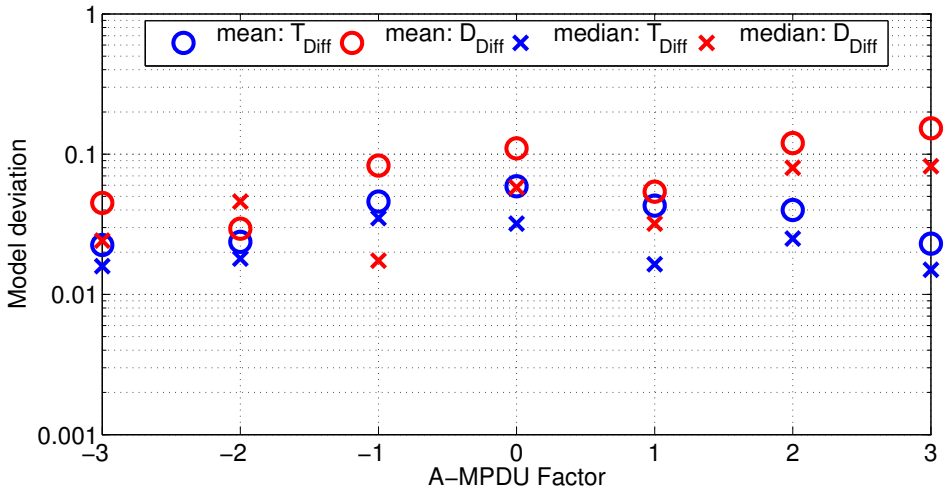

Figure 28: Deviation 802.11n MAC layer extensions (long-distance links)

Interim summary Before proceeding to the next chapter of using the modeling approach and optimizing 802.11 point-to-point links a short summary will be provided in this section. The purpose of this summary is to provide an aggregated view on the capabilities and limitations of the introduced model for 802.11a and 802.11n. Besides the contemplated higher deviations between model and measurement for 802.11n and the higher aggregation factor (which is more accurate now assuming lower buffer-sizes) the overall model accuracy is good. The reader is reminded that the validations presented in the last section were conducted by evaluating approximately 5000 different measurements for

- Different links and distances
- Modulations
- MAC parameters (CW_{min} and the maximum retry count (R))
- Physical and MAC layer extensions of 802.11n
- Different payload sizes.

This extensive measurement and evaluation of the introduced modeling approach lead to the possibility of a validated usage in the following sections.

7. Model utilization and link optimization

After the successful development of the modeling approach for 802.11a and 802.11n long-distance point-to-point links, the purpose of this section is to use this development for further considerations. The first part of this sections will provide the reader with several useful aspects to consider when designing networks of long-distance point-to-point links. These considerations will utilize the default values as described in the 802.11a [iee12] and 802.11n [iee12] standard. Another focus will be laid on the influence of different MAC layer parameter for this type of links.

The second part of this section will provide a detailed calculation with the goal to find the optimum parameters for this type of WiFi connections. These parameters shall be used to maximize the throughput under the goal of moderate delay which improves the QoS and therefore the user experiences in WiLD deployments. In the following sections it will be explicitly refereed to the case of 802.11a or 802.11n.

7.1. General facts for 802.11 point-to-point links

The goal of this subsection is to provide the reader with general considerations about the dependencies resulting from MAC layer and propagation parameters. Since 802.11n offers various different combinations of parameters like MIMO and SISO, 20 MHz and 40 MHz bandwidth and the different aggregation factors, only a subset of possibilities can be described in the following.

7.1.1. Influence of the distance

Despite the physical layer constraints (described in section 2.2.1) which can be overcome with the usage of high gain directional antennas and high-power WiFi cards the increased propagation time bounds the maximum distance of long-distance WiFi links as well. Mainly due to the increased slot time needed for the back-off protocol the overall possible throughput in the bi-directional case decreases with the distance. For the 802.11a standard this is pictured in figure 29. This figure presents the model calculations up to a distance of 50 km for three different modulations.

It can be observed that the maximum saturation throughput decreases non-linear. The decrease is steep at the beginning and flattens for higher distances. The decrease is also stronger for higher modulations since the ratio between transmission and idle times is generally larger. While the transmission time increases with the distance linearly due to the additional propagation time for each packet and the acknowledgement, the idle times increases even more since the propagation time is included in every back-off slot

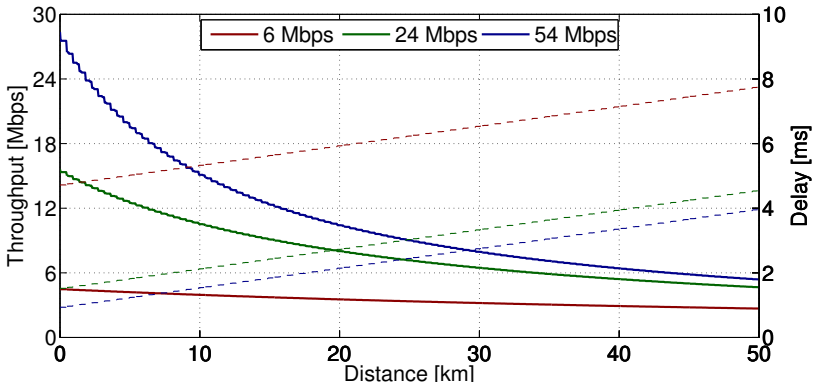

Figure 29: Saturation throughput for 802.11a (distance) (no-buffer)

as well. This leads to the pictured form of the throughput. By closely observing the throughput curve a stepwise decrease takes place. These steps are not related to the number of calculation points, moreover, they represent the increase in the coverage class. As described in previous sections an adaption of the MAC layer timings takes place for every additional 450 m distance leading to approximately 11 steps for the first 5 km.

In contrasts the delay increases linear according to the distance. The delay increase only arises from the additional timings for the back-off slot and the propagation time for a packet. The increase is therefore independent from the used MCS. The pitch depends on the used MAC layer parameters like CW_{min} which permits the usage of a simple overall linear approximation at this point.

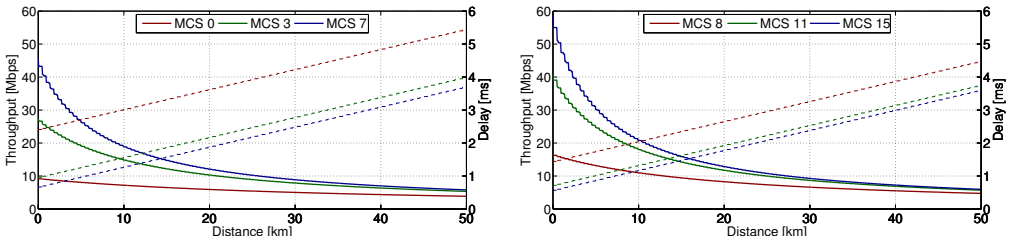

(a) 40 MHz (b) 40 MHz MIMO

Figure 30: Physical layer extensions 802.11n (distance)

The usage of high throughput physical layer extensions provided by 802.11n are not capable of influencing the decrease of the throughput according to the distance which is shown in figure 30. The plot 30a shows the maximum link capacity for a 40 MHz 802.11n connection and in plot 30a a two times two MIMO capability is considered. It can be observed that the overall form of the curves is identical to 802.11a. In fact, the influence of physical extensions significantly decreases with the distance. This leads to the fact that the throughput for all three plots (802.11a, 802.11n HT-40 and 802.11

HT-40 MIMO) at a distance of 50 km is nearly identical. This effect can be grounded again through the ratio between back-off and transmission time. Both 802.11n physical layer extensions bisect the number of needed OFDM-Symbols to transmit the payload. However, these extensions have no influence on the overall idle time on the medium since the needed time for the back-off and propagation delay is not affected. Since 50 km is not a typical WiLD distance it is more useful to compare these effects at a more probable link distance of 5 km. Taking the highest possible MCS into account[53] the throughput increases from 17 Mbps to 21 Mbps and 22 Mbps for 11n-40MHz and 11n-40MHz-MIMO compared to 802.1a. Due the contemplated ratio this increase is significantly less than the doubling of the physical data rate.

A huge advantage of the physical layer extensions of 802.11n is that the average delay decreases compared to 802.11a while the throughput increases. Since physical layer extensions do not influence any MAC layer timings the small decrease in the transmission time leads to an overall decrease in the delay for all different distances.

Besides the physical extensions the aggregation techniques of 802.11n provide a high throughput possibility at the MAC layer. For the uni-directional traffic case this technique has been evaluated in [RKJ13] leading to a maximum throughput of 200 Mbps for a physical data-rate of 300 Mbps [RKJ13]. However, [RKJ13] does not account for precise delay considerations and the usual bi-directional traffic.

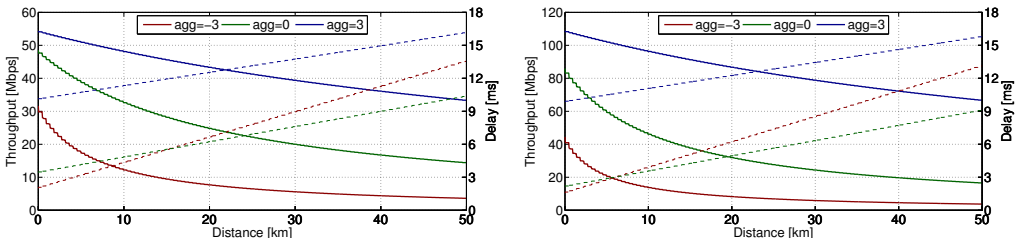

(a) MCS 7 (b) MCS 15

Figure 31: A-MPDU aggregation of 802.11n (distance)

While the usage of MIMO does not provide any known disadvantage [RKJ13] the usage of 40 MHz channels may not be available at all locations since the increased channel bandwidth comes with the need for a free 40 MHz part in the spectrum. The ISM-band (even for 5 GHz) is usually crowed by many participants and the usage of this physical layer enhancement is optional. Figure 31 evaluates the usage of different A-MPDU factors for diverse link distance. A payload of 1450 Bytes, the default MAC values for 802.11n and 20 MHz bandwidth is considered as well as the highest possible MCS of 7 for the SISO and 15 for the MIMO case.

[53] Which is usually available at a link distance of 5 km using high gain antennas.

While isolatedly considered the 802.11n physical layer enhancements do not provide a throughput enhancement for long-distance WiFi links, the MAC layer extensions do. Even for the considered bi-directional traffic the usage of aggregation factors provides an efficient usage of the spectrum. The influence of the distance decreases with higher aggregation factors since the ratio between transmission times and back-off times decreases as well. Using MIMO and the highest aggregation factor leads for a link distance up to 10 km to an aggregated link capacity of approximately 100 Mbps for both stations combined and in bi-directional saturated traffic conditions. For the highest approximation factor an increase in the delay is observable. This delay increase is mainly a results of the needed buffer rather than the propagation time. The influence of distance on this delay is comparable to the increase for 802.11a long-distance links.

7.1.2. Influence of the payload size

The influence of the payload size can be evaluated similar as done in last paragraph with the distance. Setting the distance fixed to 5 km (which is a typical value occurring in WiLD [SPNB08] [RC07]) figure 32 provides a plot for the maximum throughput as well as the delay.

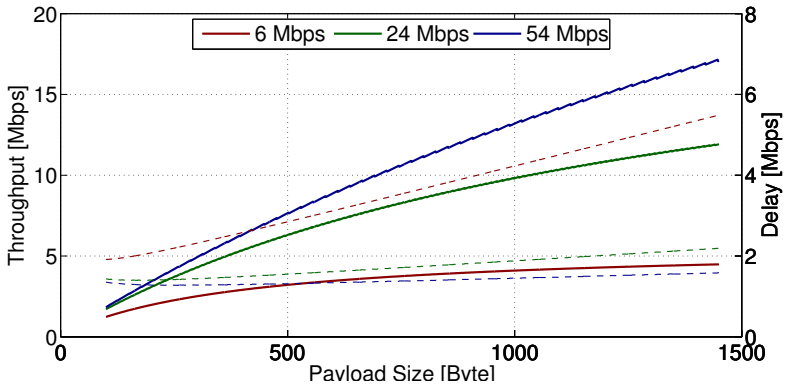

Figure 32: Saturation throughput 802.11a (payload)

It can be ascertained that the maximum link capacity increases for all modulations with a steeper increase for the higher ones. This was expected since a greater payload leads to the transmission of more data after a station has won the contention. This leads overall to less idle time on the medium. An interesting results can be observed regarding the delay. For the highest modulation an increase in the delay is almost non-observable in the plot. In fact, when evaluating the calculations the delay increase is just about 0.3 ms between the lowest and the highest possible payload size. This small increase shows that delay is induced during idle times, mainly during the back-off. The increase due to a

longer transmission time which means additional sending of a few OFDM-Symbols is negligible for higher MCS.

For the 802.11n case the isolated view on the physical layer extensions is skipped and the A-MPDU aggregation case is considered directly in figure 33.

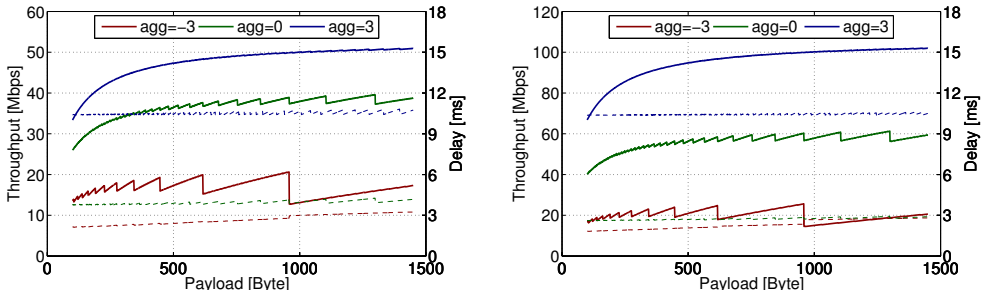

(a) MCS 7 (b) MCS 15

Figure 33: A-MPDU aggregation of 802.11n (payload)

The results for different packet sizes show an unusual behavior for throughput and delay measurements since it results in a chainsaw wave-like curve. This behavior is especially evident for the throughput measurement. Since the A-MPDU technique aggregates fully formated MAC frames, the result is not a straight line parallel to the x-axis. Frequent and steep decreases occur for an increasing payload sizes. These steep drops results from the possibility to send one frame less in the A-MPDU frame format. The optimum exploitation of the A-MPDU technique for different payload sizes takes place at the top of every segment. For the highest aggregation factor this behavior is not directly observable since a larger number of packets is aggregated and therefore the frequency of these decreases is not noticeable with the resolution of the conducted calculations. When evaluating the tops of every segment as well as the highest aggregation factor for the SISO and MIMO case an overall increase of the throughput occurs. The A-MPDU technique is capable of reducing the idle times on the medium but it suffers from MAC overhead[54]. The delay on the other hand is nearly constant for different payload sizes besides a small chainsaw wave-like behavior as well. The number of aggregated packets has no influence on the transmission or access timings and (as described in section 4.4.2) the size of the buffer was chosen equal to the number of aggregated packets as a trade-off between delay and throughput[55].

[54]For the case of A-MSDU this effect would not take places since this aggregation technique works above the MAC layer [RKJ13].

[55]If the buffer size was chosen to a fixed size in Bytes a delay increase for smaller payload would be observable.

7.1.3. Influence of the Packet Error Rate

Since long-distance 802.11 links usually suffer from a higher PER due to a greater possibility for interferences the knowledge about the influence of this factor is desirable. Keeping the introduced plotting scheme, figure 34 pictures this influence for different PER and modulations.

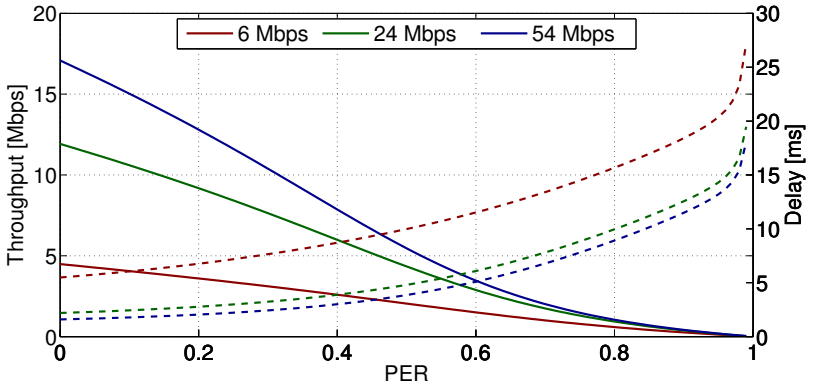

Figure 34: Saturation throughput for 802.11a (PER)

It is observable that a high PER has huge influence on the throughput and the delay respectively. While the throughput decreases non-linear the delay increases. This non-linear behavior results from the fact that besides the non-usable data leading to a retry of the erroneous frames the exponential back-off scheme doubles the contention window. This doubling leads to an additional decrease in the throughput due to higher idle times on the medium.

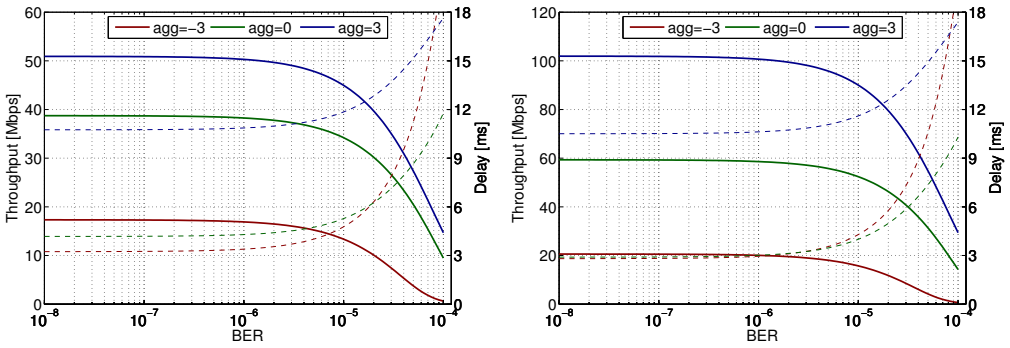

(a) MCS 7 (b) MCS 15

Figure 35: A-MPDU aggregation of 802.11n (distance)

The influence of the erroneous links on 802.11n A-MPDU is evaluated in figure 35. In this case different values for the BER are compared against various aggregation factors for the highest possible modulations. The reader is invited to use equation (52) for a conversion to PER. A noticeable throughput decrease as well as a delay increase takes place at a BER of $5 * 10^{-5}$ for the presented MCS. After this value, the throughput greatly decreases for all aggregation factors. Compared to 802.11a the delay increase is steeper since a reordering at the receiver takes place.

In [KHB+12] we introduced an alternative algorithm for link calibration in self-managed wireless back-haul networks. This algorithm tries to estimate the most suitable MCS for the current link with binary search like propping. The introduced modeling approach is capable to account for errors on the wireless link and can therefore be used to determine a tolerable factor of packet loss before switching to a lower modulation should be considered. An example for these considerations is provided in plot 36 for the case of 802.11a point-to-point links with 1450 Bytes average payload and a distance of 5 km.

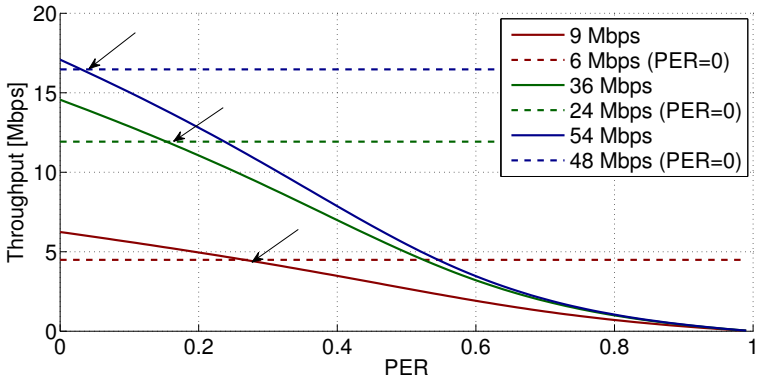

Figure 36: Visualization of the switching PER

It can be noticed that the switching-PER from a higher MCS to a lower MCS strongly depends on the used MCS. While a switch from 54 Mbps to 48 Mbps should be considered for a PER of 3% a switch from 9 Mbps to 6 Mbps is under the premise of throughput maximization desirable for a much higher PER. This should be considered as an example for these considerations since this switch is depended on other factors as well. Several tables (table 17-18) have been generated and calculated which are available in the appendix of this work to provide an overview of the switch factor for the maximum throughput. The overall tendency is that the tolerable PER for a certain MCS increases with a greater payload size. This effect can be explained using the results from figure 34 which shows the influence of the payload size on the link capacity. For a small payload size the throughput differences between different MCS are low since the influence of the

back-off timing increases. These small differences introduce a generally lower tolerable PER since even a small PER leads to a decrease of the throughput below the adjacent lower MCS. The influence of the distance to the maximum tolerable PER compared to the payload is especially for higher MCS negligible.

It should be noted that higher PERs generally increase the number of retransmission on the wireless point-to-point link. This higher retransmission rate could lead to additional delay which is not desirable for applications like Voice over Internet Protocol (VoIP). When the maximum number of retransmission is also limited to a low value, a higher PER also leads to an increased packet loss which transport protocols like TCP may induce to reduce their window size.

7.2. Optimization

After describing general dependencies of long-distance point-to-point links in the last section this chapter will deal with the optimization of MAC parameters for the case of saturation throughput. Since the choice of the MAC parameters has an influence on the throughput and the delay similarly, both parameters should be taken into account. This section will first deal with the optimization of 802.11a and afterwards the 802.11n standard. Since several combinations of different link parameters are possible the following will provide an example of possible optimizations. If possible a general statement about the optimal link parameter will be provided.

7.2.1. 802.11a

To start the process of optimization for 802.11a figure 37 provides an overview about the main idea behind this optimization process. For a typical link distance of 5 km the figure shows the dependencies of throughput and delay to the parameterizable MAC layer parameters for 802.11a - CW_{min} and the number of retries. The results are rounded to two defining numbers and the value for $CW_{min} = 1$ is excluded. This value will not be considered any further since the presented experiments in the last section have shown that the accuracy of the model is significantly worse for this number. While an estimation with this factor seems still a valid approach an optimization should be not considered. In fact the modeling approach overestimates the quality of throughput and delay for this factor compared to the experiments.

For the presented example in figure 37 the maximum throughput is present at a CW_{min} value of three and the maximum number of retries. The minimum delay is given at a $CW_{min} = 7$ with no possibility to retry the frame. Some tendencies are already noticeable.

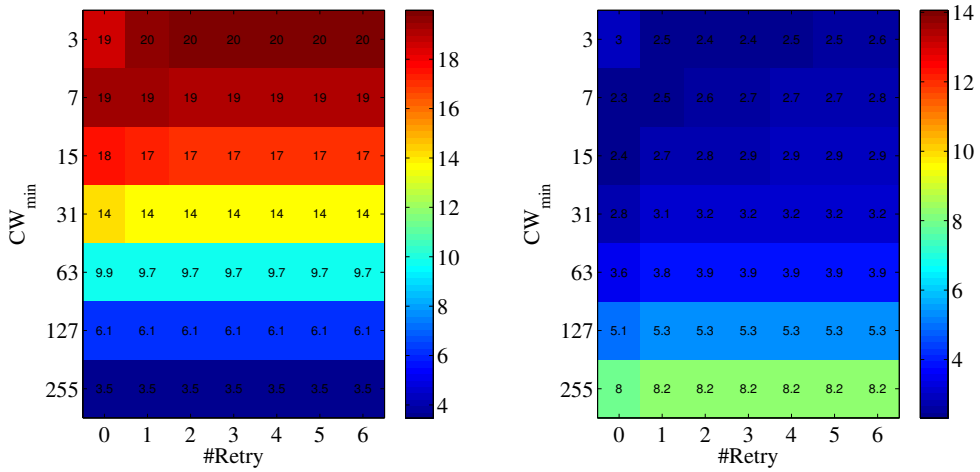

(a) Throughput [Mbps] (b) Delay [ms]

Figure 37: MAC layer parameter influence 802.11a

The best values are present at the lower values for CW_{min} and the quality decreases constantly for higher values of this MAC parameter. The differences in delay and throughput for different chances to retry a frame are comparably low especially for the higher values of CW_{min} since the probability for a retransmission is significantly less. In the following the optimal parameter combination compared to the distance and different sizes of payload and modulations will be evaluated. The assumption is a strong dependency of these values to the contemplated parameters.

The process of optimization is however a non-trivial task since common techniques[56] are not applicable. These optimization techniques focus on a so called single-objective optimization. The underlying problem in this case is clearly related to a multi-objective optimization problem as the schematic drawing in figure 38 indicates.

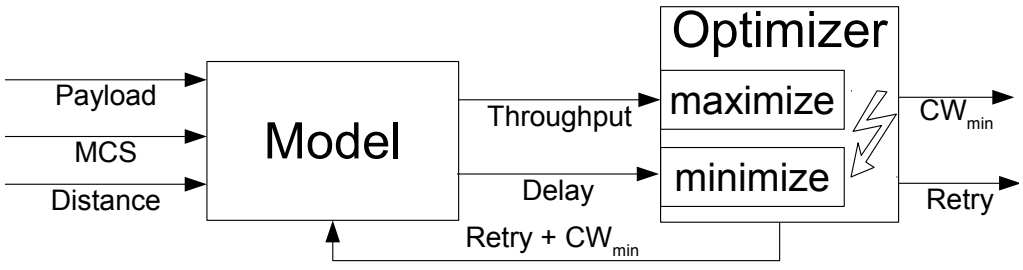

Figure 38: Multi-objective optimization problem for 802.11a

[56] E.g. deviation, Newton's method, nonlinear programming, gradient descent [Lan13].

The situation is even more complicated because the goals of the multi-objective problem are different. While the throughput should be maximized the goal to is to find a minimized delay. The nature of multi-objective problems prevents the existence of a single solution, moreover, several solutions may be valid and equal in the case of their quality. These solutions are called: Pareto[57] optimal solutions [Lan13]. To find this set of values several techniques were developed. The comparison of different technique is out of scope of this thesis but the reader is invited to use [Lan13] for further research.

This thesis will utilize the idea of "scalarizing a multi-objective optimization problem" [CS03]. This technique describes a transformation from a multi-objective optimization problem to a single-optimization problem. Instead of maximizing the throughput and minimizing the delay the ratio defined through a utility function will be used. This function maps both goals to a single goal which can be optimized using well known techniques. This utility function needs to be carefully defined for a valid output of optimized parameters. To define this utility function a general knowledge about the dependencies between delay and throughput for different combinations of the MAC layer parameters is needed. In the following the definition of this function is described.

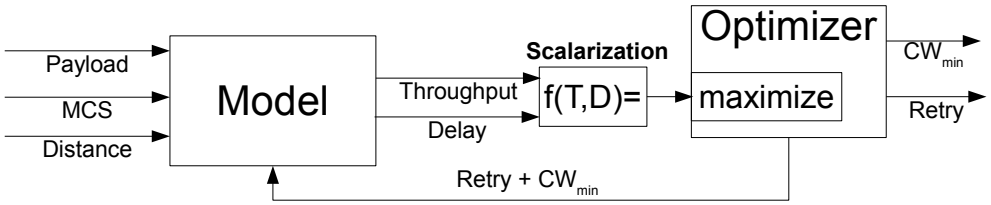

Figure 39: Single-objective optimization problem for 802.11a

For a single[58] experiment all values for the throughput and the delay are calculated using the developed modeling approach. This results in data which defines a value for throughput an delay for every combination of CW_{min} and the maximum number of retries. Figure 40a shows a graph of this data with the throughput plotted on the x- and the delay on the y-axis. For this single experiment the graph shows the dependency between delay and throughput for different MAC layer parameter combinations. By analyzing the graph it is observable that the dependency between delay and throughput follows a $\frac{1}{x}$ mathematical function. Figure 40b provides a re-plot of the same data with the y-axis defined as the reciprocal delay. This plotting leads to a linearization of the data. In this representation the Pareto optimal solutions are exemplary marked (red points). These values represent the optimal MAC layer parameter combination for a minimum delay and a maximum throughput.

[57] Named after the Italian engineer Vilfredo Pareto (1848–1923).
[58] With a fixed payload size, modulation and distance

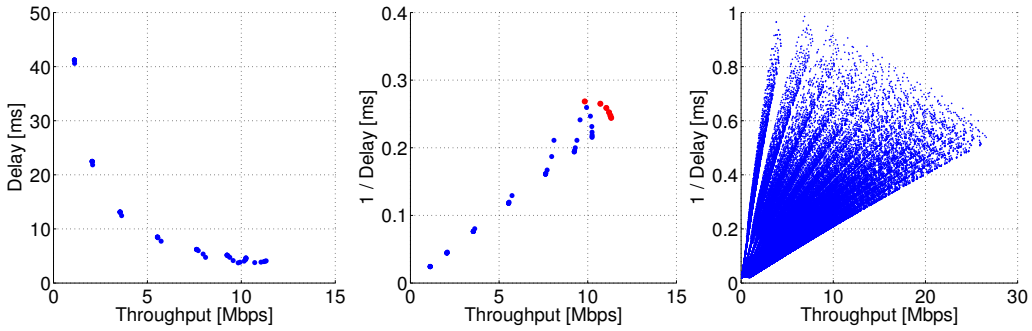

(a) Raw data (b) Linearization (c) All combinations

Figure 40: Dependency between throughput and delay optimization

Figures 40a and 40b are visualizations of a single experiments with fixed input parameters. For a general utility function this dependency between delay and throughput needs to be applicable for all combinations of parameters. This evaluation is pictured in figure 40c for a payload size from 100 to 1450 Bytes, 1 to 10 km link distance and all available modulations[59]. The same tendency for the relationship between throughput and delay is noticeable for all combinations as well. This leads to the possibility of scalarizing the multi-objective optimization problem in the following way. The point of interest which defines the best combination of MAC layer parameters is given at the point which maximizes the addition of a reciprocal delay and throughput. In the graphical representation of the linearized case this is the point with the maximum distance to the source of the plot. This range can be calculated by utilizing the Pythagorean theorem[60] and leads to the following optimization problem:

$$\text{maximize} \left(\sqrt{(\frac{1}{\mathrm{D}})^2 + (\mathrm{S})^2} \right). \tag{64}$$

This definition needs further improvement due the different numerical values for the delay and throughput. Since the throughput is (for most cases) given with a higher numerical value expressed in Mbps compared to the delay declared in ms, a normalization is needed. The goal of this normalization is to map both goals to a comparable numerical value by first calculating the maximum value for delay and throughput for every isolated (fixed input parameters) experiment. Every calculated value depending on the modeled parameters will then be weighted with the maximum possible value for this case. One possible use case of this optimization will be the ability to pick the optimum solution which is closer to an optimum delay or throughput. To address this issue a factor (F) can be added to the optimization problem which weights the influence of the delay. This leads to the following final definition:

[59] This leads to 125440 conducted throughput and delay calculations.
[60] Another possible explanation is through the usage of the generalized calculation of a circle radius.

$$\text{maximize} \left(\sqrt{\left(\frac{F}{\frac{\mathrm{D}_i}{\mathrm{D}_{max}}} \right)^2 + \left(\frac{\mathrm{S}_i}{\mathrm{S}_{max}} \right)^2} \right). \tag{65}$$

The delay influence factor depend on the current traffic situation on the link. In the following this factor will be defined to one and further research is needed to evaluate its influence.

The optimization problem will be solved using MATLAB. The results will be the optimum MAC parameters depending on the defined input variables: modulation, payload and distance for the 802.11a case. Since the graphical representation of three input parameters and two outputs is challenging for a single plot, first the influence of the payload size and afterwards the dependency of the distance for different modulations is evaluated.

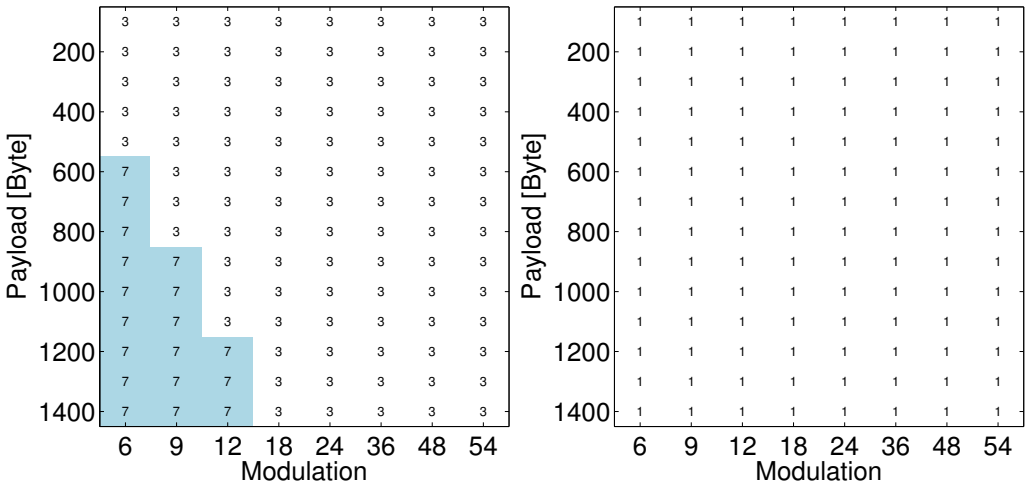

(a) CW_{min} (b) Retry

Figure 41: Optimized parameter for 802.11a (fix. distance)

The first consideration is the influence of the payload and different modulations on the optimum values for CW_{min} and the retry. Figure 41 represents the optimum values for the parameters CW_{min} and the maximum number of retries for a fixed link distance of 5 km. For both values the parameter variance is less than assumed. For the number of retries the optimum value is fixed to one which is equivalent to a single chance for a retransmission. The CW_{min} value varies for this link distance between two values: three and seven. For lower modulation in combination with larger payload the value seven is preferred. Since the transmission time for this combination is larger, the retransmission of a packet is comparatively expensive and should be avoided.

For completeness the isolated results for the multi-objective problem are plotted in the same schematic representation in the appendix of this work (cf. figure 48). The reader is invited to use this plots to compare these results to the single-objective approach presented in figure 41.

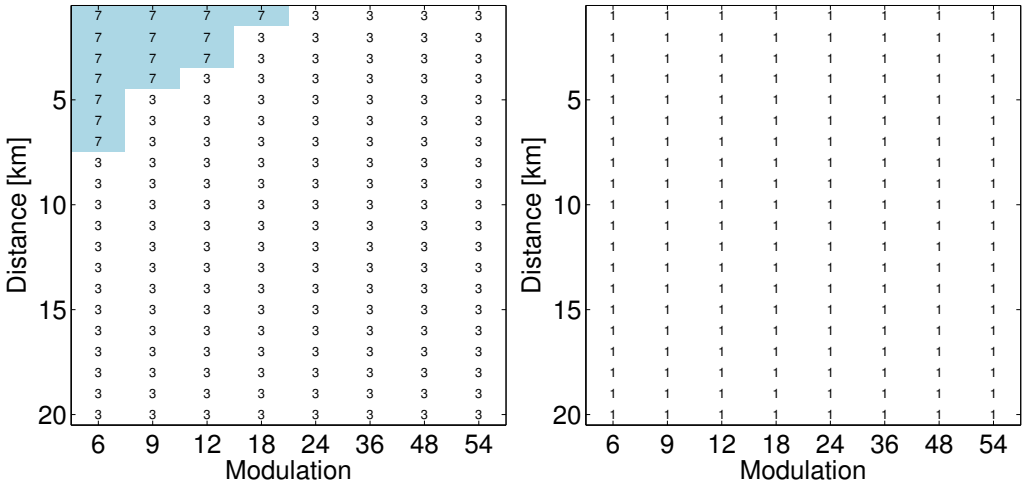

(a) CW_{min} (b) Retry

Figure 42: Optimized parameter for 802.11a (fix. payload)

To complete the optimization of 802.11a the influence of the distance to the optimum MAC layer parameters still needs to be addressed. The payload is fixed to a size of 750 Bytes representing the mean value of possible payload sizes, the distance is varied and all possible modulations for this standard are used. The results are presented in figure 42 and for the multi-objective problems in the appendix in figure 49.

For the number of retransmission the optimum value is again fixed to one. For the minimal number of back-off slots values of 3 and 7 occur while a CW_{min} of 3 is clearly preferential. A value of 7 only occurs for the combination of low modulations and low distances alike. A small distance reduces the idle time during the back-off because of the overall smaller coverage class. A lower modulation however increases the transmission time of the frame. For this combination collisions should occur less often to maximize the throughput.

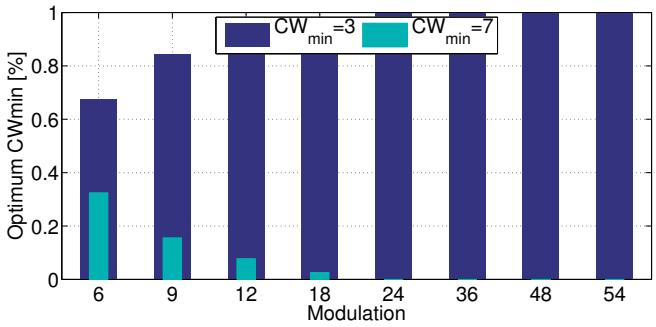

Figure 43: Optimized parameter 802.11a

To provide an overall idea for setting the optimum MAC parameter every possible combination of input factors has been calculated similar to the approach in figure 40c.

The results of these calculations for the factor of CW_{min} are pictured in figure 43. Despite of the link distance and the average payload of the frames, a CW_{min} value of three should be used for all higher modulations in the case of point-to-point links. Even for the lower modulations the usage of this value seems valid since it represents still the majority compared to the other optimum of $CW_{min} = 7$. This finding provides the designer of long-distance 802.11a links with an easy decision rule for the optimum link parameters. As already described, for the number of retries a value of one should be applied which represents the optimum value for all possible parameter combinations.

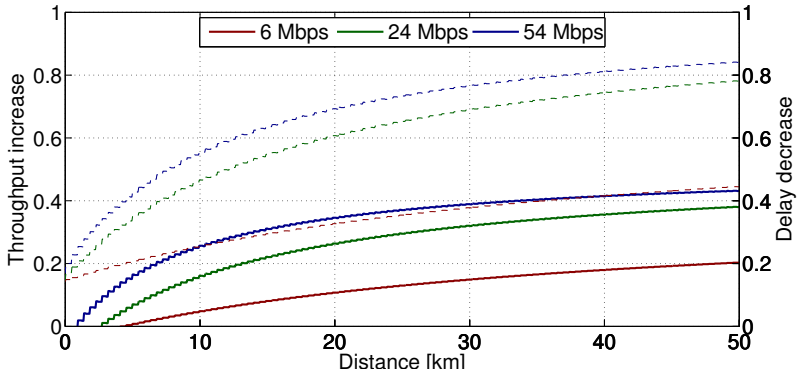

Figure 44: Optimization gain 802.11a

To provide an idea about the gain resulting from the optimized parameters for 802.11a figure 44 provides the throughput increase as well as the delay decrease compared to the default values of the standard (cf. table 1). Especially on longer distances the optimization provides a throughput gain up to 40 % and a delay decrease up to 80 %. For shorter link distances the optimization potential decreases since the influence of the back-off time in comparison to the overall transmission time decreases.

7.2.2. 802.11n

After the optimization of 802.11a, the 802.11n standard will be addressed in this section. For this process the same utility function introduced for 802.11a is used. Due to the numerous possibilities for parameter combination the challenge of this section will be to provide an adequate representation of the results. For this standard the following variables can be addressed to the optimization function

- Bandwith (20 MHz / 40 MHz)
- Aggregation factor (-3,..,3)
- Payload size (50,..,1450 Bytes)
- MCS (0,..,7 SISO and 7,..,15 MIMO)
- Distance (1,..,20 km)

and the goal is to find again the optimum values for CW_{min} and as well the maximum number of retries. To reduce this amount of input factors for a possible representation two factors will be excluded for the first part of this section. Besides the chainsaw-like effect for lower aggregation factors the influence of the payload size plays a tangential role due to the aggregation technique. In the following, this factor will be fixed to an average payload size of 750 Bytes which is statically valid following the measurements conducted in [Ams13]. For the channel width, 20 MHz are assumed due to the usually spare spectrum in the ISM-Band. This reduces the covered input factors to three, similar to the 802.11a case.

To optimize 802.11n links the influence of the distance to different MCS are considered first assuming different A-MPDU factors in range from zero to three. Lower aggregation factors are not considered since this issue has already been addressed for the case of 802.11a. The results are presented in figure 45b to 45d.

For all different aggregation factors the optimum retry value is again fixed to one and therefore not plotted in this section. Since this effect now occurred for all optimization results (for 802.11a as well) a short explanation will be given. With the contemplated utility function the optimum retry value (as well as CW_{min}) is a trade-off between throughput and delay. While the throughput increase for additional chances of retransmission is relatively low, the increase in delay is comparable large since a packet may wait several times for a successful transmission including a larger back-off interval due to the exponential back-off scheme.

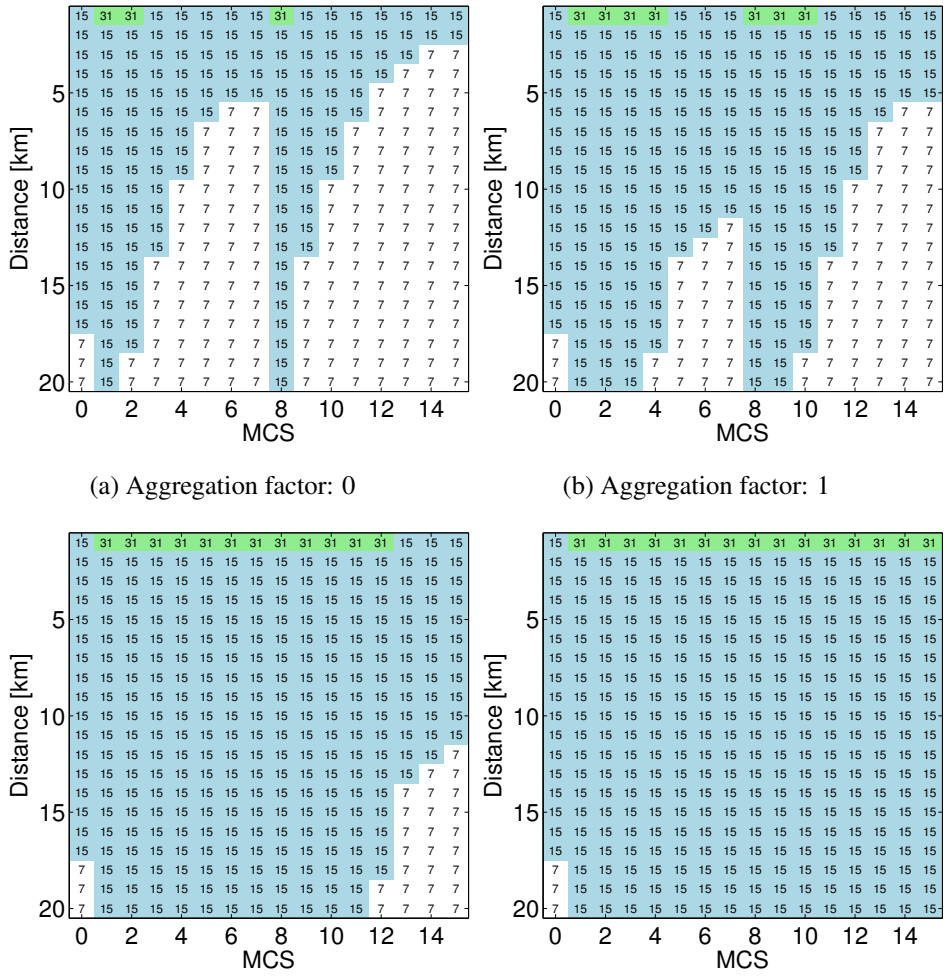

(a) Aggregation factor: 0

(b) Aggregation factor: 1

(c) Aggregation factor: 2

(d) Aggregation factor: 3

Figure 45: Optimized parameter for 802.11n (fix. payload)

The optimum CW_{min} value iterates between 7 and 15 for all calculated A-MPDU factors. The biggest variance is observable for an A-MPDU factor of zero. A value of 15 defines the optimum CW_{min} solution for lower distance up to 5 km and for lower MCS 0-3 (8 for the MIMO case). The explanation of this behavior is identical to the 802.11a case. For lower distances and modulations collisions should be avoided since the transmission time has a bigger influence compared to the back-off timings. With an increasing A-MPDU factor a value of 15 becomes more and more the majority of the optimum. For the highest A-MPDU factor of three a value of 7 should not be considered anymore.

The described effects bare an easy decision process based on a single link feature as provided for 802.11a where it was possible to draw a approximate decision exclusively based on the modulation (cf. figure 43). A designer of 802.11n long-distance links should base its decision of the optimum MAC layer parameters following a schematic

decision. If a high A-MPDU factor is used a CW_{min} value of 15 should be chosen. For moderate A-MPDU factors zero and one, the link distance is an important factor. For short links less than 5 km a value of 15 is the optimum choice. For links greater than 5 km, the decision needs to take the used MCS into account.

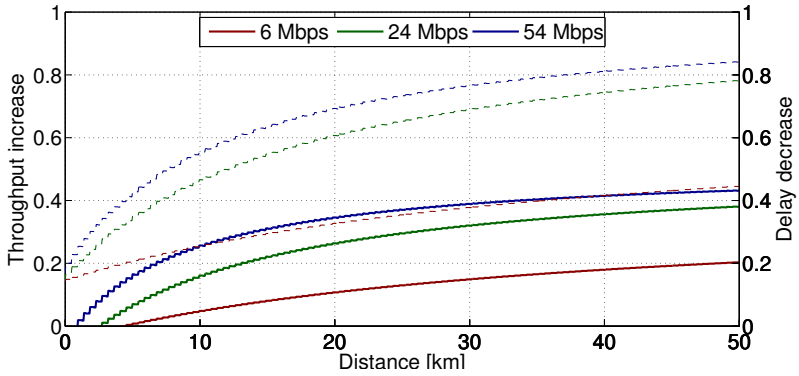

Figure 46: Optimization gain 802.11n

Since the optimum MAC layer values for CW_{min} for long-distance are already close to the default values for 802.11n (cf.table 1), the throughput increase is compared to 802.11a small. Just for the longer distances and the smaller aggregation factors (when the optimum value changes to $CW_{min} = 7$) a throughput increase is measurable. For the delay the improvement is higher since the optimum value for the number of retries reduces the overall chances to transmit a packet leading to a lower delay. The conducted calculations proof the presence of an optimum CW_{min} for 802.11n as well.

7.2.3. Traffic Class Separation

After describing the optimization and estimation of 802.11a and 802.11n DCF for long-distance links, traffic class separation utilizing the Enhanced Distributed Coordination Access (EDCA) still needs to be addressed. As described in section 2.1.2 the EDCA is capable of protecting high priority traffic through allocated slots. Mainly two different techniques can be applied to protect these slots [Bin08]:

- CW_{min} differentiation
- AIFS differentiation.

Instead of developing and implementing an additional modeling approaches for traffic class differentiation in 802.11 networks, this section reuses already conducted results in [Bin08] and [RMSS07][61].

[61] In fact, a complete modeling approach taking 802.11n traffic class differentiation with A-MPDU aggregation on lossy links is (to the best of the authors knowledge) not developed at the moment.

In [Bin08] the two contemplated differentiation techniques for EDCA are compared comprehensively. For CW_{min} differentiation the developed modeling approach for 802.11 long-distance links could be adapted to account for different traffic classes. However, an extension to account for AIFS differentiation is not possible as described in [Bin08] due to the following reason. The uniform per-slot collision probability is not valid anymore. The number of stations which can access a given slot is not constant, it strongly depends on the time which has elapsed from the last transmission. When comparing both differentiation techniques [Bin08] concludes for the CW_{min} technique that "the throughput repartition [...] is almost independent on the network load". This leads to the effect that for an increased network congestion to saturation, both access classes "suffer proportionate throughput degradation as the collision probability increases". For a carrier-grade network offering QoS this is not a desirable behavior.

In fact the AIFS differentiation results in a complementary behavior when comparing it to CW_{min}. For this case, [Bin08] concludes that "the higher the load, the greater the effectiveness of AIFS differentiation in protecting the high priority class". This is a desirable behavior for QoS aware networks since even for the case of congestion on the network, desired services like VoIP should provide an adequate user experience.

These observations are confirmed by [RMSS07] (one of the publications focusing on optimization of the 802.11 MAC layer). As described in section 3.3 they conclude that the optimal value for CW and $retry$ should be used for all traffic classes and that the usage of different values for AIFS provides a good possibility for traffic class differentiation as defined by the standard.

For optimization of the 802.11 MAC in the presence of different traffic classes this thesis proposes the following approach. At first, the optimum MAC parameters for each traffic class need to be determined based on the variable link properties like the distance, different MCS or the average payload size. These optimum values should be applied to each traffic class. Afterwards, a value for the AIFS needs to be chosen to protect the highest priority traffic class from the other. An idea of determining this value is provided in [Bin08] and will be described in the following.

To not leave out capacities on the link and for ease of calculation it is assumed that the highest traffic class is provided with an AIFS value of zero[62]. The interesting case (where QoS factors are important) is found in the saturation case. In this case a certain amount of link capacity should be reserved to the higher traffic class.

[62] Just the difference between the two AIFS values is important.

This amount of link capacity can be calculated as a ratio between the two traffic classes and for the case of point-to-point links as described in [Bin08] with the following equation:

$$\frac{S_j}{S_k} \approx \frac{0.5(1-\tau)^{2\delta_j}}{1-0.5(1-\tau)^{2\delta_j}} \tag{66}$$

where the fixed numbers in that equation occur to due the point-to-point links case and δ_j describes the increased AIFS value of the lower prioritized traffic class (i.e. best-effort and indicated through index j).

This calculation described in [Bin08] only holds for an equal average payload size for the different traffic classes. This assumption does not hold for different services which use diverse payload sizes. In this work this equation will be reformulated to described the ratio between the packets per second for different traffic classes.[63]

$$\frac{PPS_j}{PPS_k} \approx \frac{0.5(1-\tau)^{2\delta_j}}{1-0.5(1-\tau)^{2\delta_j}} \tag{67}$$

To validate this proposed equation a single test in the laboratory environment was conducted using two different traffic streams. The first stream is labeled (using the IPV4 TOS bit) to best effort and assumes a high payload size of 1450 Bytes. The second stream is labeled to VoIP and assumes an average payload size of 160 Bytes as a possible VoIP packet payload described in [Pre06]. The result of this test is presented in figure 47.

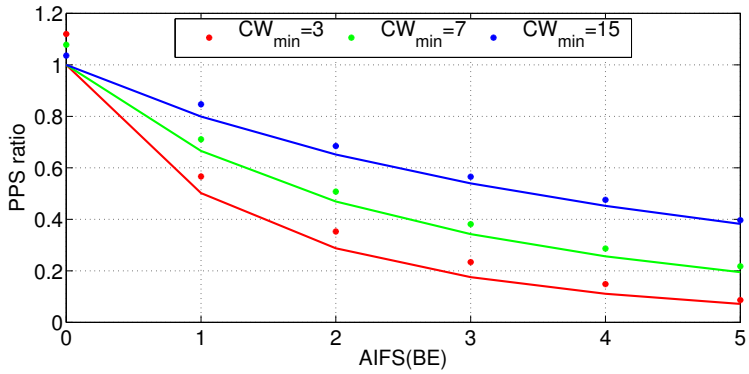

Figure 47: Traffic class separation using AIFS

It can be observed that the approximation using equation (67) holds (despite their simplicity) well. The conducted measurements (points in the plot) show a static deviation to a higher throughput ratio. An unexpected result is that even for the same value of AIFS

[63] This is an approximation as well since it assumes an equal transmission time of the packets. It is much more accurate than the one introduce in [Bin08].

for the voice and the best-effort stream the ratio between the two traffic streams is not equal. The voice stream is prioritized due to an additional and unspecified fact. A possible explanation is the prioritization in a queue before the MAC layer has an influence on the packets. Further research is needed. However, the conducted experiments provide the additional finding that the prioritization of traffic classes depends on the CW_{min}, value although it is set equal for both traffic classes.

For lower values of CW_{min} even a small difference in the AIFS value between the two traffic classes has a strong impact on the prioritization of the voice class. For a typical optimum value of $CW_{min} = 3$ and an AIFS difference of one for lower traffic class this results in an approximately 0.5 throughput ratio. In different words, the packets per second (or precisely the chance for a transmission) for the voice class are twice as much as for the best-effort class. For a CW_{min} value of 15 this increases to a ratio of 0.85. For a higher value of AIFS the ratio decreases constantly.

For the design and operation of WiLD these results play an important role for the QoS assurance in a network. Using a higher AIFS value provides the operator with the opportunity to reserve link capacity for different traffic classes and therefore (under the assumption of a proper classification) service like VoIP. However, a large value for AIFS comes with trade-off that the best-effort class suffers from a low capacity in the case of contention on the medium. Another important fact to consider is that a large value of AIFS for the lower traffic classes introduces additional time on the medium. For the case when no VoIP calls are present on the medium the increased AIFS for the best-effort class will be held as well and therefore introduces additional idle times. The results presented in figure 47 show that even with small values of AIFS a sufficient traffic class separation is possible.

8. Discussion and conclusion

To summarize the results of this work this section can be seen as a brief guideline for MAC layer properties of 802.11 WiLD links. In a separate part the contribution to the evaluated state of the art will be described. This thesis closes providing a prospect on future work items. These items include already discovered possible additions from previous sections which will be substantiated and new ideas from a more general point-of-view.

As defined in the beginning of this work one of the main targets was to estimate the MAC layer performance of 802.11 long-distance links. For this purpose a unified modeling approach for 802.11a and 802.11n long-distance links was successfully developed. This model is based on a well known approach but offers extended capabilities to account for

- Current 802.11 standards: Instead of using the outdated (although easier to model) 802.11b standard this work extended the well known approach to account for 802.11a and 802.11n. These extensions were conducted by using results from several publications and proposing new additions including an approximation to account for finite buffers which is an important factor for an accurate modeling.
- Long-distance 802.11 links: The well known approach has been enriched with the MAC layer constrains of WiLDs to account for this type of connections.

The well known approach and the conducted extension were extensively verified against different distances and various combinations of link and MAC parameters leading to approximately 5000 evaluated measurements. The accuracy of the model was pictured for different use cases and shows an overall sufficiently low deviation between model and measurements. Especially for 802.11a, a model accuracy of 99.5 % was reached due to several described adaption to account for real deployments. The only non-negligible inaccuracy was present for the delay calculation of 802.11n in combination with high aggregation factors which can be mainly attributed to the huge buffer sizes during the measurements.

The developed modeling approach has been used to exemplary evaluate and estimate different dependencies for long-distance 802.11 links. By calculating the throughput and the delay for a wide range of distances (up to 50 km) it is possible to define the limits of WiLDs. The results show that the saturation throughput gracefully decreases with the distance when using the 802.11a standard. This decrease is mainly induced by the enlarged slot times which lead to more idle time on the medium. The same effect leads to an increase of the delay on these links nearly linear with the distance. For

802.11a, these effects seem to be unavoidable since the increased slot times are an important factor for the Distributed Coordination Function (DCF) on long-distances. The average packet size has been identified as an additional factor influencing the throughput on WiLDs. The presence of exclusively small payloads significantly decreases the maximum throughput.

For the 802.11n standard it has been evaluated that the physical layer extensions provide an additional throughput increase just for short distances up to 5 km. For larger links, the increase in throughput as well the decrease in delay is negligible compared to 802.11a. The physical layer extensions induce a small change in the transmission time while the ratio to the overall increased back-off stays almost constant. In contrast, the 802.11n A-MPDU aggregation technique provides a way to deliver high data-rates on long-distances as well. The transmission of an aggregated block significantly lowers the influence of the enlarged back-off timings[64]. However, the aggregation technique suffers from an enlarged delay. This trade-off[65] between the two QoS parameters has been comprehensively described in this work. A smaller buffer for the aggregation technique leads to a throughput decrease, while a larger buffer significantly increases the delay. Fur further considerations this buffer was chosen comparably low leading to a small reduction in throughput but to a significant decrease for the delay. The influence of the average packet-size to the aggregation techniques results in a chainsaw-like behavior. However, with exception of exclusively small packets the influence is evident compared to 802.11a and results mainly from the MAC overhead.

The affect of erroneous long-distance links has been described for both regarded standards. For 802.11a the throughput decreases nearly linear with an increasing packet error rate. The switching PER has been calculated which defines the border before a switch to the adjacent lower modulations should be considered. For the 802.11n aggregation technique the influence of the BER has been pictured. Starting with a BER of 10^{-6} the throughput decreases heavily. An additional problem of a high BER on 802.11n links is the delay increase. Despite the fact that erroneous packets need to be resend, the reordering procedure of these packets at the receiver increases the delay even more. If possible, a high BER should be avoided on long-distance 802.11n links.

With the developed modeling approach the possibility to process the second goal of this work arose - the MAC layer optimization of WiLD links. This process aimed at providing the optimum values for CW_{min} and the maximum number of retries. To conduct an optimization of the throughput and the delay alike, a utility function was introduced

[64] These results enrich the already publicized findings in [RKJ13] with bi-directional traffic and delay considerations.

[65] Which is usually not considered in other publications excluding the influence of buffering.

which transforms the multi-objective optimization problem to a single-objective problem using the well known scalarization technique.

At the beginning of this work the assumption that the optimum MAC parameters underly a large variance was formulated. After the conducted process of optimization this assumption is not confirmed. For 802.11a, a simple dependency between the modulation used and the optimum value for CW_{min} is present. For the lower modulations a CW_{min} of 7, for the higher ones a CW_{min} value of 3 in combination with a single chance of retransmission provides the optimum values independent from the link distance. The usage of this optimization provides (compared to the default parameters) an increase up to 40% in throughput and a decrease of 80% in delay especially on long links.

The same optimization process was conducted for the 802.11n standard. Independent from link or traffic related parameters a retry value of one defines the optimum value similar to 802.11a. The optimized CW_{min} parameter was mainly found between 7 and 15 depending on the link properties. Since the standard already defines a default value $CW_{min} = 15$, the throughput increase due to the optimization is less compared to 802.11a. However, using the optimum value of a single retry decreases the average delay.

To provide traffic class separation on 802.11 links the preferable usage of AIFS compared to different values for CW_{min} has been justified. The presented equation to calculate the relationship between transmission probabilities of different traffic classes shows that even small values of AIFS are sufficient to reserve link capacity for different services.

8.1. Contribution

This work contributes to the current state of the art (described in section 3) with two main results. The extended and adapted modeling approach for long-distance 802.11 links is capable of predicting 802.11a and 802.11n. The particular definition of all needed parameters provides the possibility to calculate the saturated MAC layer throughput for bi-directional traffic in WiLD networks. It accounts for erroneous propagation environments, 802.11n A-MPDU aggregation and provides an approximation for the finite buffer case for the calculation of delay and throughput. The conducted optimizations provide operators of WiLD with the possibility to improve the QoS in these type of networks.

A second addition to the state of the art was reached besides the main goal of this thesis, the careful verification of the well known modeling approach by Bianchi against current WiFi hardware instead of the usually conducted simulations.

8.2. Future work

The experiments and results of this work lead to several possible future work items. Selected ideas will be described in the following.

Two additional factors were introduced in this work with desirable further research. First, the optimal buffer size of 802.11n long-distance connections needs additional investigation. The current definition of this parameter provides an equal trade-off between delay and throughput. However, for networks without delay critical services (i.e. a pure distribution of files or video broadcast) this factor can be redefined to use the complete possible throughput despite of the increased delay. The same trade-off between delay and throughput applies for the defined utility function to scalarize the multi-objective problem. The current approach uses the Pareto optimal solution of the minimum delay and the maximum throughput. Depending on the usage of the network a more intelligent approach for choosing one of the possible solutions maybe desirable. Since both factors apply to the same problem a unified consideration seems to be possible.

An additional possible parameter to include in the utility function is the average expected loss. However, it is assumed that this parameter is indirectly covered through the throughput and the delay. An increased weighting in the utility function could lead to a larger optimum value for the number of retransmissions which is a trade-off to the lower delay but is conceivably important for different transport layer protocols.

This work focuses on the optimization of 802.11 point-to-point links. Deployments of WiLD [SPNB08, RC07, RC07] usually consist of several links forming a topology. An evaluation of the optimized MAC parameters regarding the influence of a multi-hop environment can be addressed.

Different WMN protocols operate on the same frequency forming large ad-hoc cells. With the usage of suitable antennas a visibility among several stations occurs. Despite the capacity sharing of the medium among these stations an additional decrease for the throughput may occur. Most parts of the developed modeling approach are not limited to point-to-point links. So this work can be used to estimate the throughput decrease for ad-hoc cells with numerous participants and large distances in between. Depending on the results of this additional work item a complex frequency planing and the multi-radio approach of WiBACK could be mathematically justified.

The approach can be easily adapted to any technology using the DCF. A possible further application is the usage for Sub-GHz WiFi connections which are currently evaluated to provide connectivity to rural ares exploiting the TV White Space (TVWS) band [BA+13].

With the availably of statistically sufficient data about an average Internet connection of an end-user (e.g. household) several possibilities for future work items arise. The first interesting statistic is the relation between up- and downlink. Common contracts of Internet Service Providers (ISPs) do not provide synchronous link capacities so it is desirable to control this ratio on WiLD links as well. The default 802.11 MAC provides several possibilities for a capacity shift when the average utilization of the link reaches the contention case. Through the usage of different AIFS values for up- and downlink the access probability of the two directions can be influenced towards a desired ratio. Without changing the access probabilities, different A-MPDU factors provide the same effect for 802.11n.

Using the contemplated data, a dynamical adaption of the MAC parameters to the current traffic situation is possible. Due to the knowledge about peak times for certain traffic patterns (which could be obtained using machine learning algorithms) a dynamic adaption could lead to a better user experience. An example is the need for more VoIP connections during the day, while in the evening the need for high down-link capacity increases due to an increased demand for video streaming or file downloads.

Since the goal of this thesis is to provide a QoS optimization at layer two, additional research is needed for the inclusion of different transport layer protocols to the model. Especially the extension to account for TCP requires additional effort. The behavior of the congestion window and the slow start mechanism need to be studied. The challenges of TCP on wireless links are well-known [MCG+01]. Current TCP algorithms like Reno, Cubic or Tahoe use packet loss as an indication for congestion to adapt their window size. For a wired network, congestion is the main reason for packet loss. However, on wireless links the PER or collisions on the MAC layer are additional factors to consider [MCG+01]. The common Reno algorithm reacts to packet loss with a drastic decrease of its windows size leading to on overall decreased throughput. Different techniques to address this problem were published over the last years [MCG+01] [MLAW99] introducing new algorithms like Westwood or Vegas and researchers compared their throughput on wireless links against previous algorithms [BPSK97]. Using their results could lead to an accurate modeling for throughput and delay on layer four with using a desired average traffic mix.

Different researchers have already proposed alternative MAC layer approaches for 802.11. Most of these proposals focus on a Time Division Multiple Access (TDMA) based approach. An example is provided in [SSN08] with the name WiLD MAC. However, this approach offers no throughput increase compared to the default MAC. Moreover, it suffers from an increased delay compared to 802.11a. However, their MAC approach focuses on long-distance mesh networks with visibility among several stations. The main issue in their implementation is the accurate synchronization of time slots in this dis-

tributed network. In case of long-distance 802.11 point-to-point links other approaches are imaginable. During the conducted evaluation of the default 802.11 MAC layer two unsophisticated ideas for different MAC layers approaches arose which will be formulated in the following as the last possible future work items of this thesis.

The first idea describes a Frequency-division duplexing (FDD) for long-distance links. This can be realized using separate interfaces (WiFi cards) for up- and downlink. Assuming a free spectrum, the back-off mechanisms of the current 802.11 MAC layer are expendable in this approach. However, the acknowledgements and the IFS still lead to idle times on the medium. In the current Linux driver implementation the NO-ACK option provides the possibility to surrender completely for acknowledgements at the MAC layer. However, surrendering ACKs on a typical erroneous WiFi link would require that other protocols care for lost packets and induce a retransmission. To still provide the possibility for retransmissions on lower layers in this FDD approach, the following technique is proposed. The correct reception of a packet on the downlink is acknowledgement through the next frame in the uplink using a piggybacked flag added to the data. The usage of two WiFi cards requires more CAPEX as well additional spectrum and the efficiency of this approach needs to be evaluated [66].

The second idea of new MAC layer for long-distance 802.11 links follows the well-known approach of a network token. A recent publication [ESB13] compared a SoftToken MAC to the evaluated 802.11a MAC. Their comparison focused on ad-hoc cells with several stations and the authors measured a throughput decrease compared to 802.11a. They conclude that the implemented SoftToken approach outperforms the DCF in terms of traffic class differentiation since a deterministic QoS provision is possible. In the case of point-to-point links the situation is simpler. Instead of using a ring topology as specified in the IEEE802.5 standard [iee01] or numerous stations as described in [ESB13] the token will be passed only between two participants. A node which is in possession of the token and has at least one packet queued will be provided with the opportunity to transmit until a certain threshold is reached. The token will be passed together with the transmission of the data packets. However, this approach needs further investigation for example to handle the case of a lost token as well as possible gain in QoS compared to the default MAC.

[66] A similar approach to this idea was already introduced by the company Ubiquiti networks with a technology called airFiber [net13].

References

[Air12] Airberry GmbH. Tailored Wireless Mesh Solutions. `http://www.airberry.com/`, 2012. Online; Accessed: 12-12-2013.

[Ams13] Amsterdam Internet Exchange. Frame size distribution. `https://www.ams-ix.net/technical/statistics/sflow-stats/frame-size-distribution`, Nov 2013. Online; Accessed: 14-11-2013.

[Ant03] J. Antony. *Design of Experiments for Engineers and Scientists*. Butterworth-Heinemann, Oxford, 1. edition, 2003.

[ASS03] F. Alizadeh-Shabdiz and S. Subramaniam. A Finite Load Analytical Model for the IEEE 802.11 Distributed Coordination Function MAC. In *Workshop Modeling Optimization Mobile Ad Hoc Wireless Networks*, pages 321–322, 2003.

[BA+13] P. Batroff, O. Aliu, E. , Schuetz, M. Kretschmer, C. Niephaus, and K. Jonas. Unified Solution Towards Deoployment of TV White Space in Africa. In *Fifth International IEEE EAI Conference on e-Infrastructure and eServices for Developing Counties*, Oct 2013.

[Ber09] J. Berg. The 802.11 subsystems - for kernel developers. `http://wireless.kernel.org/80211books/`, 2009. Online; Accessed: 8-11-2013.

[BF+06] K. Behrendt, K. Fodero, et al. The perfect time: An examination of time-synchronization techniques. In *Proceedings of the 60th Annual Georgia Tech Protective Relaying Conference*, 2006.

[Bia98] G. Bianchi. Performance analysis of the IEEE 802.11 distributed coordination function. *IEEE Journal on Selected Areas in Communications*, 18(3):535–547, 1998.

[Bin08] B. Bing. *Emerging Technologies in Wireless LANs - Theory, Design, and Deployment*. Cambridge University Press, Cambridge, 1. edition, 2008.

[BPSK97] H. Balakrishnan, V. N. Padmanabhan, S. Seshan, and R. H. Katz. A comparison of mechanisms for improving TCP performance over wireless links. *, IEEE/ACM Transactions on Networking*, 5(6):756–769, 1997.

[BT05] G. Bianchi and I. Tinnirello. Remarks on IEEE 802.11 DCF performance analysis. *Communications Letters, IEEE*, 9(8):765–767, 2005.

[Bun07] Allgemeinzuteilung der Frequenzen im Frequenzbereich 5755 MHz – 5875 MHz für gewerblich öffentliche, breitbandige, ortsfeste Verteilsysteme; Broadband Fixed Wireless Access (BFWA). Vfg. 47. Technical report, Bundesnetzagentur, 2007.

[BV05] A. Banchs and L. Vollero. A delay model for IEEE 802.11e EDCA. *Communications Letters, IEEE*, 9(6):508–510, 2005.

[CBV05] P. Chatzimisios, A. C. Boucouvalas, and V. Vitsas. Performance analysis of the IEEE 802.11 MAC protocol for wireless LANs. *International Journal of Communication Systems*, 18(6):545–569, 2005.

[CCG98] F. Cali, M. Conti, and E. Gregori. IEEE 802.11 wireless LAN: capacity analysis and protocol enhancement. In *Seventeenth Annual Joint Conference of the IEEE Computer and Communications Societies*, pages 142–149, 1998.

[CCG00] F. Cali, M. Conti, and E. Gregori. Dynamic tuning of the IEEE 802.11 protocol to achieve a theoretical throughput limit. *IEEE/ACM Transactions on Networking*, 8(6):785–799, 2000.

[Che12] H. Chen. Throughput Analysis of Block-Ack in IEEE 802.11n. In *International Conference on Computer Application and System Modeling*, volume 2, 2012.

[CNB+00] G. R. Cantieni, Q. Ni, C. Barakat, T. Turletti, P. Group, and I. S. Antipolis. Performance analysis under finite load and improvements for multirate 802.11. *Elsivier Computer Communications*, pages 1095–1109, 2000.

[CS03] Y. Collette and P. Siarry. *Multiobjective Optimization - Principles and Case Studies*. Springer, Berlin, Heidelberg, 2. edition, 2003.

[DV05] X. Dong and P. Varaiya. Saturation throughput analysis of IEEE 802.11 wireless LANs for a lossy channel. *Communications Letters, IEEE*, 9(2):100–102, 2005.

[Eid06] J. C. Eidson. *Measurement, Control, and Communication Using IEEE 1588*. Springer, Berlin, Heidelberg, 2006.

[EO05] P. Engelstad and O. Osterbo. Delay and Throughput Analysis of IEEE 802.11e EDCA with Starvation Prediction. In *The IEEE Conference on Local Computer Networks*, pages 647–655, 2005.

[ESB13] L. Eznarriaga, C. Senguly, and N. Bayer. Experiences with SoftToken: a token-based coordination layer for WLANs. *International Journal of Communication Systems*, 2013.

[FT05] C. H. Foh and J. Tantra. Comments on IEEE 802.11 saturation throughput analysis with freezing of backoff counters. *Communications Letters, IEEE*, 9(2):130–132, 2005.

[Han13] S. Han. NUSE: Networking Stack in Userspace. `http://www.eecs.berkeley.edu/~sangjin/2013/01/14/NUSE.html`, 2013. Accessed: 22/11/2013.

[Har13] E. Harris. Precision Time Protocol Daemon - ptpd2. `http://sourceforge.net/projects/ptpd2/`, Apr 2013. Online; Accessed: 10-11-2013.

[HD05] J. Hui and M. Devetsikiotis. A unified model for the performance analysis of IEEE 802.11e EDCA. *IEEE Transactions on Communications*, 53(9):1498–1510, 2005.

[HEKN11] D. Henkel, S. Englander, M. Kretschmer, and C. Niephaus. Connecting the unconnected; Economic constraints and technical requirements towards a back-haul network for rural areas. In *GLOBECOM Workshops*, pages 1039–1044, 2011.

[HS11] W. J. Hopp and M. L. Spearman. *Factory Physics*. Waveland Press, Reading, 3. edition, 2011.

[iee01] IEEE Standard for Information Technology - Telecommunications and Information Exchange Between Systems - Local and Metropolitan Area Networks - Specific Requirements. Part 5: Token Ring Access Method and Physical Layer Specifications. Amendment 5: Gigabit Token Ring Operation. *IEEE 802.5v-2001*, 2001.

[iee07] IEEE Standard for Information Technology - Telecommunications and Information Exchange Between Systems - Local and Metropolitan Area Networks - Specific Requirements - Part 11: Wireless LAN Medium Access Control (MAC) and Physical Layer (PHY) Specifications. *IEEE Std 802.11-2007 (Revision of IEEE Std 802.11-1999)*, pages 1–1076, Dec 2007.

[iee08] IEEE Standard for a Precision Clock Synchronization Protocol for Networked Measurement and Control Systems. *IEEE Std 1588-2008 (Revision of IEEE Std 1588-2002)*, 2008.

[iee09] IEEE Standard for Information technology- Local and metropolitan area networks– Specific requirements- Part 11: Wireless LAN Medium Access Control (MAC)and Physical Layer (PHY) Specifications Amendment 5: Enhancements for Higher Throughput. *IEEE Std 802.11n-2009(Amendment to IEEE Std 802.11-2007)*, pages 1 –565, Sep 2009.

[iee12] IEEE Standard for Information technology-Telecommunications and information exchange between systems Local and metropolitan area networks-Specific requirements Part 11: Wireless LAN Medium Access Control (MAC) and Physical Layer (PHY) Specifications. *IEEE Std 802.11-2012 (Revision of IEEE Std 802.11-2007)*, pages 1–2793, Feb 2012.

[It03] U. It. ITU-T Recommendation G.114. Technical report, International Telecommunication Union, May 2003.

[JCH84] R. Jain, D.-M. Chiu, and W. R. Hawe. A quantitative measure of fairness and discrimination for resource allocation in shared computer system. 1984.

[JDB99] R. Jain, A. Durresi, and G. Babic. Throughput fairness index: An explanation. Technical report, Ohio State University, 1999.

[Joh07] JohannesBerg. radiotap.org defined-fields/TSFT. `http://www.radiotap.org/defined-fields/TSFT`, Dec 2007. Online; Accessed: 12-11-2013.

[KHB+12] M. Kretschmer, T. Horstmann, P. Batroff, M. Rademacher, and G. Ghinea. Link calibration and property estimation in self-managed wireless back-haul networks. In *18th Asia-Pacific Conference on Communications*, pages 232–237, 2012.

[KNG+04] D. Kotz, C. Newport, R. S. Gray, J. Liu, Y. Yuan, and C. Elliott. Experimental evaluation of wireless simulation assumptions. In *Proceedings of the 7th ACM international symposium on Modeling, analysis and simulation of wireless and mobile systems*, pages 78–82, 2004.

[KTBG04] Z.-N. Kong, D. H. K. Tsang, B. Bensaou, and D. Gao. Performance analysis of IEEE 802.11e contention-based channel access. *IEEE Journal on Selected Areas in Communications*, 22(10):2095–2106, 2004.

[LÖ7] C. Lüders. *Lokale Funknetze - Wireless LANs (IEEE 802.11), Bluetooth, DECT*. Vogel Verlag Und Druck, Würzburg, 1. edition, 2007.

[Lab04] N. R. Laboratory. MGEN - The Multi-Generator Toolset. `http://cs.itd.nrl.navy.mil/work/mgen/index.php`, 2004. Online; Accessed: 09-11-2013.

[Lan13] K. Lange. *Optimization*. Springer, Berlin, Heidelberg, 2. edition, 2013.

[Lin12] Linux Wireless. About ath9k. `http://linuxwireless.org/en/users/Drivers/ath9k`, 2012. Accessed: 10-11-2013.

[LMCW02] K. Leung, B. McNair, L. Cimini, and J. Winters. Outdoor IEEE 802.11 cellular networks: MAC protocol design and performance. In *IEEE International Conference on Communications*, volume 1, pages 595–599, 2002.

[LSC10] R. P. Liu, G. Sutton, and I. Collings. A New Queueing Model for QoS Analysis of IEEE 802.11 DCF with Finite Buffer and Load. *IEEE Transactions on Wireless Communications*, 9(8):2664–2675, 2010.

[LW06] Y. Lin and V. W. Wong. Frame aggregation and optimal frame size adaptation for IEEE 802.11 n WLANs. In *Global Telecommunications Conference, IEEE*, pages 1–6. IEEE, 2006.

[MAT13] MATLAB. *8.1.0.604 (R2013a)*. The MathWorks Inc., Natick, Massachusetts, 2013.

[MCG+01] S. Mascolo, C. Casetti, M. Gerla, M. Y. Sanadidi, and R. Wang. TCP westwood: Bandwidth estimation for enhanced transport over wireless links. In *Proceedings of the 7th annual international conference on Mobile computing and networking*, pages 287–297, 2001.

[MFL05] A. Martínez-Fernández and D. M. López. Rural telemedicine infrastructure and services in the Department of Cauca, Colombia. *Telemedicine journal and e-health*, 11(4):451–459, Jun 2005.

[MHW03] S. Mangold, G. Hiertz, and B. Walke. IEEE 802.11e wireless LAN - resource sharing with contention based medium access. In *Proceedings on 14th IEEE Personal, Indoor and Mobile Radio Communications*, volume 3, pages 2019–2026, 2003.

[MLAW99] J. Mo, R. J. La, V. Anantharam, and J. Walrand. Analysis and comparison of TCP Reno and Vegas. In *Eighteenth Annual Joint Conference of the IEEE Computer and Communications Societies*, volume 3, pages 1556–1563, 1999.

[net13] U. networks. airFiber Carrier Class Point-to-Point Gigabit Radio. `http://dl.ubnt.com/datasheets/airfiber/airFiber_DS.pdf`, 2013. Accessed: 03-01-2014.

[Pit95] J. Pitman. *Probability*. Springer texts in statistics. Springer, 1995.

[PNS+07] R. Patra, S. Nedevschi, S. Surana, A. Sheth, L. Subramanian, and E. Brewer. WiLdnet: design and implementation of high performancewifi based long distance networks. In *Proceedings of the 4th USENIX conference on Networked systems design and implementation*, 2007.

[Pre06] C. Press. Voice Over IP - Per Call Bandwidth Consumption. `http://www.cisco.com/en/US/tech/tk652/tk698/technologies_tech_note09186a0080094ae2.shtml`, 2006. Accessed: 28/12/2013.

[PS10] E. Perahia and R. Stacey. *Next Generation Wireless LANs - Throughput, Robustness, and Reliability in 802.11n*. Cambridge University Press, Cambridge, 1. edition, 2010.

[PSGS12] D. Paudel, K. Sato, B. Gautam, and D. Shrestha. Design and implementation of partial mesh community wireless network in Himalayan region. In *Third Asian Himalayas International Conference on Internet*, pages 1–6, 2012.

[Rad11] M. Rademacher. Lanstrecken-WLAN-Verbindungen für Wireless Mesh-Netzwerke. Bachelor thesis, FH-SWF Meschede, Mar 2011.

[RC07] B. Raman and K. Chebrolu. Experiences in using WiFi for rural internet in India. *IEEE Communications Magazine*, 45(1):104–110, 2007.

[Rec12] J. Rech. *Wireless LANs: 802.11-WLAN-Technologie und praktische Umsetzung im Detail*. Heise Heinz, Hannover, 4. edition, 2012.

[RKJ13] M. Rademacher, M. Kretschmer, and K. Jonas. Exploiting IEEE802.11n MIMO Technology for Cost-Effective Broadband Back-Hauling. In *Fifth International IEEE EAI Conference on e-Infrastructure and eServices for Developing Countries*, Oct 2013.

[RMSS07] J. Ramiro, A. Martinez, S. Salmerón, and J. Simó. Traffic engineering in rural wireless networks for developing countries using IEEE 802.11 EDCA. *Wireless Rural and Emergency Communications*, Jan 2007.

[RR04] J. Robinson and T. Randhawa. Saturation throughput analysis of IEEE 802.11e enhanced distributed coordination function. *IEEE Journal on Selected Areas in Communications*, 22(5):917–928, 2004.

[sen10] SENF: The Simple and Extensible Network Framework. `http://senf.berlios.de/api/trunk/doc/html/`, 2010. Online; Accessed: 09-11-2013.

[Ser99] R. Serfozo. *Introduction to Stochastic Networks*. Springer, Berlin, Heidelberg, 1999.

[Sie13] D. Siemon. Queueing in the Linux Network Stack. *Linux J.*, 231, Jul 2013.

[SMFRLSP10] J. Simo-Reigadas, A. Martinez-Fernandez, J. Ramos-Lopez, and J. Seoane-Pascual. Modeling and Optimizing IEEE 802.11 DCF for Long-Distance Links. *IEEE Transactions on Mobile Computing*, 9(6):881–896, 2010.

[SNC+08] D. Skordoulis, Q. Ni, H.-H. Chen, A. Stephens, C. Liu, and A. Jamalipour. IEEE 802.11n MAC frame aggregation mechanisms for next-generation high-throughput WLANs. *IEEE Transactions on Wireless Communications*, 15(1):40–47, Feb 2008.

[SPNB08] S. Surana, R. Patra, S. Nedevschi, and E. Brewer. Deploying a Rural Wireless Telemedicine System: Experiences in Sustainability. *Computer*, 41(6):48–56, 2008.

[SSN08] R. P. S Salmerón-Ntutumu, J Simó-Reigadas. Comparison of MAC Protocols for 802.11-Based Long Distance Networks. In *Proceedings of the 1st Workshop Wireless For Development*, Aug 2008.

[TBS04] I. Tinnirello, G. Bianchi, and L. Scalia. Performance evaluation of differentiated access mechanisms effectiveness in 802.11 networks. In *Global Telecommunications Conference, IEEE*, volume 5, pages 3007–3011, 2004.

[TBX10] I. Tinnirello, G. Bianchi, and Y. Xiao. Refinements on IEEE 802.11 Distributed Coordination Function Modeling Approaches. *IEEE Transactions on Vehicular Technology*, 59(3):1055–1067, 2010.

[TC05] I. Tinnirello and S. Choi. Efficiency analysis of burst transmissions with block ACK in contention-based 802.11e WLANs. In *IEEE International Conference on Communications*, volume 5, 2005.

[TWCM10] K. Tan, D. Wu, A. Chan, and P. Mohapatra. Comparing simulation tools and experimental testbeds for wireless mesh networks. In *IEEE International Symposium on a World of Wireless Mobile and Multimedia Networks*, pages 1–9, 2010.

[WD06] U. Windl and D. Dalton. The NTP FAQ and HOWTO: Understanding and using the Network Time Protocol - Frequency Error. `http://www.ntp.org/ntpfaq/NTP-s-sw-clocks-quality.htm`, Nov 2006. Online; Accessed: 09-11-2013.

[YWA05] J. Yin, X. Wang, and D. P. Agrawal. Modeling and optimization of wireless local area network. *Computer Communication*, 28(10):1204–1213, 2005.

[ZAZA02] E. Ziouva, T. Antonakopoulos, E. Ziouva, and T. Antonakopoulos. Reprint CSMA/CA Performance under High Traffic Conditions: Throughput and Delay analysis, Feb 2002.

A. List of equation variables

Variable	Explanation
CW_i	Contention Windows size in back-off stage i
$DIFS$	Time of a DCF Interframe Space (DIFS) in $[\mu s]$
$SIFS$	Time of a Short Interframe Space (SIFS) $[\mu s]$
$SlotTime$,σ	Time of a back-off slot in $[\mu s]$
$EIFS$	Time of Extended Interframe Space (EIFS) in $[\mu s]$
$ACKTxTime$	Overall transmission time of an ACK in $[\mu s]$
$AIFS(AC)$	Time of Arbitration Interframe Space (AIFS) per AC in $[\mu s]$
$AIFSN(AC)$	Number of AIFS for an AC
$ACKTimeout$	ACKTimeout at the receiver in $[\mu s]$
$AirPropTime$	Propagation time for long-distance links in $[\mu s]$
S	Saturation throughput in Mbps
$E[\ ]$	Expected value
$Payload$,P	Payload in Bit
T_{Frame}	Time for a complete frame transmission process without back-off in $[\mu s]$
T_{MPDU}	Time for the transmission of a MPDU in $[\mu s]$
T_{ACK}	Time for the transmission of an ACK
T_{PREAM}	Time for the transmission of the preamble in $[\mu s]$
T_{PCLP}	Time for the transmission of the PLCP in $[\mu s]$
MAC-HDR	MAC Header in Byte
T_{SYM}	Time of an OFDM Symbol
N_{DBPS}	Number of data bits per OFDM Symbol
P_{idle}	Probability for an idle slot
$P_{success}$	Probability for "one station picks a slot"
$P_{collsion}$	Probability for collision due to several stations pick a slot"
T_s	Time of a successful transmission in $[\mu s]$
T_c	Time of for a collision in $[\mu s]$
τ,$P\{TX\}$	Constant probability that a specified station transmits in a slot
p	Constant collision Probability
B_i	Number of back-off slots in the current back-off stage
W	$CW_{min}+1$, Number of slots for CW_{min}
β_i	Back-off scheme
R	Number of possible retries
N	Number of stations in the ad-hoc cell
ζ	Transmitted frame is corrupted because of noisy channel conditions
d	Distance between two stations in [m]
cc	Coverage class
N_B	Number of aggregated frames in an A-MPDU block
$N_{\text{B-calc}}$	Number of A-MPDU frames based on the max. aggregation factors
$N_{\text{B-4ms}}$	Number of A-MPDU frames based on 4 ms limit
BER	Bit Error Rate after the FEC
T_{Reorder}	Waiting time for the re-orderer at the receiver
D	Delay measured or model
D_{System}	System delay including buffer and processing times
D_{Access}	Access Delay of packet after becoming HOL
N_{Buffer}	Number of buffered frames in packets
δ_j	Difference in AIFSN between two traffic classes

B. Tables and Values

Table 12: Achievable OFDM-datarates for IEEE802.11a [Rec12, iee07]

Modulation	Bits/ subcarrier	Bits/ OFDM-Symbol (N_{CBPS})	FEC Coderate (R)	Datenbits/ OFDM-Symbol (N_{DBPS})	Datarate MBit/s
BPSK	1	48	1/2	24	6
BPSK	1	48	3/4	36	9
QPSK	2	96	1/2	48	12
QPSK	2	96	3/4	72	18
16-QAM	4	192	1/2	96	24
16-QAM	4	192	3/4	144	36
64-QAM	6	288	2/3	192	48
64-QAM	6	288	3/4	216	54

Table 13: Achievable OFDM-datarates for IEEE802.11n [Rec12, iee09, iee12]

MCS	Modulation	Bits/ subcarrier	Bits/ OFDM-Symbol (N_{CBPS})	FEC Coderate (R)	Datenbits/ OFDM-Symbol (N_{DBPS})	Datarate MBit/s LGI	Datarate MBit/s SGI
0	BPSK	1	52	1/2	26	6.5	7.2
1	QPSK	2	104	1/2	52	13	14.4
2	QPSK	2	104	3/4	78	19.5	21.7
3	16-QAM	4	208	1/2	104	26	28.9
4	16-QAM	4	208	3/4	156	39	43.3
5	64-QAM	6	312	2/3	208	52	57.8
6	64-QAM	6	312	3/4	234	58.5	65
7	64-QAM	6	312	5/6	260	65	72.2
8	BPSK	1	52	1/2	26	13	14.4
9	QPSK	2	104	1/2	52	26	28.9
10	QPSK	2	104	3/4	78	39	43.3
11	16-QAM	4	208	1/2	104	52	57.8
12	16-QAM	4	208	3/4	156	78	86.7
13	64-QAM	6	312	2/3	208	104	115.6
14	64-QAM	6	312	3/4	234	117	130
15	64-QAM	6	312	5/6	260	130	144.4

Table 14: 4ms limit for frame aggregation [iee12]

MHz.MCS	0	1	2	3	4	5	6	7
HT20	3212	6432	9648	12864	19300	25736	28952	32172
HT40	6680	13360	20044	26724	40092	53456	60140	65532

Table 15: 4ms limit for frame aggregation MIMO [iee12]

MHz.MCS	8	9	10	11	12	13	14	15
HT20	6424	12852	19280	25708	38568	51424	57852	64280
HT40	13348	26700	40052	53400	65532	65532	65532	65532

Table 16: Assumed physical layer times for 802.11 in μs [Rec12, iee12]

Parameter	Time OFDM-Symbol	Time Preamble	Time PLCP
802.11a	4	16	4
802.11n(5 GHz) SISO	4	16	4
802.11n(5 GHz) YxY-MIMO	4	16+Y*4	4

Table 17: Switching PER. IEEE802.11a, 5000m

	200	400	600	800	1000	1200	1400
9	0.14	0.18	0.21	0.23	0.24	0.25	0.26
12	0.07	0.10	0.13	0.14	0.16	0.17	0.18
18	0.08	0.12	0.15	0.17	0.18	0.20	0.21
24	0.05	0.07	0.09	0.10	0.12	0.13	0.14
36	0.05	0.08	0.10	0.11	0.13	0.14	0.15
48	0.03	0.04	0.05	0.07	0.08	0.09	0.09
54	0.01	0.01	0.02	0.02	0.03	0.03	0.03

Table 18: Switching PER. IEEE802.11a, 1450 Byte Payload

	1000	2000	3000	4000	5000	10000	2000
9	0.31	0.30	0.29	0.28	0.27	0.23	0.30
12	0.22	0.21	0.20	0.19	0.18	0.15	0.21
18	0.27	0.25	0.24	0.23	0.21	0.17	0.25
24	0.19	0.17	0.16	0.15	0.14	0.11	0.17
36	0.22	0.20	0.18	0.17	0.15	0.11	0.20
48	0.15	0.13	0.12	0.11	0.10	0.07	0.13
54	0.05	0.04	0.04	0.03	0.03	0.02	0.04

C. Plots

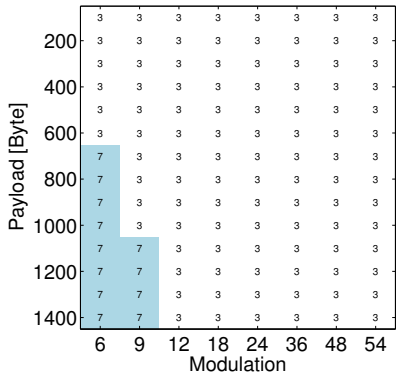

(a) CW_{min} and delay

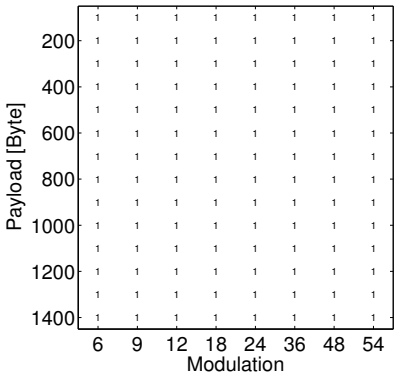

(b) Retry and delay

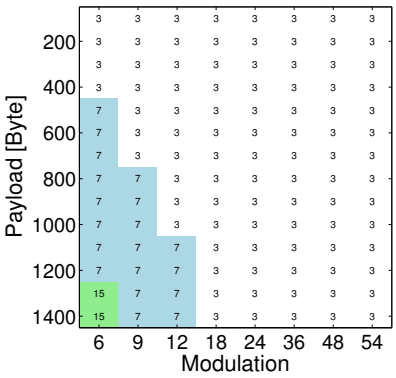

(c) CW_{min} and throughput

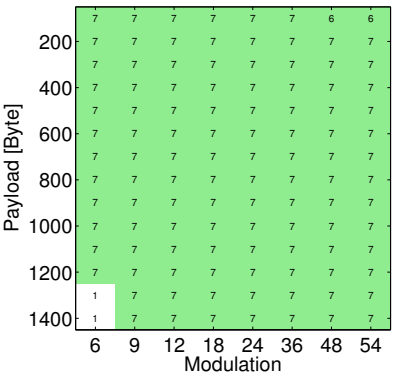

(d) Retry and throughput

Figure 48: Optimization 802.11a - seperate throughput delay (payload)

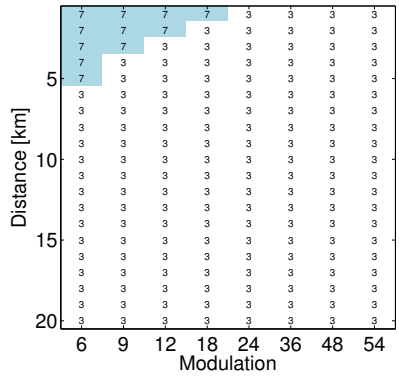

(a) CW_{min} optimization delay

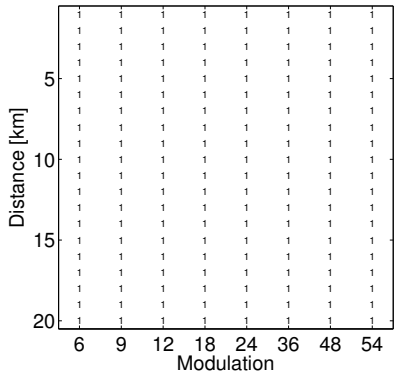

(b) Retry optimization delay

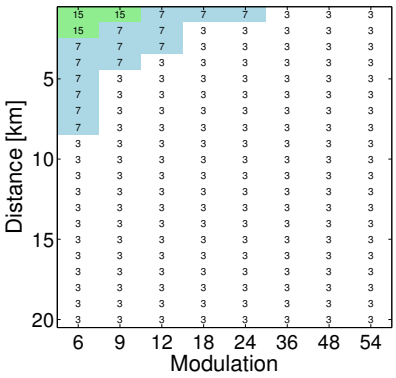

(c) CW_{min} optimization throughput

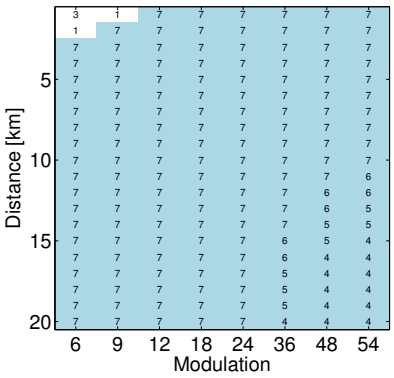

(d) Retry optimization throughput

Figure 49: Optimization 802.11a stand allone throughput and delay depending on the distance

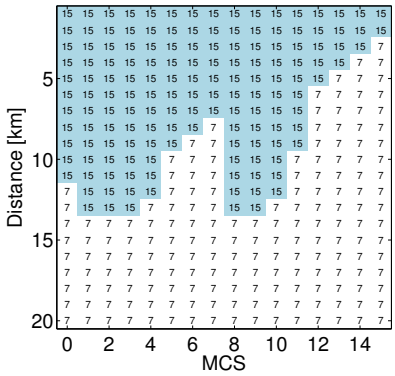

(a) CW_{min} optimization delay

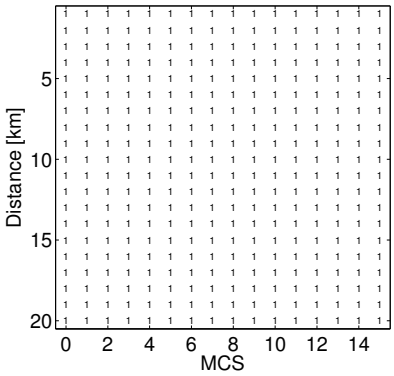

(b) Retry optimization delay

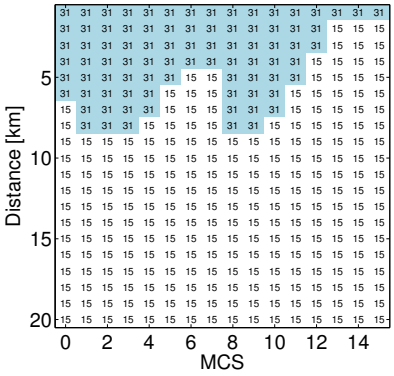

(c) CW_{min} optimization throughput

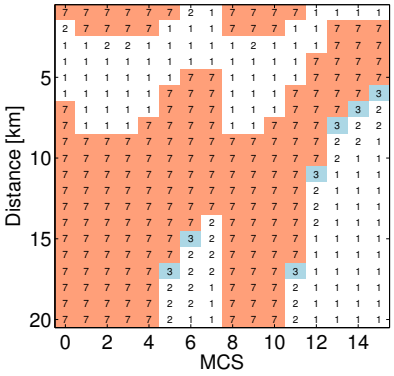

(d) Retry optimization throughput

Figure 50: Optimization 802.11n - seperate throughput delay (distance,factor 1)

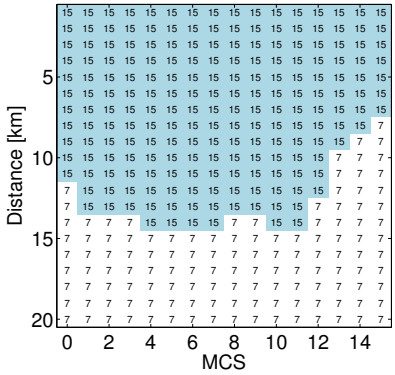

(a) CW_{min} optimization delay

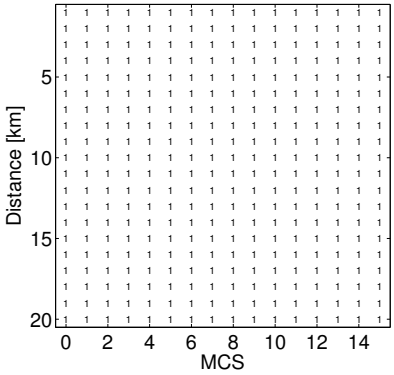

(b) Retry optimization delay

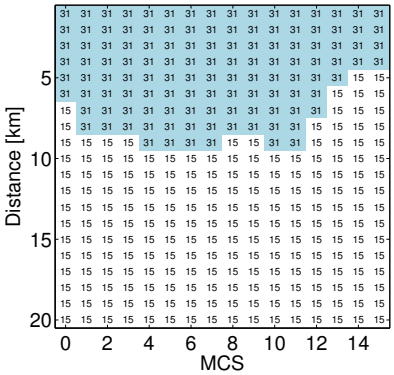

(c) CW_{min} optimization throughput

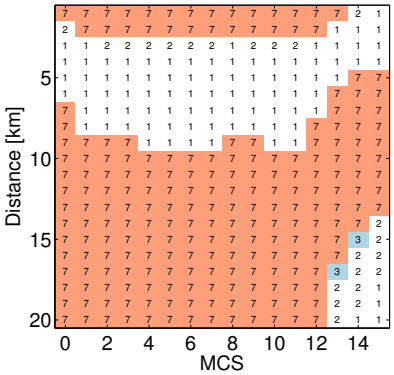

(d) Retry optimization throughput

Figure 51: Optimization 802.11n - seperate throughput delay (distance,factor 2)

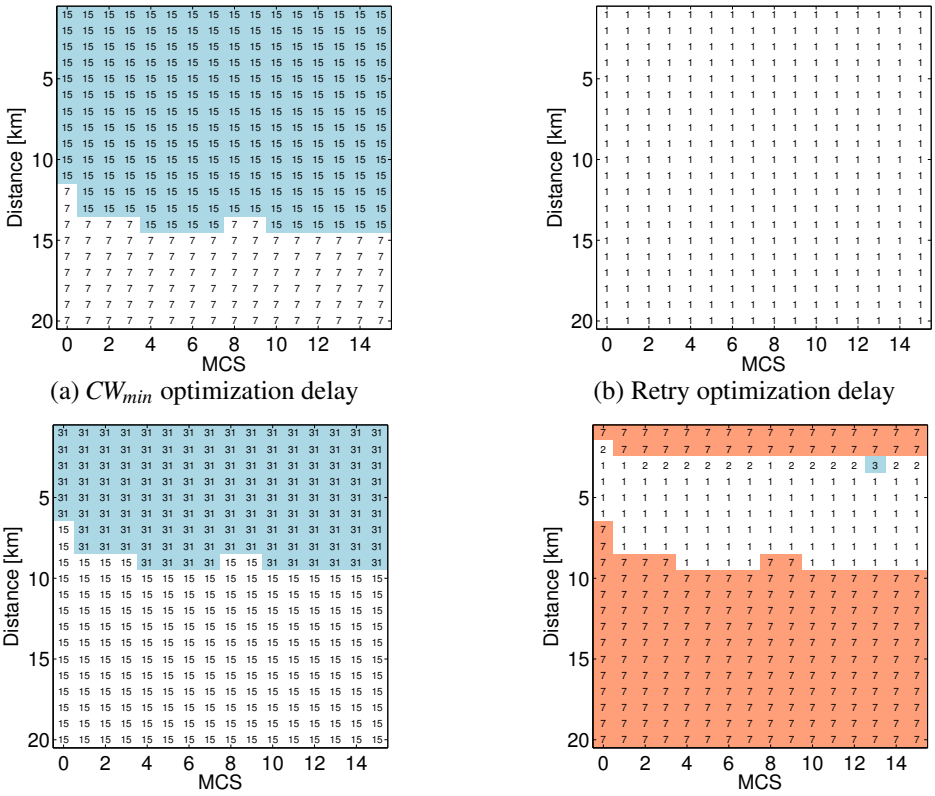

(a) CW_{min} optimization delay

(b) Retry optimization delay

(c) CW_{min} optimization throughput

(d) Retry optimization throughput

Figure 52: Optimization 802.11n - seperate throughput delay (distance,factor 3)